Characterization of a Functional *Comt1* Haplotype in Inbred Strains of Mice

Samantha Katherine Segall

A dissertation submitted to the faculty of the University of North Carolina at Chapel Hill in partial fulfillment of the requirements for the degree of Doctor of Philosophy in the Curriculum in Genetics and Molecular Biology

Chapel Hill
2010

Approved by:

Luda Diatchenko

Eric Everett

Beverly Koller

Andrea G. Nackley-Neeley

David Threadgill

Tim Wiltshire

ABSTRACT

Samantha Segall: Characterization of a Functional *Comt1* Haplotype in Inbred Strains of Mice
(Under the direction of Tim Wiltshire and Luda Diatchenko)

We have pursued a genome-wide approach to examining strain-specific variations in gene expression in the brain of 29 inbred strains of mice. The highest association was found within the locus of the Catechol-O-Methyltransferase (*Comt1)* gene, coding for an ubiquitously expressed enzyme that maintains basic biologic functions by inactivating catecholamines. In human and mouse, COMT has been associated with multiple behavioral phenotypes, including pain sensitivity and stress response. Multiple brain regions in 29 inbred strains of mice were analyzed for *Comt1* expression levels using a genome wide array. Differential expression levels, validated with qPCR, were observed for *Comt1*. A B2 Short Interspersed Nucleotide Element (SINE) was identified as an insertion in the 3'UTR of *Comt1* in 14 strains of a shared haplotype. Experiments using mammalian expression vectors of full length cDNA clones with and without the SINE element present demonstrate the SINE haplotype (+SINE) to have greater Comt1 enzymatic activity. Within strains examined to date, +SINE mice have increased enzymatic function, decreased sensitivity for thermal and chemical- induced pain assays and behavioral differences in several

anxiety assays. These results suggest that a haplotype, defined by a 3'UTR B2 SINE element, regulates *Comt1* expression and mouse behavior.

ACKNOWLEDGEMENTS

This dissertation is dedicated to the following women who profoundly influenced my life. Without a doubt, I never would have graduated without the help from each.

Annelore Butler

Luda Diatchenko

Beverly Koller

Charlene Segall Slayton

Rita Svec

And to my father, Scott Segall, who bought me my first microscope, first mouse, and built my first mouse maze. And to my mother, Joy Segall, who is the reason I chose this life.

TABLE OF CONTENTS

LIST OF TABLES

Table

LIST OF FIGURES

LIST OF ABBREVIATIONS AND SYMBOLS

3-OMD	3-methoxydopa
3'UTR	3' Untranslated region
5'UTR	5' Untranslated region
7SL	RNA component of the signal recognition particle
µl	Microliter
µM	Micromolar
A	Adenine
aa	Amino acid
AC	Anterior commisure
ActD	Actinomyosin D
ADHD	Attention deficit hyperactivity disorder
ANOVA	Analysis of variance
APS	Average pain sensitivity
BAC	Bacterial artificial chromosome
BCA	Bicinchoninic acid
Bp	Base pair
BV-2	Murine microglia cells
C	Celsius
CDF	Cumultive distribution function
cDNA	Complementary DNA
CDTA	Trans-1,2-Cyclohexanediaminetetra Acetic Acid

Chr	Chromosome
COMT	Catechol-O-methyltransferase gene (human)
COMT	Catechol-O-methyltransferase enzyme (human)
COMT1	Catechol-O-methyltransferase enzyme (mouse)
Comt1	Catechol-O-methyltransferase gene (mouse)
$Comt1^{+}$	Catechol-O-methyltransferase gene (mouse), ancestral
$Comt1^{B2i}$	Catechol-O-methyltransferase gene (mouse), B2 insertion in 3'UTR
COS1	**C**V-1 (African green monkey) in **O**rigin, carrying **S**V40 genetic material
DHPG	Dihydroxyphenylglycol
DOPAC	3,4-dihydroxyphenylacetic acid
DiProPerm	Direction Projection Permutation
DNA	Deoxyribonucleic acid
DWD	Distance weighted discrimination
E	Epinephrine
E.Coli	*Escherichia coli*
EDTA	Ethylenediaminetetraacetic acid
ELISA	Enzyme-linked immunosorbent assay
EPM	Elevated plus maze, total distance
eQTL	Expression quantitative trait loci
F	Fixation indices
G	Guanine
GCRMA	GC-Robust multi-array average
GNF	Genomics Institute of the Novartis Research Foundation

HAM	Haplotype association mapping
HDLSS	High Dimension Low Sample Size
HEK 293	Human Embryonic Kidney cell line
Het	Heterozygous
HPLC	High-performance liquid chromatography
HPS	High pain sensitivity
HVA	Homovanillic acid
i.e.	Id est (“that is” *Latin*)
IL-6	Interleukin-6
I.M.A.G.E	Integrated Molecular Analysis of Genomes and their Expression
i.p.	Intraperitoneal injection
Kb	Kilobase
Kbp	Kilobase pair
KO	Knockout
LDB	Light/dark box, % time spent in light
LPS	Low pain sensitivity
MAO	Monoamine oxidase
MB -	Membrane bound form
MB	Megabase
Met	Methionine
Mg^{2+}	Magnesium ion
MHPG	Methoxyhydroxyphenylglycol
miRNA	microRNA

mL	Mililiter
mM	Millimolar
mRNA	Messenger RNA
NCBI	National Center for Biotechnology Information
NE	L-norepinephrine
NE/E	Norepinephrine and epinephrine
NET	Norepinephrine Transporter
Ng	Nanogram
NIH	National Institutes of Health
nM	Nanomolar
NMN	Normetanephrine
OFD	Open field, total distance
OFR	Open field, rearing
PC-12	Pheochromocytoma cells
PCR	Polymerase chain reaction
qPCR	Quantitative polymerase chain reaction
QTL	Quantitative trait loci
RIPA	Radio-Immunoprecipitation Assay
RNA	Ribonucleic acid
rRNA	Ribosomal RNA
rs4680	Polymorphic nucleotide for valine or methionine aa in human COMT
S -	Soluble form
SAH	S-adenosyl homocysteine

SAMe	S-adenosyl methionine
SEM	Standard error of the mean
SINE	Short Interspersed Nucleotide Element
SK-N-Be(2)	Human neuroblastoma cell line
SMP	Sympathetically maintained pain
S_N2	Bimolecular nucleophilic substitution
SNP	Single nucleotide polymorphism
SPF	Specific Pathogen Free
Tg	Transgenic
TH	Tyrosine hydroxylase
THP-2	Human acute monocytic leukemia **cell** line
TMD	Temporomandibular Disorder
TNFα	Tumor necrosis factor-alpha
tRNA	Transfer RNA
Val	Valine
WT	Wild-type

CHAPTER 1: COMT ENZYME STRUCTURE AND FUNCTION

Introduction

Dysregulation of catecholamine signaling has been linked strongly to a variety of neuropsychiatric disorders (reviewed by Harrison & Tunbridge 2008 and Lachman 2008). Catechol-*O*-methyltransferase, or *COMT*, a gene encoding an enzyme of the same name, was among the first candidate genes in anxiety studies, as the COMT enzyme reduces the activity of catecholamines. Catecholamines are molecules derived from tyrosine, conserved in structure from worm to human, and function as neuromodulators or hormones. Catecholamines epinephrine and norepinephrine, are the molecules that warn of danger, and prepare the organism for immediate action (the fight-or-flight response). Both physiological and psychological stressors induce the release of catecholamines (Guyton, 1991). COMT enzymatic activity regulates the amounts of dopamine and norepinephrine in the brain and is associated with mood, memory, and other cognitive processes (reviewed by Mannisto & Kaakkola, 1999). A decrease of catecholamine metabolism is linked to disproportionate anxiety response (Domschke *et.al.,* 2007, Evans *et.al.,* 2009, Hettema *et.al.,* 2008), Obsessive-Compulsive Disorder (Pooley *et.al.,* 2007), cognition (Sheldrick *et.al.,* 2008) heightened pain perception (reviewed by Andersen & Skorpen, 2009), clearly demonstrating wide-ranging implications in a number of biological processes.

COMT Enzyme Function

Julius Axelrod and Robert Tomchick were the first to isolate and describe the enzymatic properties of a protein isolated from liver in their seminal paper: *Enzymatic 0-Methylation of Epinephrine and Other Catechols* (Axelrod & Tomchick 1958), the first of many discoveries which was recognized by a Nobel Prize in Physiology or Medicine for Axelrod in 1970. In the original paper, Axelrod and Tomchick speculated, "that O-methyl transferase is of paramount importance in the metabolism of catechol amine hormones and perhaps other normally occurring and foreign catechols." Indeed, the general function of COMT is the elimination of toxic or biologically active catechols and other hydroxylated metabolites (Mannisto & Kaakkola 1999). COMT enzyme is found in plants, microorganisms, and animals (Mannisto *et.al.,* 1992).

Substrates for COMT include the precursor molecule for the catecholamines, L-dopa, and the catecholamines dopamine, epinephrine and norepinephrine, their hydroxylated metabolites, catecholestrogens (Ball & Knuppen 1980), ascorbic acid, intermediates of melanin, and dietary and medicinal products (Mannisto & Kaakkola 1999). COMT shields the placenta and developing embryo in the first trimester of pregnancy from activated hydroxylated compounds formed from aryl hydrocarbons by hydroxylases (Barnea & Avigdor, 1990). COMT acts as a detoxifying enzyme between blood and other tissues, protecting the body from xenobiotics (Mannisto & Kaakkola 1999).

COMT is a member of the methyltransferase class of enzymes. The

enzymatic action is a transfer of a methyl group from the sulfur of S-adenosyl-L-methionine (SAMe) to one of the hydroxyls on a catechol structure in the presence of Mg^{2+} ions (Guldberg & Marsden, 1975), shown in Figure 1.1. The methyl transfer occurs by a S_N2 reaction (Woodard *et. al.,* 1980). In the COMT enzymatic reaction, the 3' or 4' hydroxyl group of the catechol substrate makes a direct nucleophilic attack on the methyl carbon of SAM. COMT itself does not become a methylated enzyme intermediate.

COMT Expression Profiles

Comt1 is widely expressed across a number of tissues. A comprehensive expression profile of *Comt1* mRNA in mouse is freely available on the public website BioGPS (http://biogps.gnf.org, Wu *et.al.,* 2009). Expression is highest in mouse in the liver, followed by kidney, likely due to the function of metabolic breakdown of catecholamines (Figure 1.2). In human expression, liver is also highest in two of the RNA probe sets, but the expression in other tissues is variable between probe sets (data not shown).

COMT Metabolism in the Brain

COMT is likely very important in the brain where regulation of catecholamines is critical for many neurological functions. There is considerable debate as to where catecholamine metabolism via COMT is most important (Professor William Maixner, UNC Center for Neurosensory Disorders, personal communication). Presynaptic neurons have no known COMT activity; the primary course of halting synaptic action of catecholamines is termed $uptake_1$, and occurs in presynaptic nerve terminals where catecholamines are either

metabolized by MAO-A or returned to storage vesicles (Huotari *et.al.,* 2002). As uptake$_1$ is the primary elimination system (Kopin 1985, Cass *et.al.,* 1993), COMT activity under basal conditions is likely low (Huotari *et.al.,* 2002). Glial cells provide a less important route of catecholamine clearing, termed uptake$_2$, where catecholamines are metabolized by COMT and/or monoamine oxidase (MAO)-B (Huotari *et.al.,* 2002).

COMT Structure: Membrane Bound and Soluble Forms

COMT is a single gene with six exons that maps in humans to chromosome 22q11.21 (Grossman *et.al.,* 1992). There are two major isoforms of COMT recognized in humans, a membrane bound form MB-COMT and a soluble form S-COMT, Figure 1.3 (Assicot & Bohoun 1971, Borchardt*, et.al.,* 1974, Nissinen 1984, Jeffery & Roth 1985). Both MB- and S- forms of the enzyme are made from the same transcript by two different promoters (Tenhunen *et.al.,* 1993). In humans, transcripts from at least one of the two forms have been identified in every tissue (Mannisto & Kaakkola 1999). As S- and MB- forms are found in different cellular compartments, the contribution of the two forms on different substrates possibly depends on not only the kinetic properties of the two forms but on the intracellular distribution of the substrates (Lotta *et.al.,* 1995).

Human *MB-COMT* transcript has two 5'UTR exons and four coding exons (Figure 1.4). MB-COMT has 271 amino acids. The first 50 (amino-terminal) amino acids are the hydrophobic membrane-anchoring signal. MB-COMT is found intracellularly on the rough endoplasmic reticulum (Lotta *et.al.,* 1995)

predominantly expressed in the brain, preferentially catabolizes dopamine, and is localized to: astrocytic processes surrounding synapses, postsynaptic dendritic spines, and capillary walls (Karhunen *et.al.,* 1995, Lundstrom *et.al.,* 1995, Mannisto & Kaakkola 1999).

S-COMT does not have 5'UTR exons or a targeting sequence, and has 4 exons (Figure 1. 3). The protein contains 221 amino acids and is the more abundant form. S-COMT is found in cytosol and in the nuclear envelope (Lotta *et.al.,* 1995) highly expressed in liver and kidney, and has much higher affinity for epinephrine.

While MB- and S- enzymes have been cloned and characterized, other *COMT* transcripts with alternative splicing have been isolated from human cadaver brains (Tunbridge *et. al.,* 2007). It is therefore probable that COMT enzyme forms other than MB- or S- exist.

COMT Sequence in Other Mammals

A COMT amino acid sequence from different mammalian species is highly similar (Vidgren *et.al.,* 1994). S-COMT from human is 81% identical with rat (Lotta *et.al.,* 1995) and 80% identical with mouse (Segall *et.al.,* 2010) (Figure 1.4, alignment with publically available software Clustal 2.0.8). RNA secondary structure is also highly conserved (Nackley *et. al.,* 2006). However, transcript structure between human and mouse for what is presumably S-COMT is not as well conserved (Figure 1.3). In mouse, three major isoforms have been identified, but from transcript structure, it is unclear which transcripts correspond to the S- form, as both have 5'UTRs.

COMT Sex-by-Gene Interaction

There is a growing body of evidence that COMT's effects are sexually dimorphic (Harrison & Tunbridge, 2008). Human COMT activity in erythrocytes (Boudikova *et.al.,* 1990, Weinshilboum *et.al.,* 1999) and liver (De Santi *et.al.,* 1998) is lower in females, possibly because it has been shown that estrogens down regulate COMT expression (Xie *et.al.,* 1999). In human postmortem prefrontal cortex, COMT activity is 17% lower in females than in males (Chen *et.al.,* 2004). In inbred strains of mice, female mice have lower *Comt1* RNA expression (Segall *et.al.,* 2010).

The Human Val/Met Polymorphism

COMT enzymatic activity is genetically polymorphic in humans. Family studies of erythrocyte (red blood cell) lysates showed a trimodal distribution of high, intermediate and low activities and the results of segregation analysis were consistent with a Mendelian inheritance pattern of two autosomal codominant alleles (Boudikova *et.al.,* 1990, Floderus & Wetterberg 1981, Grossman *et. al.,* 1992, Jeanjean *et.al.,* 1997, Siervogel *et.al.,* 1984, Spielman & Weinshilboum 1979, Weinshilboum & Raymond 1977). Furthermore, COMT activity in erythrocytes correlated to activity levels in other tissues, such as liver, lung, and kidney (Boudikova *et.al.,* 1999, Weinshilboum 1978). As the molecular mechanism for the allelic variation had not been identified, *COMT* was designated $COMT^{L}$ and $COMT^{H}$ for low and high activity, respectively. Erythrocyte lysates were thermo labile in subjects homozygous for the low activity allele, which led to the conclusion that the low activity was due to a

structural change in the COMT protein from an alternation in amino acid sequence (Boudikova *et.al.,* 1990, Scanlon *et.al.,* 1979, Spielman & Weinshilboum 1981).

When human *S-COMT* was sequenced, two sequences differed at amino acid residue 108 (G→A, SNP rs4680 at S-COMT 108 or MB-COMT 158). The first published sequence had a Methionine (*met*) (Bertocci, *et. al.,* 1991) and the second published sequence had a Valine (*val*) at this position (Lundstrom *et. al.,* 1992). To determine if either of these sequences were $COMT^{L}$, human *val108* and *met108 S-COMT* cDNA was expressed in *E. coli* to measure catalytic activity (Lotta *et.al.,* 1995). The catalytic activities were basically the same but as shown experimentally in human erythrocytes, the *met* enzyme was more thermo labile at physiological temperature of 37^{o}C (Lotta *et.al.,* 1995). This experiment was repeated in COS-1 and HEK293 cell constructs (Shield *et. al*., 2004), which unlike the *E.coli* transfections, showed a 40% reduction in COMT activity in the Met108 construct. In human tissue samples, a significant decrease in immunoreactive protein was found in liver biopsy samples from individuals homozygous for the *met* allele (Shield *et.al.,* 2004). In postmortem, dorso-lateral prefrontal cortex tissue, individuals homozygous for *met* showed an approximately 38% reduction in COMT activity from homozygous *val* (Chen *et.al.,* 2004).

Effect of Val^{158}Met on Behavioral Phenotypes

As a low activity allele presumably would lead to decreased catecholamine metabolism, genetic studies have attempted to link *val/met* rs4680 to an

assortment of diseases and personality traits. The first conformation of the low activity allele was conducted in liver biopsy with PCR (Lachman *et.al.,*1995) but with the ease of genotyping, a “cottage industry” of hundreds of studies have since been published in which the functional SNP rs4680 was examined for multiple psychiatric disorders (Lachman, 2008). The *met* allele, which is the reduced activity allele, has been correlated to better neurocognition in the general population (Egan *et.al.,* 2001, Malhotra *et.al.,* 2002) and greater anxiety (Drabant *et.al.,* 2006, Meir *et.al.,* 2009, Stein *et.al.,* 2006), possibly through the greater bioavailability of dopamine, epinephrine and norepinephrine in these individuals. However, correlations between the *val*158*met* polymorphism and disease state are often not reproducible (Lachman 2008, Barnett *et.al.,* 2009.)

The Three Haplotypes of *COMT* in Humans

Until recently, there was no mechanistic explanation for lowered enzymatic efficiency other than the reduced stability of the *met* allele. Dr. Luda Diatchenko and Dr. Andrea Nackley clarified the contribution of rs4680 by revealing three major haplotypes, as opposed to two, with the *val* allele encoding the most and least efficient enzyme.

Diatchenko and Nackley used pain sensitivity measurements and common SNPs in *COMT* transcript to define *COMT* haplotypes, and evaluate the contributions of common SNPs with rs4680 (Diatchenko *et.al.,* 2005). Three haplotypes were found to be present in 96% of subjects (Figure 1.7 a). These haplotypes were analyzed against a universal measure of pain perception to test whether they correlated with pain sensitivity. Haplotypes aligned to increasing

pain sensitivity and were designated high (HPS), average (APS) and low (LPS) pain sensitivity (Figure 1.7b). In addition to pain perception, haplotype status also correlated with enzymatic efficacy, with the LPS haplotype producing the most efficient enzyme and HPS the least efficient. A highly efficient COMT would limit catecholamine signaling to adrenergic receptors; therefore it was reasonable to expect nociceptive pain sensitivity to diminish with high COMT activity. However, the LPS and HPS were both *val* variants, so enzyme stability could not be the only explanation for higher activity of the LPS allele.

Transcript stability was examined next, with mRNA structure and Gibbs free energy predicted for the three haplotypes (Nackley *et. al.,* 2006). LPS had the least stable transcript, and HPS the most stable transcript. Transcript stability directly correlated to protein levels, and enzymatic efficacy. Site directed mutagenesis of the nucleotide interacting with rs4680 in the HPS transcript destroys the stable stem-loop structure and reverted it to the LPS haplotype, restoring the high level of translated protein. Thus, a molecular explanation for high, average, and low pain sensitivity from nociceptive thermal, pressure and ischemic stimuli directly correlates with low, average and high COMT activity.

Since all previous linkage studies grouped both *val* alleles together, it is not surprising that studies often were not reproducible, as the haplotype encoding for the *least* and *greatest* efficient enzyme would be grouped together, if only rs4680 were genotyped. Terminology and haplotype analysis is currently changing from *val/met*, to the haplotypes christened HPS, APS and LPS. Since the haplotypes were discovered, studies have found correlations of haplotype to

syndrome or disease of investigation, such as for cognitive function (Barnett *et.al.,* 2009) severity of hyperactivity symptoms in adults (Halleland *et.al.,* 2008), experimental pain (George *et.al.,* 2010) or pain post-surgical procedure (George *et.al.,* 2008).

COMT and 22q11 Deletion Syndrome

COMT is localized to 22q11.2 (Grossman *et.al.,* 1992), within the region hemizygously deleted in 22q11 Deletion Syndrome (22q11DS), or DiGeorge Syndrome (Driscoll *et. al.,* 1992). 22q11DS is the most common of the rare chromosomal disorders, with a frequency rate of 1:4000 (Oskarsdóttir *et.al.,* 2004). As 22q11DS individuals have only one copy of *COMT,* extensive studies of the *val/met* polymorphism have been conducted, although none yet with the haplotype as defined by Diatchenko *et.al*. However, there is a consistent biological theme, which manifests itself in 22q11DS: low COMT activity (from having one copy of the gene) correlates to high anxiety. The incidence of anxiety disorders among 22q11DS individuals is nearly 50% (Baker & Skuse 2005, Gothelf *et.al.,* 2007, Jolin *et.al.,* 2009, Shashi *et.al.,* 2010). We will show further evidence of the correlation of COMT function and anxiety in Chapter 2.

COMT activity in other mammals

COMT activity is variable in inbred and out bred strains of rats (Roth *et. al.,* 1990, Goldstein *et.al.,* 1990, Weinshilboum & Raymond 1977) although the genetic source of the difference has not yet been identified. A recent report by Masuda *et. al.* found inter-breed variations of *COMT* genotypes in five common dog breeds (Masuda *et.al.,* 2004). Although the authors speculated on the

affects of the polymorphisms, they did not quantify the relative activities of *COMT* in blood or tissue from the surveyed dog breeds. In inbred strains of mice, differences in catecholamine metabolism between C57BL/6J and DBA/2J had been reported previously (Eleftheriou 1975). This study found that COMT1 activity varies with brain region, age, and stress (Figure 1.6).

Other species do not have either a Valine or Methionine at the human polymorphic position. Rat and pig (Salminen *et. al.,* 1990, Malherbe *et.al.,* 1992) mouse and monkey (Papaleo *et.al.,* 2008) have Leucine at this position. On the Santa Cruz Genome Browser (http://genome.ucsc.edu), the two Neanderthal sequences available are Valine at this position, as are the great apes chimpanzee and orangutan (Green *et.al.,* 2010, Kent, *et.al.,* 2002, Lander *et.al.,* 2001, Rhead *et.al.,* 2010).

Further comparisons between COMT of different species showed experimentally that the first Kozak sequence evolved to favor translation of MB-form of COMT in the brain (Papaleo *et.al.,* 2008). It has been suggested that COMT activity has been lowered with evolutionary pressure as higher cortical function emerged (Chen *et.al.,* 2004) and COMT became more important in central neurotransmission, in contrast to its original role in peripheral detoxification (Papaleo *et.al.,* 2008). The Neanderthal and Great Ape species *val* at this position support this hypothesis.

The COMT1 Knockout and *Comt-Val-Tg* Mouse

A strain of mice with the *Comt1* gene disrupted has been generated (Gogos *et. al,* 1998). A disrupted *Comt1* transcript originally was introduced into

a mixed C57BL/6J/129Sv background and has been backcrossed into C57BL/6J. The mouse is able to be maintained by homozygous crosses, and is normal in appearance.

In pharmacological studies, *Comt1* deficiency does not affect basal brain dopamine and norepinephrine levels, although when *Comt1* null and heterozygous (het) mice are challenged with levodopa (the precursor to dopamine), the catecholamine metabolites and dopamine accumulate in the cortex and hypothalamus (Huotari *et. al.,* 2002). Figure 1.5 shows levels of catecholamines and metabolites in cortex of wild type, heterozygous and null *Comt1* mice. The effect is *Comt1* dosage dependent and specific to brain region. Additionally, the effect is sexually dimorphic, as male wt and het mice show greater 3- methoxydopa (3-OMD) than female wt and het mice. In *Comt1* knockout mice, frontal cortical dopamine levels are affected in male, but not female *Comt1* null mice (Gogos *et.al.,* 1998). Of note: the authors did not find any protein differences in basal levels of catecholamine-metabolizing enzymes (MAO-A/B, phenyltransferase) or catecholamine synthesizing enzymes (tyrosine hydroxylase, dopa decarboxylase, or dopamine β- hydroxylase). In contrast, tyrosine hydroxylase (TH) is up regulated in a transgenic mouse over expressing the human *COMT-Val* variant *(COMT-Val-tg)* (Papaleo *et.al.,* 2008). As TH is the rate-limiting enzyme in dopamine synthesis, higher TH protein levels in *COMT-Val-tg mice,* which have higher COMT enzymatic activity, would be consistent with a compensatory effect from greater dopamine degradation in *COMT-Val-tg* mice (Papaleo *et.al,* 2008).

Under stressful conditions, COMT1 deficiency reveals behavioral phenotypes. Male heterozygous mice are more aggressive (Gogos *et. al.,* 1998). *Comt1* null and heterozygous mice have an increased stress reactivity, increased acoustic startle stimulus, improved working memory and increased thermal pain sensitivity (Papaleo *et. al.,* 2008). These phenotypes mirror human studies of individuals with a low activity *COMT* allele.

Novel findings regarding the activity and function of *Comt1* in inbred strains of mice are presented in Chapter 2. While inbred strains of mice led to our *Comt1* findings, two other publications in BXD recombinant mice (Li *et.al.,* 2010) and HS out bred mice (Kember *et.al.,* 2010) simultaneously mirrored some of our findings. However, there is a large dataset of information, which did not coalesce into a paper, which will be presented in subsequent chapters.

References

Andersen, S. & Skorpen, F. (2009) Variation in the COMT gene: implications for pain perception and pain treatment. *Pharmacogenomics,* **10,** 669-684.

Assicot, M. & Bohuon, C. (1971) Presence of two distinct catechol -O-methyltransferase activities in red blood cells. *Biochimie,* **53,** 871-874.

Axelrod, J. & Tomchick, R. (1958) Enzymatic O-methylation of epinephrine and other catechols. *J Biol Chem,* **233,** 702-705.

Baker, K., Baldeweg, T., Sivagnanasundaram, S., Scambler, P. & Skuse, D. (2005) COMT Val108/158 Met modifies mismatch negativity and cognitive function in 22q11 deletion syndrome. *Biol Psychiatry,* **58,** 23-31.

Ball, P. & Knuppen, R. (1980) Catecholoestrogens (2-and 4-hydroxyoestrogens): chemistry, biogenesis, metabolism, occurrence and physiological significance. *Acta Endocrinol Suppl (Copenh),* **232,** 1-127.

Barnea, E.R. & Avigdor, S. (1990) Coordinated induction of estrogen hydroxylase and catechol-O-methyl transferase by xenobiotics in first trimester human placental explants. *J Steroid Biochem,* **35,** 327-331.

Barnett, J.H., Heron, J., Goldman, D., Jones, P.B. & Xu, K. (2009) Effects of catechol-O-methyltransferase on normal variation in the cognitive function of children. *Am J Psychiatry,* **166,** 909-916.

Bertocci, B., Miggiano, V., Da Prada, M., Dembic, Z., Lahm, H.W. & Malherbe, P. (1991) Human catechol-O-methyltransferase: cloning and expression of the membrane-associated form. *Proc Natl Acad Sci U S A,* **88,** 1416-1420.

Borchardt, R.T., Cheng, C.F. & Cooke, P.H. (1974) The purification and kinetic properties of liver microsomal-catechol-o-methyltransferase. *Life Sci,* **14,** 1089-1100.

Boudikova, B., Szumlanski, C., Maidak, B. & Weinshilboum, R. (1990) Human liver catechol-O-methyltransferase pharmacogenetics. *Clin Pharmacol Ther,* **48,** 381-389.

Cass, W.A., Zahniser, N.R., Flach, K.A. & Gerhardt, G.A. (1993) Clearance of exogenous dopamine in rat dorsal striatum and nucleus accumbens: role of metabolism and effects of locally applied uptake inhibitors. *J Neurochem,* **61,** 2269-2278.

Chen, J., Lipska, B.K., Halim, N., Ma, Q.D., Matsumoto, M., Melhem, S.,

Kolachana, B.S., Hyde, T.M., Herman, M.M., Apud, J., Egan, M.F., Kleinman, J.E. & Weinberger, D.R. (2004) Functional analysis of genetic variation in catechol-O-methyltransferase (COMT): effects on mRNA, protein, and enzyme activity in postmortem human brain. *Am J Hum Genet,* **75,** 807-821.

De Santi, C., Giulianotti, P.C., Pietrabissa, A., Mosca, F. & Pacifici, G.M. (1998) Catechol-O-methyltransferase: variation in enzyme activity and inhibition by entacapone and tolcapone. *Eur J Clin Pharmacol,* **54,** 215-219.

Diatchenko, L., Anderson, A.D., Slade, G.D., Fillingim, R.B., Shabalina, S.A., Higgins, T.J., Sama, S., Belfer, I., Goldman, D., Max, M.B., Weir, B.S. & Maixner, W. (2006) Three major haplotypes of the beta2 adrenergic receptor define psychological profile, blood pressure, and the risk for development of a common musculoskeletal pain disorder. *Am J Med Genet B Neuropsychiatr Genet,* **141B,** 449-462.

Diatchenko, L., Slade, G.D., Nackley, A.G., Bhalang, K., Sigurdsson, A., Belfer, I., Goldman, D., Xu, K., Shabalina, S.A., Shagin, D., Max, M.B., Makarov, S.S. & Maixner, W. (2005) Genetic basis for individual variations in pain perception and the development of a chronic pain condition. *Hum Mol Genet,* **14,** 135-143.

Domschke, K., Deckert, J., O'Donovan M, C. & Glatt, S.J. (2007) Meta-analysis of COMT val158met in panic disorder: ethnic heterogeneity and gender specificity. *Am J Med Genet B Neuropsychiatr Genet,* **144B,** 667-673.

Drabant, E.M., Hariri, A.R., Meyer-Lindenberg, A., Munoz, K.E., Mattay, V.S., Kolachana, B.S., Egan, M.F. & Weinberger, D.R. (2006) Catechol O-methyltransferase val158met genotype and neural mechanisms related to affective arousal and regulation. *Arch Gen Psychiatry,* **63,** 1396-1406.

Driscoll, D.A., Budarf, M.L. & Emanuel, B.S. (1992) A genetic etiology for DiGeorge syndrome: consistent deletions and microdeletions of 22q11. *Am J Hum Genet,* **50,** 924-933.

Egan, M.F., Goldberg, T.E., Kolachana, B.S., Callicott, J.H., Mazzanti, C.M., Straub, R.E., Goldman, D. & Weinberger, D.R. (2001) Effect of COMT Val108/158 Met genotype on frontal lobe function and risk for schizophrenia. *Proc Natl Acad Sci U S A,* **98,** 6917-6922.

Eleftheriou, B.E. (1975) Regional brain catechol-O-methyl transferase: age related differences in the mouse. *Exp Aging Res,* **1,** 99-103.

Evans, J., Xu, K., Heron, J., Enoch, M.A., Araya, R., Lewis, G., Timpson, N., Davies, S., Nutt, D. & Goldman, D. (2009) Emotional symptoms in

children: The effect of maternal depression, life events, and COMT genotype. *Am J Med Genet B Neuropsychiatr Genet,* **150B,** 209-218.

Floderus, Y. & Wetterberg, L. (1981) The inheritance of human erythrocyte catechol-O-methyltransferase activity. *Clin Genet,* **19,** 392-395.

Fvasconcellos (2007) Structural diagram of normetanephrine. In Normetanephrine.svg (ed), *http://www.acdlabs.com/download/chemsk.html ACD/ChemSketch 10.0] and {{w|Inkscape}}. |Source= Own work.*, p. Structural diagram of normetanephrine. Created using ACD/ChemSketch 10.10 and Inkscape.

George, S.Z., Wallace, M.R., Wright, T.W., Moser, M.W., Greenfield, W.H., 3rd, Sack, B.K., Herbstman, D.M. & Fillingim, R.B. (2008) Evidence for a biopsychosocial influence on shoulder pain: pain catastrophizing and catechol-O-methyltransferase (COMT) diplotype predict clinical pain ratings. *Pain,* **136,** 53-61.

Gogos, J.A., Morgan, M., Luine, V., Santha, M., Ogawa, S., Pfaff, D. & Karayiorgou, M. (1998) Catechol-O-methyltransferase-deficient mice exhibit sexually dimorphic changes in catecholamine levels and behavior. *Proc Natl Acad Sci U S A,* **95,** 9991-9996.

Goldstein, D.J., Weinshilboum, R.M., Dunnette, J.H. & Creveling, C.R. (1980) Developmental patterns of catechol-O-methyltransferase in genetically different rat strains: enzymatic and immunochemical studies. *J Neurochem,* **34,** 153-162.

Green, R.E., Krause, J., Briggs, A.W., Maricic, T., Stenzel, U., Kircher, M., Patterson, N., Li, H., Zhai, W., Fritz, M.H., Hansen, N.F., Durand, E.Y., Malaspinas, A.S., Jensen, J.D., Marques-Bonet, T., Alkan, C., Prufer, K., Meyer, M., Burbano, H.A., Good, J.M., Schultz, R., Aximu-Petri, A., Butthof, A., Hober, B., Hoffner, B., Siegemund, M., Weihmann, A., Nusbaum, C., Lander, E.S., Russ, C., Novod, N., Affourtit, J., Egholm, M., Verna, C., Rudan, P., Brajkovic, D., Kucan, Z., Gusic, I., Doronichev, V.B., Golovanova, L.V., Lalueza-Fox, C., de la Rasilla, M., Fortea, J., Rosas, A., Schmitz, R.W., Johnson, P.L., Eichler, E.E., Falush, D., Birney, E., Mullikin, J.C., Slatkin, M., Nielsen, R., Kelso, J., Lachmann, M., Reich, D. & Paabo, S. (2010) A draft sequence of the Neandertal genome. *Science,* **328,** 710-722.

Grossman, M.H., Emanuel, B.S. & Budarf, M.L. (1992) Chromosomal mapping of the human catechol-O-methyltransferase gene to 22q11.1----q11.2. *Genomics,* **12,** 822-825.

Guldberg, H.C. & Marsden, C.A. (1975) Catechol-O-methyl transferase:

pharmacological aspects and physiological role. *Pharmacol Rev,* **27,** 135-206.

Guyton, A.C. (1991) Textbook of Medical Physiology. In Wonsiewicz, M.J. (ed), W.B. Saunders Company, Philadelphia, p. 676.

Halleland, H., Lundervold, A.J., Halmoy, A., Haavik, J. & Johansson, S. (2009) Association between catechol O-methyltransferase (COMT) haplotypes and severity of hyperactivity symptoms in adults. *Am J Med Genet B Neuropsychiatr Genet,* **150B,** 403-410.

Harrison, P.J. & Tunbridge, E.M. (2008) Catechol-O-methyltransferase (COMT): a gene contributing to sex differences in brain function, and to sexual dimorphism in the predisposition to psychiatric disorders. *Neuropsychopharmacology,* **33,** 3037-3045.

Hettema, J.M., An, S.S., Bukszar, J., van den Oord, E.J., Neale, M.C., Kendler, K.S. & Chen, X. (2008) Catechol-O-methyltransferase contributes to genetic susceptibility shared among anxiety spectrum phenotypes. *Biol Psychiatry,* **64,** 302-310.

Huotari, M., Gogos, J.A., Karayiorgou, M., Koponen, O., Forsberg, M., Raasmaja, A., Hyttinen, J. & Mannisto, P.T. (2002) Brain catecholamine metabolism in catechol-O-methyltransferase (COMT)-deficient mice. *Eur J Neurosci,* **15,** 246-256.

Jeanjean, A.P., Laterre, E.C. & Maloteaux, J.M. (1997) Neuroleptic binding to sigma receptors: possible involvement in neuroleptic-induced acute dystonia. *Biol Psychiatry,* **41,** 1010-1019.

Jeffery, D.R. & Roth, J.A. (1985) Purification and kinetic mechanism of human brain soluble catechol-O-methyltransferase. *J Neurochem,* **44,** 881-885.

Jolin, E.M., Weller, R.A., Jessani, N.R., Zackai, E.H., McDonald-McGinn, D.M. & Weller, E.B. (2009) Affective disorders and other psychiatric diagnoses in children and adolescents with 22q11.2 Deletion Syndrome. *J Affect Disord,* **119,** 177-180.

Karhunen, T., Tilgmann, C., Ulmanen, I. & Panula, P. (1995) Neuronal and non-neuronal catechol-O-methyltransferase in primary cultures of rat brain cells. *Int J Dev Neurosci,* **13,** 825-834.

Kent, W.J., Sugnet, C.W., Furey, T.S., Roskin, K.M., Pringle, T.H., Zahler, A.M. & Haussler, D. (2002) The human genome browser at UCSC. *Genome Res,* **12,** 996-1006.

Kopin, I.J. (1985) Catecholamine metabolism: basic aspects and clinical

significance. *Pharmacol Rev,* **37,** 333-364.

Lachman, H.M. (2008) Does COMT val158met affect behavioral phenotypes: yes, no, maybe? *Neuropsychopharmacology,* **33,** 3027-3029.

Lachman, H.M., Papolos, D.F., Saito, T., Yu, Y.M., Szumlanski, C.L. & Weinshilboum, R.M. (1996) Human catechol-O-methyltransferase pharmacogenetics: description of a functional polymorphism and its potential application to neuropsychiatric disorders. *Pharmacogenetics,* **6,** 243-250.

Lander, E.S. & Linton, L.M. & Birren, B. & Nusbaum, C. & Zody, M.C. & Baldwin, J. & Devon, K. & Dewar, K. & Doyle, M. & FitzHugh, W. & Funke, R. & Gage, D. & Harris, K. & Heaford, A. & Howland, J. & Kann, L. & Lehoczky, J. & LeVine, R. & McEwan, P. & McKernan, K. & Meldrim, J. & Mesirov, J.P. & Miranda, C. & Morris, W. & Naylor, J. & Raymond, C. & Rosetti, M. & Santos, R. & Sheridan, A. & Sougnez, C. & Stange-Thomann, N. & Stojanovic, N. & Subramanian, A. & Wyman, D. & Rogers, J. & Sulston, J. & Ainscough, R. & Beck, S. & Bentley, D. & Burton, J. & Clee, C. & Carter, N. & Coulson, A. & Deadman, R. & Deloukas, P. & Dunham, A. & Dunham, I. & Durbin, R. & French, L. & Grafham, D. & Gregory, S. & Hubbard, T. & Humphray, S. & Hunt, A. & Jones, M. & Lloyd, C. & McMurray, A. & Matthews, L. & Mercer, S. & Milne, S. & Mullikin, J.C. & Mungall, A. & Plumb, R. & Ross, M. & Shownkeen, R. & Sims, S. & Waterston, R.H. & Wilson, R.K. & Hillier, L.W. & McPherson, J.D. & Marra, M.A. & Mardis, E.R. & Fulton, L.A. & Chinwalla, A.T. & Pepin, K.H. & Gish, W.R. & Chissoe, S.L. & Wendl, M.C. & Delehaunty, K.D. & Miner, T.L. & Delehaunty, A. & Kramer, J.B. & Cook, L.L. & Fulton, R.S. & Johnson, D.L. & Minx, P.J. & Clifton, S.W. & Hawkins, T. & Branscomb, E. & Predki, P. & Richardson, P. & Wenning, S. & Slezak, T. & Doggett, N. & Cheng, J.F. & Olsen, A. & Lucas, S. & Elkin, C. & Uberbacher, E. & Frazier, M., et al. (2001) Initial sequencing and analysis of the human genome. *Nature,* **409,** 860-921.

Li, Z., Mulligan, M.K., Wang, X., Miles. M., Lu, L., Williams, R.W. (2010) A Transposon in Comt Generates mRNA Variants and Causes Widespread Expression and Behavioral Differences among Mice. *PLOS One,* **5,** 1-11.

Lotta, T., Vidgren, J., Tilgmann, C., Ulmanen, I., Melen, K., Julkunen, I. & Taskinen, J. (1995) Kinetics of human soluble and membrane-bound catechol O-methyltransferase: a revised mechanism and description of the thermolabile variant of the enzyme. *Biochemistry,* **34,** 4202-4210.

Lundstrom, K., Tenhunen, J., Tilgmann, C., Karhunen, T., Panula, P. & Ulmanen, I. (1995) Cloning, expression and structure of catechol-O-methyltransferase. *Biochim Biophys Acta,* **1251,** 1-10.

Lundstrom, K., Tilgmann, C., Peranen, J., Kalkkinen, N. & Ulmanen, I. (1992) Expression of enzymatically active rat liver and human placental catechol-O-methyltransferase in Escherichia coli; purification and partial characterization of the enzyme. *Biochim Biophys Acta,* **1129,** 149-154.

Malherbe, P., Bertocci, B., Caspers, P., Zurcher, G. & Da Prada, M. (1992) Expression of functional membrane-bound and soluble catechol-O-methyltransferase in Escherichia coli and a mammalian cell line. *J Neurochem,* **58,** 1782-1789.

Malhotra, A.K., Kestler, L.J., Mazzanti, C., Bates, J.A., Goldberg, T. & Goldman, D. (2002) A functional polymorphism in the COMT gene and performance on a test of prefrontal cognition. *Am J Psychiatry,* **159,** 652-654.

Mannisto, P.T. & Kaakkola, S. (1999) Catechol-O-methyltransferase (COMT): biochemistry, molecular biology, pharmacology, and clinical efficacy of the new selective COMT inhibitors. *Pharmacol Rev,* **51,** 593-628.

Mannisto, P.T., Ulmanen, I., Lundstrom, K., Taskinen, J., Tenhunen, J., Tilgmann, C. & Kaakkola, S. (1992) Characteristics of catechol O-methyltransferase (COMT) and properties of selective COMT inhibitors. *Prog Drug Res,* **39,** 291-350.

Masuda, K., Hashizume, C., Kikusui, T., Takeuchi, Y. & Mori, Y. (2004) Breed differences in genotype and allele frequency of catechol O-methyltransferase gene polymorphic regions in dogs. *J Vet Med Sci,* **66,** 183-187.

Mier, D., Kirsch, P. & Meyer-Lindenberg, A. (2009) Neural substrates of pleiotropic action of genetic variation in COMT: a meta-analysis. *Mol Psychiatry*.

Nackley, A.G., Shabalina, S.A., Tchivileva, I.E., Satterfield, K., Korchynskyi, O., Makarov, S.S., Maixner, W. & Diatchenko, L. (2006) Human catechol-O-methyltransferase haplotypes modulate protein expression by altering mRNA secondary structure. *Science,* **314,** 1930-1933.

NEUROtiker (2007) In Catecholamines_biosynthesis.svg (ed), *Multi-license with GFDL and Creative Commons CC-BY-SA-2.5 and older versions (2.0 and 1.0).* pp. Biosynthesis of catecholamines adrenaline (epinephrine) and noradrenaline (norepinephrine), intermediates DOPA and dopamine.

Nissinen, E. & Mannisto, P. (1984) Determination of catechol-O-methyltransferase activity by high-performance liquid chromatography with electrochemical detection. *Anal Biochem,* **137,** 69-73.

Oskarsdottir, S., Vujic, M. & Fasth, A. (2004) Incidence and prevalence of the 22q11 deletion syndrome: a population-based study in Western Sweden. *Arch Dis Child,* **89,** 148-151.

Papaleo, F., Crawley, J.N., Song, J., Lipska, B.K., Pickel, J., Weinberger, D.R. & Chen, J. (2008) Genetic dissection of the role of catechol-O-methyltransferase in cognition and stress reactivity in mice. *J Neurosci,* **28,** 8709-8723.

Pooley, E.C., Fineberg, N. & Harrison, P.J. (2007) The met(158) allele of catechol-O-methyltransferase (COMT) is associated with obsessive-compulsive disorder in men: case-control study and meta-analysis. *Mol Psychiatry,* **12,** 556-561.

Rhead, B., Karolchik, D., Kuhn, R.M., Hinrichs, A.S., Zweig, A.S., Fujita, P.A., Diekhans, M., Smith, K.E., Rosenbloom, K.R., Raney, B.J., Pohl, A., Pheasant, M., Meyer, L.R., Learned, K., Hsu, F., Hillman-Jackson, J., Harte, R.A., Giardine, B., Dreszer, T.R., Clawson, H., Barber, G.P., Haussler, D. & Kent, W.J. (2010) The UCSC Genome Browser database: update 2010. *Nucleic Acids Res,* **38,** D613-619.

Roth, J.A., Grossman, M.H. & Adolf, M. (1990) Variation in hepatic membrane-bound catechol-O-methyltransferase activity in Fischer and Wistar-Furth strains of rat. *Biochem Pharmacol,* **40,** 1151-1153.

Salminen, M., Lundstrom, K., Tilgmann, C., Savolainen, R., Kalkkinen, N. & Ulmanen, I. (1990) Molecular cloning and characterization of rat liver catechol-O-methyltransferase. *Gene,* **93,** 241-247.

Scanlon, P.D., Raymond, F.A. & Weinshilboum, R.M. (1979) Catechol-O-methyltransferase: thermolabile enzyme in erythrocytes of subjects homozygous for allele for low activity. *Science,* **203,** 63-65.

Segall, S., Nackley, A.G., Diatchenko, L., Lariviere, W.R., Lu, X., Marron, J.S., Grabowski-Boase, L., Walker, J.R., Slade, G., Gauthier, J., Bailey, J.S., Steffy, B.M., Maynard, T.M., Tarantino, L.M. & Wiltshire, T. (2010) Comt1 Genotype and Expression Predicts Anxiety and Nociceptive Sensitivity in Inbred Strains of Mice. . *Genes Brain Behav.*

Shashi, V., Howard, T.D., Keshavan, M.S., Kaczorowski, J., Berry, M.N., Schoch, K., Spence, E.J. & Kwapil, T.R. (2010) COMT and anxiety and cognition in children with chromosome 22q11.2 deletion syndrome. *Psychiatry Res,* **178,** 433-436.

Sheldrick, A.J., Krug, A., Markov, V., Leube, D., Michel, T.M., Zerres, K.,

Eggermann, T. & Kircher, T. (2008) Effect of COMT val158met genotype on cognition and personality. *Eur Psychiatry,* **23,** 385-389.

Shield, A.J., Thomae, B.A., Eckloff, B.W., Wieben, E.D. & Weinshilboum, R.M. (2004) Human catechol O-methyltransferase genetic variation: gene resequencing and functional characterization of variant allozymes. *Mol Psychiatry,* **9,** 151-160.

Siervogel, R.M., Weinshilboum, R., Wilson, A.F. & Elston, R.C. (1984) Major gene model for the inheritance of catechol-O-methyltransferase activity in five large families. *Am J Med Genet,* **19,** 315-323.

Spielman, R.S. & Weinshilboum, R.M. (1981) Genetics of red cell COMT activity: analysis of thermal stability and family data. *Am J Med Genet,* **10,** 279-290.

Stein, D.J., Newman, T.K., Savitz, J. & Ramesar, R. (2006) Warriors versus worriers: the role of COMT gene variants. *CNS Spectr,* **11,** 745-748.

Tenhunen, J., Salminen, M., Jalanko, A., Ukkonen, S. & Ulmanen, I. (1993) Structure of the rat catechol-O-methyltransferase gene: separate promoters are used to produce mRNAs for soluble and membrane-bound forms of the enzyme. *DNA Cell Biol,* **12,** 253-263.

Thompson, J.D., Higgins, D.G. & Gibson, T.J. (1994) CLUSTAL W: improving the sensitivity of progressive multiple sequence alignment through sequence weighting, position-specific gap penalties and weight matrix choice. *Nucleic Acids Res,* **22,** 4673-4680.

Tunbridge, E.M., Lane, T.A. & Harrison, P.J. (2007) Expression of multiple catechol-o-methyltransferase (COMT) mRNA variants in human brain. *Am J Med Genet B Neuropsychiatr Genet,* **144B,** 834-839.

Weinshilboum, R., Raymond, F. (1977) Variations in Catechol-O-Methyltransferase Activity In Inbred Strains of Rats. *Neuropharmacology,* **16,** 703-706.

Weinshilboum, R.M., Otterness, D.M. & Szumlanski, C.L. (1999) Methylation pharmacogenetics: catechol O-methyltransferase, thiopurine methyltransferase, and histamine N-methyltransferase. *Annu Rev Pharmacol Toxicol,* **39,** 19-52.

Weinshilboum, R.M. & Raymond, F.A. (1977) Inheritance of low erythrocyte catechol-o-methyltransferase activity in man. *Am J Hum Genet,* **29,** 125-135.

Woodard, R.W., Tsai, M.D., Floss, H.G., Crooks, P.A. & Coward, J.K. (1980) Stereochemical course of the transmethylation catalyzed by catechol O-methyltransferase. *J Biol Chem,* **255,** 9124-9127.

Wu, C., Orozco, C., Boyer, J., Leglise, M., Goodale, J., Batalov, S., Hodge, C.L., Haase, J., Janes, J., Huss, J.W., 3rd & Su, A.I. (2009) BioGPS: an extensible and customizable portal for querying and organizing gene annotation resources. *Genome Biol,* **10,** R130.

Xie, T., Ho, S.L. & Ramsden, D. (1999) Characterization and implications of estrogenic down-regulation of human catechol-O-methyltransferase gene transcription. *Mol Pharmacol,* **56,** 31-38.

Figure 1.1 Catecholamine substrates and methylated metabolites of COMT (Axelrod & Tomchick, 1958). The most common positions for methylation are circled in red. *Adapted from catecholamine structures drawn by NEUROtiker, 2007 and Fvasconcellos, 2007.*

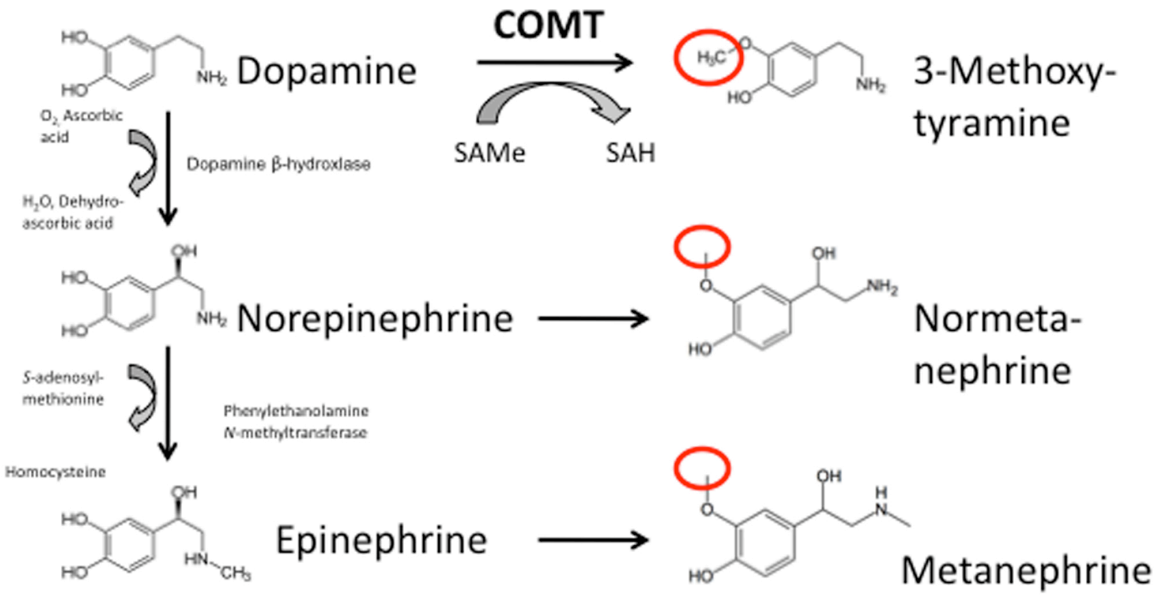

Figure 1.2 Affymetrix Genechip 430v2 *Comt1* coding probe set 1449183_at in a variety of mouse tissues and cell lines. Highest RNA expression in liver. *Adapted from data deposited onto http://biogps.gnf.org by Wu et.al., 2009.*

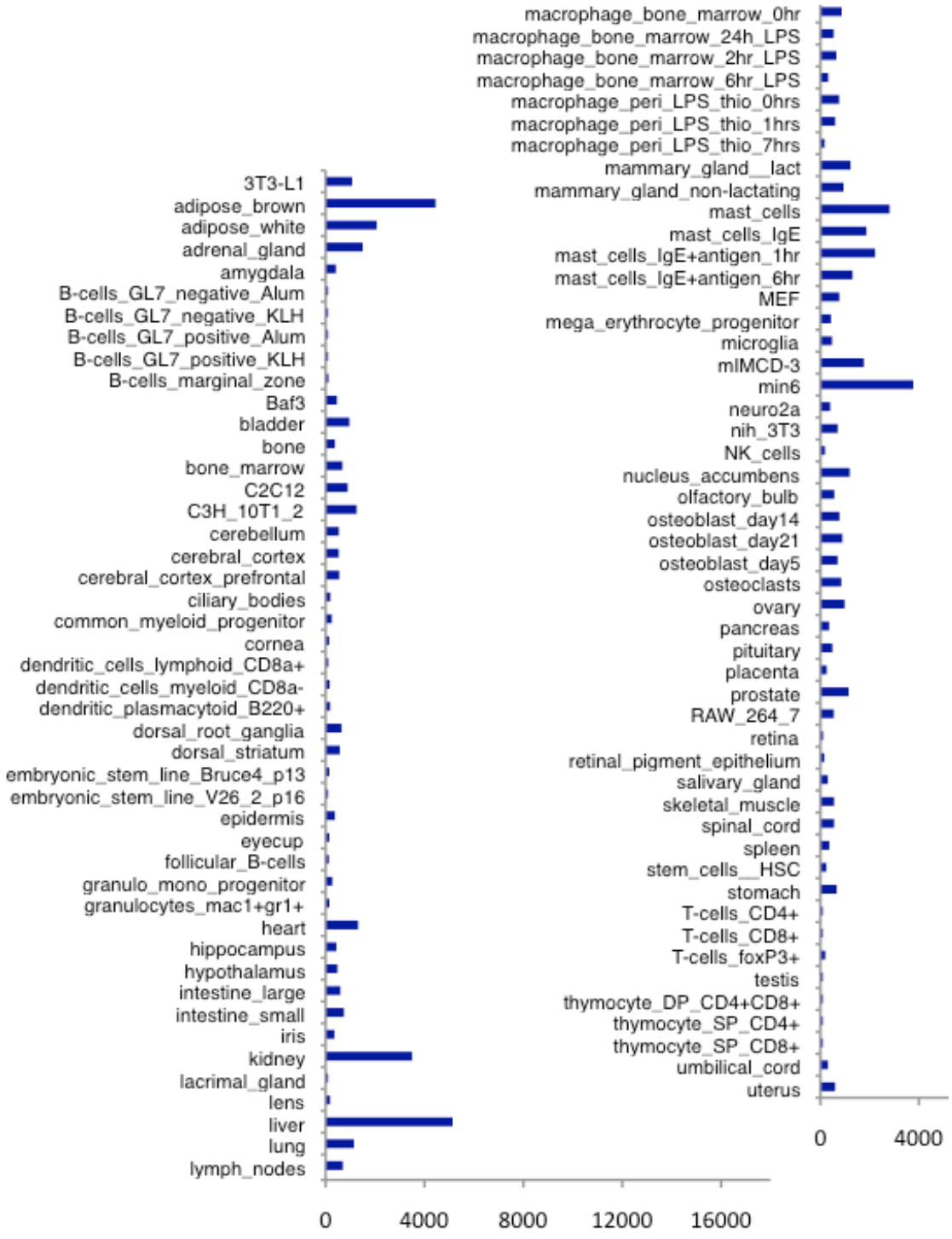

Figure 1.3 Comparison of human and mouse *COMT* gene structures: One gene transcript with splice varients forms the membrane-bound (MB-) or soluble (S-) forms of the enzyme. 5' and 3' UTR exons are depected in white, coding exons are blue. The first exon in *S-COMT* has a 5'UTR that is not spliced but immediately precedes the AUG start cite. MB- and S- forms of the gene have been annotated in human but have not been in mouse. It is not clear which isoform in mouse corresponds to the *S-COMT* identified in human.

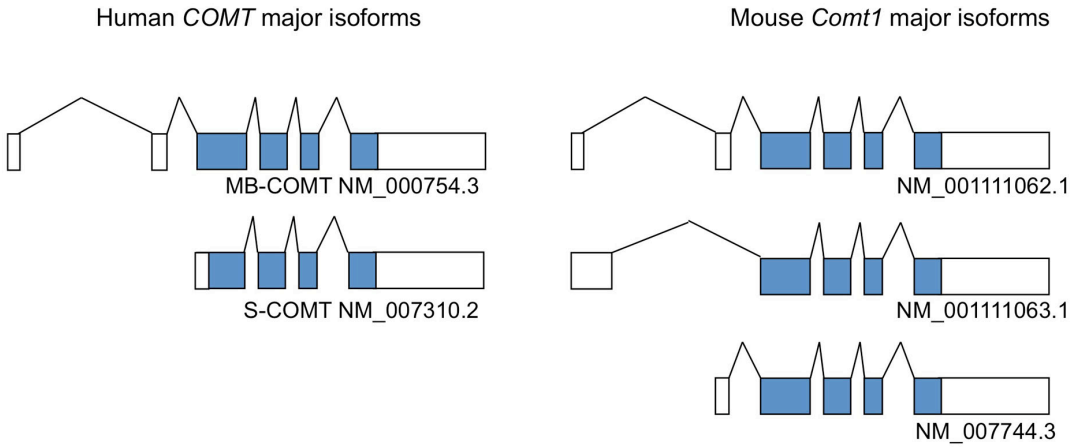

Figure 1.4 Comparison of amino acid sequence from mouse COMT1 and human COMT. *AUG MB- and **AUG S- for human COMT. Yellow highlighted amino acid sequence identical between mouse and human. Red arrow points to position of the val/met polymorphism in human. The orthologous residue in mouse is Leucine. *Adapted from NCBI Reference Sequence human NP_000745.1 and mouse NP_001104532.1 run on publically available software, http://www.ebi.ac.uk/Tools/clustalw2/index.html, Thompson et.al., 1994.*

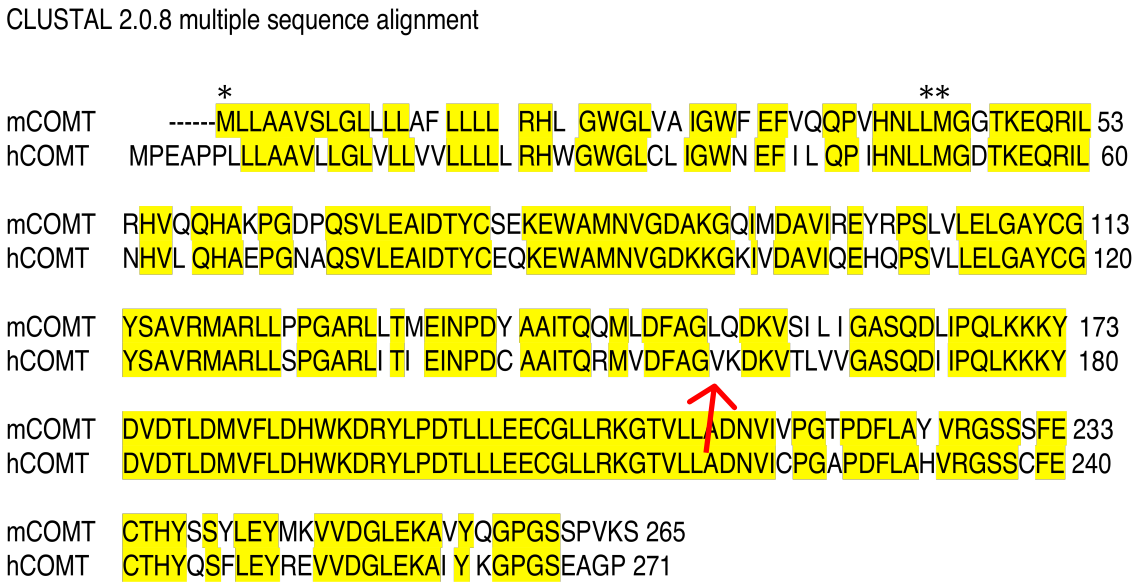

Figure 1.5 Metabolite levels in wild-type (WT) *Comt1*$^{+/+}$, heterozygous (HET) *Comt1*$^{-/+}$, and knock-out (NULL) *Comt1*$^{-/-}$ male mice before (pale orange) and after (dark orange) i.p. injections of levodopa. Supernatants from cortex homogenate levels were analyzed in two separate HPLC runs. Note: 3-OMD, HVA and MHPG levels are undetectable in *Comt1*$^{-/-}$ mice, a metabolic confirmation of the knock-out status. Units are in ng/g of wet tissue. Error bars for S.E.M and statistically significant differences are not shown for clarity. Enyzmes italicized, COMT1 enzyme is highlighted in red. *Adapted from Huotari et.al., 2001*.

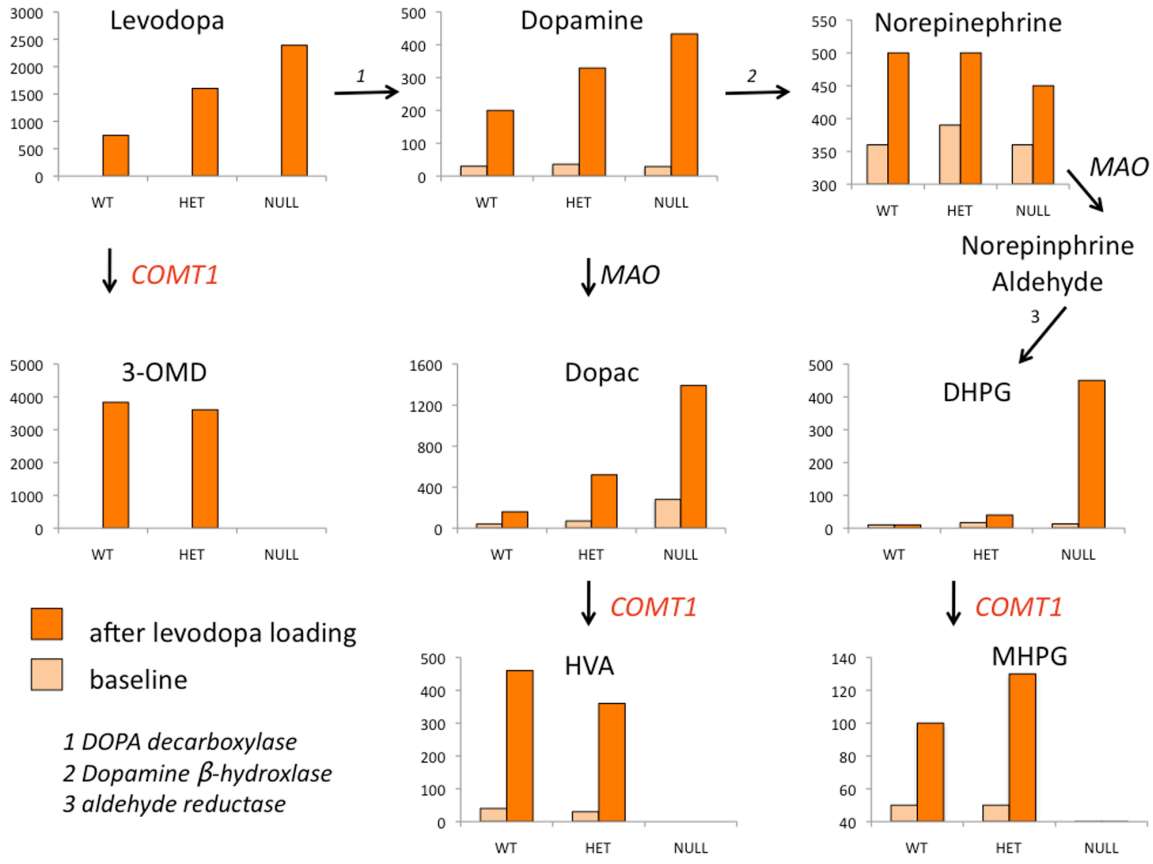

Figure 1.6 Comparison of male COMT1 activity before and after stress in two haplotypes, six developmental time points, from adolescence to advanced age in mouse. Mice were caged singly one week prior to euthanasia. One set of mice were euthanized with no stress. The other set of mice were stressed by five minutes in the open field apparatus. Thirty minutes after the open field exposure, the second set was euthanized. N= 4-7 mice per time point and strain, mon = month. *Adapted from Eleftherou, 1975*

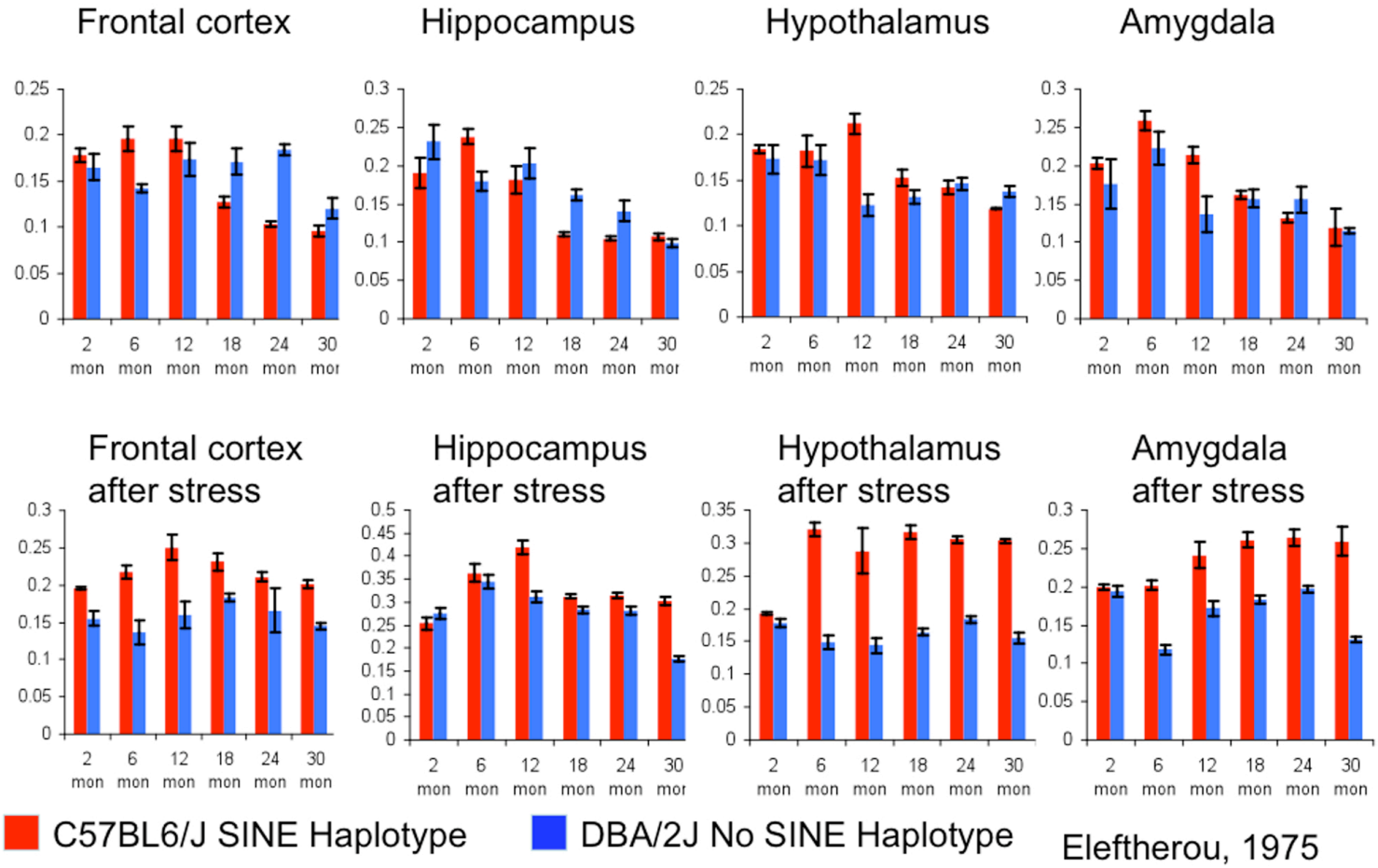

Figure 1.7 The COMT *val/met* polymorphism redefined by HPS/APS/LPS haploblocks. **a.** Haploblocks and frequency in a European population. **b.** The six haplotypes arranged by experimental pain sensitivity (note absence of *Z*-score pain data for rare HPS/HPS homozygotic women who did not complete pain study). *Adapted from Diatchenko et.al., 2005*

(a)

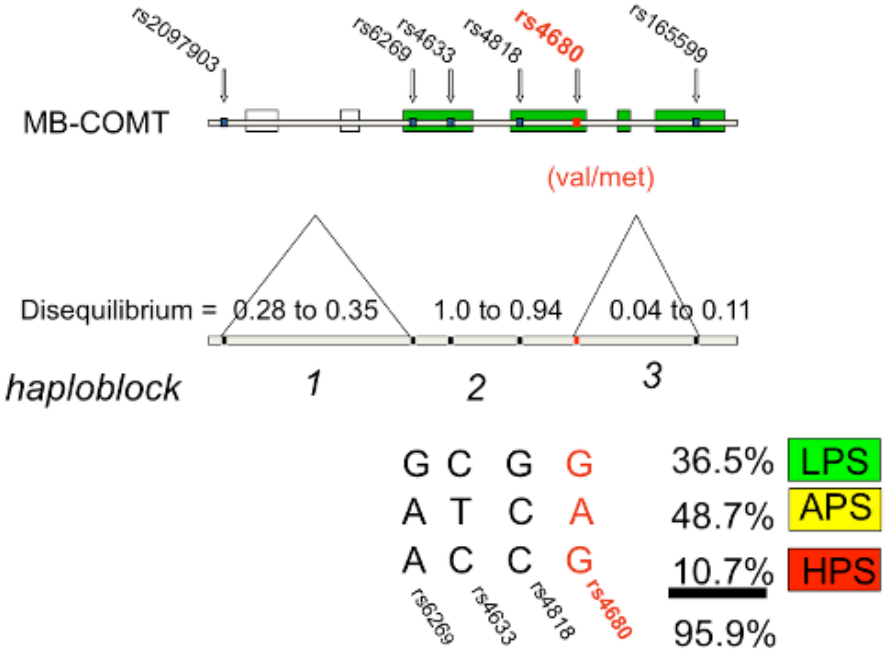

(b)

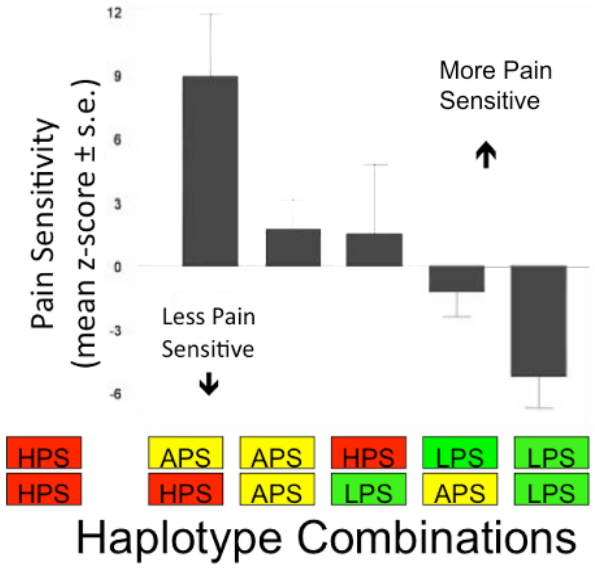

CHAPTER 2: *COMT1* GENOTYPE AND EXPRESSION PREDICTS ANXIETY AND NOCICPETIVE SENSITIVITY IN INBRED STRAINS OF MICE

SK Segall[1], AG Nackley[2], L Diatchenko[2] WR Lariviere[3], X Lu[4], JS Marron[4], L Grabowski-Boase[5], JR Walker[5], G Slade[2,6], J Gauthier[2], JS Bailey[7], BM Steffy[8], TM Maynard[9], LM Tarantino[7*], T Wiltshire[8*]

Curriculum of Genetics and Molecular Biology[1], Center for Neurosensory Disorders[2], Department of Statistics and Operations Research[4], Psychiatry[7], Department of Dental Ecology[6], Cell & Molecular Physiology[9], University of North Carolina School of Medicine, Chapel Hill, NC, USA, Eshelman School of Pharmacy[8] University of North Carolina, Chapel Hill, NC, USA

Department of Anesthesiology, University of Pittsburgh School of Medicine, Pittsburgh, PA, USA[3]

Genomics Institute of the Novartis Research Foundation, San Diego, CA[5]

[*]corresponding authors

ABSTRACT

Catechol-O-methyltransferase (COMT) is an ubiquitously expressed enzyme that maintains basic biologic functions by inactivating catechol substrates. In humans, polymorphic variance at the *COMT* locus has been associated with modulation of pain sensitivity (Andersen & Skorpen, 2009) and risk for developing psychiatric disorders (Harrison & Tunbridge, 2008). A functional

haplotype associated with increased pain sensitivity was shown to result in decreased COMT activity by altering mRNA secondary structure-dependent protein translation (Nackley *et al.*, 2006). However, the exact mechanisms whereby COMT modulates pain sensitivity and behavior remain unclear and can be further studied in animal models. We have assessed *Comt1* gene expression levels in multiple brain regions in inbred strains of mice and have discovered that *Comt1* is differentially expressed among the strains, and this differential expression is cis-regulated. A B2 Short Interspersed Element (SINE) was inserted in the 3'UTR of *Comt1* in 14 strains generating a common haplotype that correlates with gene expression. Experiments using mammalian expression vectors of full-length cDNA clones with and without the SINE element demonstrate that strains with the SINE haplotype (+SINE) have greater *Comt1* enzymatic activity. +SINE mice also exhibit behavioral differences in anxiety assays and decreased pain sensitivity. These results suggest that a haplotype, defined by a 3'UTR B2 SINE element, regulates *Comt1* expression and some mouse behaviors.

INTRODUCTION

Dysregulation of catecholamine signaling has been linked to a variety of neuropsychiatric disorders (reviewed by Harrison & Tunbridge, 2008, Lachman, 2008). The *COMT* gene encodes an enzyme of the same name and functions to eliminate catecholamines. The COMT enzyme catalyzes the transfer of a methyl group from S-adenosyl-L-methionine to one of the hydroxyls on a catechol structure (Axelrod & Tomchick, 1958) leading to catecholamine inactivation.

Catecholamines such as epinephrine and norepinephrine prepare an organism for immediate action in response to a perceived threat (the fight-or-flight response) and both physiological and psychological stressors induce the release of catecholamines (Guyton, 1991). Altered COMT enzymatic activity has been linked to disproportionate anxiety responses (Domschke *et al.*, 2007, Evans *et al.*, 2009, Pooley *et al.*, 2007), differences in pain perception (Diatchenko *et al.*, 2005, Emin Erdal *et al.*, 2001, Zubieta *et al.*, 2003) and Attention Deficit Hyperactivity Disorder (ADHD), (Deyoung *et al.*, 2010, Palmason *et al.*, 2009, Qian *et al.*, 2003) in humans.

COMT is highly conserved between mouse and human, with nearly 80% amino acid homology. Several *Comt1* mouse models have been developed. A knockout of the mouse gene, *Comt1* (Gogos *et al.*, 1998) and a transgenic line expressing human *COMT* (Papaleo *et al.*, 2008) were engineered to provide a model for understanding catecholamine processing. Experiments with the knockout and transgenic lines demonstrated that COMT activity affects stress and pain responses in a manner consistent with human studies. *Comt1* null and heterozygous mice have increased sensitivity to thermal nociception and increased stress reactivity (Papaleo *et al.*, 2008). Transgenic mice over-expressing the human gene have higher COMT enzymatic activity and a blunted thermal pain response (Papaleo *et al.*, 2008). Differences in catecholamine metabolism between C57BL/6J and DBA/2J mice has also been reported (Eleftheriou, 1975). This study found that COMT enzymatic activity varies with age and brain region and also with stress.

In the present study, we measured behavioral phenotypes and brain gene expression in 29 common inbred strains of mice. We use a method called Haplotype Association Mapping (HAM) (McClurg *et al.*, 2007, McClurg *et al.*, 2006, Pletcher *et al.*, 2004) to correlate genotypic differences with gene expression in an effort to identify regions of the genome, expression quantitative trait loci (eQTL), that contribute to inbred strain variation. This genome-wide analysis revealed *Comt1* to be differentially expressed among strains and cis-regulated. At least four haplotypes exist at the *Comt1* locus but the defining polymorphic feature is the presence of an insertion of a SINE element in the 3'UTR of the gene**.** The presence of this SINE element correlates with differential gene expression and an increase in enzymatic activity. Thus, the natural allelic variations that alter COMT1 protein levels or enzyme function, in common inbred strains of mice are of potential interest for behavioral studies.

MATERIALS AND METHODS

Animal Husbandry

All experiments conformed to the guidelines in the National Institutes of Health (NIH) Guide for the Care and Use of Laboratory Animals. Behavioral measurements and gene expression data were collected at the Genomics Institute of the Novartis Research Foundation (GNF) and all procedures were approved by the GNF Institutional Animal Care and Use Committee. Animals were housed in an SPF barrier colony and were maintained on a 12-h light: 12-h dark cycle, housed in groups of 2–4 in standard high efficiency particulate air-filtered polycarbonate mouse cages containing a layer of Bed-o-cob bedding and

one cotton nestlet. Food (Pico rodent chow 20; Purina, St Louis, MO, USA) and water were made available ad libitum. Animals used for q-PCR and ELISA experiments were housed under similar conditions as those described above and sacrificed according to guidelines set by the Institutional Animal Care and Use Committee (IACUC) at UNC Chapel Hill.

Inbred Strains

The 29 strains tested were: 129S1/SvImJ, A/J, AKR/J, BALB/cByJ, BTBR T+ tf/J, BUB/BnJ, C3H/HeJ, C57BL/6J, C57BR/cdJ, C58/J, CBA/J, CE/J, DBA/2J, FVB/NJ, I/LnJ, KK/HIJ, MA/MyJ, MRL/MpJ, NOD/LtJ, NON/LtJ, NZO/HILTJ, NZW/LacJ, P/J, PL/J, RIIIS/J, SJL/J, SM/J, SWR/J, and WSB/EiJ.

Behavioral Testing

Animals. Six to eight week old male and female mice of each strain were purchased from the Jackson Laboratory (Bar Harbor, ME, USA). The mice were habituated in quarantine for approximately 6 weeks until they were transferred to the main barrier colony. Mice were habituated to the main colony holding room for at least one week prior to behavioral testing. All behavioral testing was conducted during the light part of the light/dark cycle and occurred between the hours of 8:00AM – 12:00PM. On the day of testing, mice were transported to a quiet anteroom adjacent to the testing room and acclimated for at least one to two hours prior to the start of testing. All testing equipment was cleaned with a light bleach solution (0.1%) in between each animal. Mice were tested in two behavioral cohorts that each went through a separate series of tests. One group of mice were tested in the open field and a second group were tested on the

elevated plus maze and light/dark test. Mice were experimentally naïve for both open field and elevated plus maze testing. Animals tested in the light/dark assay had previously been tested in the elevated plus maze.

Open Field Assay (OF). The open field is a 17" × 17" × 13" arena with a white Plexiglas floor and clear Plexiglas walls (ENV-515-16; Med Associates, St Albans, VT, USA), which is surrounded by infrared detection beams on the x-, y- and z-axes that track the animals' position and activity over the course of the experiment. The apparatus is isolated within a 73.5 × 59 × 59 cm testing chamber fitted with overhead fluorescent lighting (lux level 14). Animals were removed from their home cage, immediately placed in the corner of the open field arena and allowed to freely explore the apparatus for a test interval of 10 min. Animals were scored for a number of behaviors in the open field, including total distance traveled (in cm), ambulatory episodes (number of times animal breaks user-defined number of beams before coming to rest), percent time resting, average velocity (in cm per second), number of rearings and percent time spent in the center of arena (defined as nine square-inch central part of arena). These data were recorded during testing and scored in post-session analyses using commercially available software (Activity Monitor 5.1, Med Associates). We have found in previous studies (Bailey *et al.*, 2008, Eisener-Dorman *et al.,* 2010) that factor analysis can reduce the data from the OF assay to two distinct classes of behaviors - activity-related behaviors and anxiety-related behaviors and rearing behavior represents a separate behavior. For subsequent analyses, we included only one representative behavior from each class in our analysis; total distance

(activity), percent time in the center (anxiety) and rearing behavior.

Elevated Plus Maze (EPM). The elevated plus maze (7001-0336; San Diego Instruments, San Diego, CA, USA) consists of two open arms and two closed arms [26.5" × 2.5"] that are directly opposing each other. The walls of the enclosed arms completely surround the end of the runway and are 6" high. The top of the enclosed arms is open to the testing room. The entire apparatus is 15" high and is placed on the floor for testing. A video camera above the maze captures the animal's location in the maze. Data is collected and analyzed with Actimetrics LimeLight software (Actimetrics, Wilmette, IL, USA). The animals are placed in the center of the maze and allowed to investigate the maze for 5 minutes. Data recorded include distance traveled in each region and percent time spent in the open arms of the maze.

Light/Dark Assay (LD). The light/dark enclosure (ENV-511; Med Associates) inserts into the Med-Associates open field apparatus and is a light-impermeable box that covers one third of the area of the open field. The dark box has a classic "mouse hole" entry for the animal to enter and exit the box. The animals were placed in the center of the open field directly in front of and facing the dark enclosure and allowed to explore the arena for ten minutes. Transitions between light and dark quadrants and time spent in each quadrant were assessed.

Gene Expression Studies

Tissue Collection. Eight to ten week old male and female mice of each strain were purchased from the Jackson Laboratory (Bar Harbor, ME, USA). The mice were habituated for one week prior to tissue collection. Mice were sacrificed by cervical dislocation without anesthesia to avoid gene expression differences in response to anesthetic. All dissections were conducted between the hours of 9:00AM to 11:30AM. Prefrontal cortex, amygdala, hypothalamus, hippocampus, nucleus accumbens, striatum and pituitary were dissected as follows: Immediately following euthanasia, mice were decapitated and the whole brain was removed from the skull. The hypothalamus was lifted from the ventral surface of the brain using curved forceps. The pituitary was lifted from the sella tursica in the base of the skull using microforceps. The brain was then transferred, ventral side up, to an ice-cold brain matrix with 0.5mm spacing (505C Braintree Scientific, Braintree, MA, USA). A single razor blade was placed into the first space on the brain matrix and the rostral surface of the brain was placed in the matrix and touching this blade. Thin, double-edged razor blades were placed in the twelve most anterior spaces. Following removal from the matrix, the 0.5 mm brain slices were placed flat onto an ice-cold dissection stage and specific regions dissected using anatomical landmarks as described below. The prefrontal cortex was taken from the slice corresponding to approximately 2.5 mm to 2.0 mm anterior to Bregma. To do so, a “V-shaped” wedge was made just medial to the corpus callosum with the apex terminating at about the lateral ventricle (viewed from the caudal side of the slice). Nucleus accumbens and striatum were taken from the adjacent slice approximately 2.0mm to 1.5mm

anterior to Bregma. To isolate nucleus accumbens, 1mm diameter punches were taken just ventromedial to the anterior commissure (AC). For striatum, 1mm diameter punches were taken dorsolateral to the AC, midway between the AC and corpus collosum, and lateral ventricle and corpus collosum. Amygdala was dissected from the slices corresponding to approximately 0.5mm to 1.5mm posterior to Bregma, ventromedial to the ventral boundary of the external capsule and directly below the caudate putamen. Hippocampus was dissected from slices at approximately 1.0mm to 2.0mm posterior to Bregma. The dissected regions included the following - Prefrontal cortex consists of the piriform cortex, secondary motor cortex, cingulate cortex area 1 and medial orbital cortex; nucleus accumbens consists of the anterior portion of the nucleus accumbens core and shell; striatum is a one mm diameter punch of striatum only; amygdala contains all amygdaloid nuclei plus 50% of the piriform cortex and the entire ventral endopiriform nucleus; hippocampus contains hippocampus only as it is easily peeled away from the surrounding tissue.

Gene expression analysis. After dissection tissues were immediately frozen on dry ice and stored in a -80^{o} C freezer until RNA preparation. Tissue was pulverized to a fine powder while frozen to obtain a mixture of homogeneous tissue. A small (~10mg) aliquot was homogenized using a rotor-stator (Omni TH polytron, Omni International, USA) homogenizer in Trizol (Invitrogen, Carlsbad, CA, USA) and total RNA purified with RNeasy columns (Qiagen, Valencia, CA, USA). RNA quality was tested using an Agilent Bioanalyzer (Santa Clara, CA, USA) and high quality RNA was pooled from three animals per strain to run one

microarray. Male and female samples were pooled separately and processed on separate microarrays. Gene expression analysis was performed according to standard procedures (Su *et al.*, 2004). RNA was amplified and labeled using the Affymetrix one-cycle target labeling kit. Samples were hybridized to Affymetrix GeneChip 430v2 whole-genome mouse arrays and data were processed using the gcRMA algorithm (Wu *et al.*, 2008). Raw data were deposited in GEO (http://ncbi.nih.gov/geo) under series accession GSE20160. In this study, data were filtered to remove probe sets whose expression was either undetectable (maximum expression across strains <200) or invariant across strains (ratio of maximum expression to minimum expression across strains). Although summarization algorithms are designed to be robust to single-probe outliers, the presence of SNPs in the probe sequence could theoretically lead to spurious detection of cis-eQTL. An analysis performed after removing all probes overlapping a SNP in dbSNP from the CDF file resulted in qualitatively similar results.

qPCR Validation of Affymetrix GeneChip array

Microarray data was validated by q-PCR in cDNA prepared from pituitary and cortex RNA from male animals. The first round of q-PCR used RNA remaining from the original samples prepared for the microarray. The sixteen strains (from 48 male animals) used in the first round of q-PCR validation were: BTBR T+ tf/J, C3H/HeJ, C57BL/6J, C57BR/cdJ, CBA/J, CE/J, KK/HlJ, MRL/MpJ, NOD/LtJ, NON/LtJ, NZO/HILTJ, NZW/LacJ, P/J, PL/J, RIIIS/J and SM/J. The most significant change in gene expression was validated by an ABI custom designed

Taqman assay in the 3'UTR interval (data not shown). The primer and probe sequences are: Forward primer $^{5'}$AAACCCCTCACGGTGAATCC$^{3'}$, Probe $^{5'}$TCTGCACCCAAGAACA$^{3'}$, Reverse primer $^{5'}$CATCTCACCAGTCCCCCTTTTT$^{3'}$, (Applied Biosystems Incorporated, Foster City, CA, USA). The second round of validation used cortex from four 10 week old males from strains AKR/J, BALB/cByJ, C3H/HeJ and SJL/J. The material was not pooled in the second q-PCR assay. Data was collected from sixteen individual animals, from each of four strains. Animals were housed and sacrificed as previously described. ABI TaqMAN probe Mm00514377_m1, which measures transcript in the coding region, was used for the cortex q-PCR.

Identification of B2 SINE element

BAC clone sequence for 129S6/SvEvTac (AC012399) and C57BL6/J (AC133487) was aligned with Sequencher software. A 234 bp insert was discovered in the 3'UTR. This sequence was run through Repeat Masker (http://www.repeatmasker.org), which identified it as a B2 SINE element. PCR primers flanking the region (forward primer $^{5'}$TTTCCTCAGGGCCTGTGGCT$^{3'}$ and reverse primer $^{5'}$GAGGCCATCAGGATGACACC$^{3'}$) were designed using publically available Primer3 software (http://frodo.wi.mit.edu/primer3/). PCR was performed on both DNA and cDNA. Liver and whole brain cDNA was sequenced and referenced against *Comt1 cDNA* transcript NM_001111063.1 in 129S1/SvImJ, BALB/cByJ, C57BL/6J, CBA/J and WSB/EiJ.

Development of COMT ELISA assay

COMT1 protein was measured from three pooled brain regions (two male

animals), determined by proximity: region HHA (hypothalamus, hippocampus and amygdala), region AS (nucleus accumbens and striatum) and region C (cortex). To detect the levels of COMT1 in brain lysates, the Meso Scale discovery (MSD) electrochemiluminescence (ECL) assay was performed using a MSD Sector Imager 2400 according to the manufacturer's protocol (Meso Scale Discovery, Gaithersburg, MD, USA). The MSD assay is based on a sandwich immunoassay that utilizes ECL to measure protein levels. Frozen brain regions were pulverized to a powder in liquid nitrogen. The pulverized tissue was mixed with RIPA buffer (Pierce, Thermo Fisher Scientific, Rockford, IL, USA, Cat. # PIH9901) and protease inhibitor cocktail (Pierce, Cat. # PI-78430) and were then centrifuged at 13,000 RPM for 30 min at 4 °C to obtain the supernatant. Coomassie Plus (Pierce, Cat. # PI-23200) assays were performed according to manufacturer's protocol to determine the protein concentrations in the lysates. 10 μl of primary antibody at a 1:100 concentration (Abcam, Cambridge, CA, USA Cat. #36144) was spotted in each well of a 96-well plate (MSD, Cat. # MA2400), and allowed to dry at room temperature overnight. The plate was incubated for 1 h with blocking buffer containing 3% bovine serum albumin at room temperature, then 25 mg/ml protein lysates in 50 μl lysis buffer were added to the ELISA plates. The plate was incubated at 4 °C overnight, and washed three times with 150 μl of the MSD wash buffer (50 mM Tris pH 7.5, 1.5 M NaCl, 0.2% Tween-20). 25 μl of the secondary antibody (Abcam, Cat. #51984), diluted 1:10 and labeled with the MSD SULFO-TAG detection antibody solution was added to the wells and the plates were incubated for 2 h at room temperature, while rocking. The plates

were again washed three times with the wash buffer and 150 μl of Buffer T from MSD was added to each well. The plates were analyzed with the SECTOR Imager 2400. ECL intensities obtained from the assay were normalized by the blank wells of the secondary antibody to the bovine serum albumin-coated spot with no lysate.

Enzymatic analysis of brain lysates

Sample preparation. Whole brains from two 10 week old males from strains 129S1/SvImJ, C3H/HeJ, C57BL/6J, C57BLKS/J, NZB/BINJ, NZW/LacJ, and PL/J were purchased from Jax Laboratories. Animals were killed by cervical dislocation, brains removed, frozen on dry ice, shipped, and thawed for our dissection of the frontal cortex. Tissue was pooled by strain, refrozen on dry ice, pulverized, and homogenized in 0.1mM CDTA (Sigma Chemical Company, St. Louis, MO, USA) with a 16 gauge syringe. A second round of experiments used non-pooled material from four 10 week old males from strains AKR/J, BALB/cByJ C3H/HeJ, and SJL/J. Animals were housed and sacrificed as previously described. Cortex was dissected from fresh tissue, and frozen on dry ice. Samples were then pulverized and homogenized in 0.1mM CDTA as for the first experiment. In both experiments, homogenized brain lysate was centrifuged at 2000g for 10 minutes and filtrate quantified with the Pierce BCA assay (Thermo Fisher Scientific, Rockford, IL, USA) in accordance with the manufacture's recommendation.

Enzymatic assay. COMT1 activity was assessed with the Normetanephrine ELISA kit (RE59171, IBL, Hamburg, Germany as described (Nackley &

Diatchenko 2010, Nackley *et al.*, 2006). In this method, a known amount of substrate, L-norepinephrine, is added to a biological lysate. The measure of COMT1 enzymatic activity is the amount of product, normetanephrine (NMN), produced in the reaction of lysate and added substrate. Briefly: after lysates were normalized to equal protein concentrations, 8 μl was incubated with 200μM S-adenosyl-L-methionine (SAMe; ICN Chemical, Aurora OH, USA), 7.5 mM L-norepinephrine (NE; Sigma Chemical Co.) and 2mM $MgCL_2$ in 50mM phosphate buffered saline for 1 hr at 37 C°, final volume 21μl. The reaction was terminated using 20μl of 0.4M hydrochloric acid and 1μl of 330 mM EDTA. 10μl of the halted reaction mixture was then used in the Normetanephrine ELISA kit in accordance with the manufacture's recommendation. Lysates from cortex regions of brains in four strains of the -SINE haplotype and 6 strains of the +SINE haplotype were assayed for COMT1 enzymatic activity. Four technical replicates were conducted per animal or per strain in two separate experiments. C3H/HeJ was run in both experiments and data were normalized to C3H/HeJ COMT1 activity.

Cell Construct. A *Comt1* cDNA clone in expression vector pCMV-SPORT6 was purchased from the I.M.A.G.E. Consortium (ATCC, Manassas, VA, USA, clone ID 4210097). The clone contained the full length 5'UTR and aligned to the *Comt1* NM_001111063 transcript. The full length 3'UTR was not present in the clone. To construct the +SINE and -SINE expression vectors, the truncated 3'UTR was excised by a double digestion of *Not1* and *Bsu36I.* Primers to genomic DNA were designed flanking the 3'UTR genomic region to be ligated into the double digested expression construct. The 5' primer was 5' of the *Bsu36I*

cut site, and the 3' primer had a *Not1* linker 3' of the sequence aligning to genomic sequence. C57BL6/J and WSB/J genomic DNA was PCR amplified for the 3'UTR, resulting in +SINE and -SINE 3'UTR fragment. The amplimer was double digested with *Not1* and *Bsu36I*, gel purified, and ligated into the double digested expression vector. Clones were verified by sequencing the entire insert in both directions.

Transient transfection of* Comt1 *cDNA clones. This transfection assay has been previously described (Nackley *et al.*, 2007). A rat pheochromocytoma cell line (PC12) was transiently transfected in 35-mm six well plates using FuGENE 6 Transfection Reagent (Roche, Indianapolis, IN, USA) according to manufacturer's recommendations. The amount of +SINE or -SINE construct was at a concentration of 0.9 μg/ml of media. To account for transfection efficiency, pSV-βGalactosidase vector (Promega, Madison, WI, USA) was co-transfected at 0.1 μg/ml of media. Transfection with empty vector was done for each experiment. Cell lysates were collected approximately 24 hours post-transfection.

Enzymatic analysis of cell constructs

Sample preparation and assay. After removing media, cells were washed once with ice cold 0.9% saline solution (1ml/35 mm well), and collected by scraping the wells (on ice) with 150μl/well of ice cold 0.1mM CDTA. The lysate was collected in 1.8 ml tubes and freeze/thawed (-80 C°/RT) twice. The tubes were centrifuged at 2000g for 10 min and filtrate removed. Filtrate was quantified with the Pierce BCA assay in accordance with the manufacture's recommendation and lysates normalized. The Normetanephrine ELISA kit was

also used for the cell constructs, in the same manner as for brain lysates. COMT1 activity was determined after subtracting the amount of NMN produced by endogenous enzymatic assay (transfection with empty vector). COMT1 activity was then normalized for transfection efficiency by measuring the β-galactosidase activity for each lysate. β-galactosidase activity was determined by incubating 50μg of normalized lysate with 2X β-galactosidase buffer (39.3 mM $NaH_2PO_4 \bullet H_2O$, 154.84 mM Na_2HPO_4, 4.3 mM $MgCl_2$, 4.45 mM O-Nitrophenyl β-D-galactopyranoside, 12.mM β-mercaptoethanol) in a 100μl reaction for 30 minutes at 37 C°. The lysates were then read with a luminometer at 405nM filter. The read for blank, 50μl 0.1mM CDTA and 50μl 2X β-galactosidase buffer, was subtracted from each lysate.

Statistical Analysis

***Genome-wide eQTL mapping*.** The detailed algorithm underlying the Haplotype Association Mapping (HAM) method has been previously described (McClurg *et al.*, 2007, McClurg *et al.*, 2006, Pletcher *et al.*, 2004). Briefly, HAM uses ANOVA to calculate the strength of genetic associations between an input phenotype and the ancestral haplotype structure (as inferred using a local window of three adjacent SNP alleles across the genome). A weighted bootstrap method was introduced to detect association peaks conditional on the population structure in the mouse diversity panel. At each genetic locus, the association score was represented as the negative log10-transformed P value. A score of – LogP=6 is a maximal score resultant from 10^6 permutations performed at each locus. This score is not corrected for genome-wide significance. HAM analysis

was performed for *Comt1*, across 29 strains using the web-based analysis SNPster (http://snpster.gnf.org/cgi-bin/snpster_ext.cgi) with the expression phenotype transformed to log scale. The genomic mapping of all genes and SNPs was based on Mouse Genome NCBI Build 35 (mm7).

Analysis of B2 SINE element and* Comt1 *mRNA expression and enzymatic activity. *Comt1* mRNA expression data (Affymetrix 430v2 probe set 1449183_at) was analyzed in seven brain regions using analysis of variance (ANOVA) (SPSS, v.16 for Mac, Chicago, IL USA) with sex and SINE status as independent variables.

Replicate enzymatic assays were performed and C3H/HeJ was included in all replicates. COMT1 enzymatic data were normalized to C3H/HeJ. An independent t-test (SPSS) was performed to determine differences in enzymatic activity between +SINE and -SINE strains.

Analysis of behavioral data. A total of 744 mice (355 females from 32 strains and 389 males from 31 strains) were tested in the OF assay and 223 mice (113 female and 110 males from 24 strains each) were tested in both the EPM and the LD assays as described above. Fifty-one percent of the mice tested in the OF were -SINE and forty-nine percent were +SINE. Thirty-nine percent of the mice tested in the EPM and LD assays were –SINE and sixty-one percent were +SINE. The complete data set is available on (http://www.jax.org/phenome; Project: MPD: 214). The analyses described below were conducted on the behavioral data from individual mice. However, for those results that showed significance with individual test scores we also conducted the analysis using

inbred strain means to avoid potential strain bias of uneven numbers of animals between strains. Only results that support significance by strain means as well as with individual behavioral scores were considered to have significant genotype-phenotype associations. Strain mean data and numbers of animals tested for each phenotype is listed in Table 2.4.

We used multivariate analysis to account for large numbers of data vectors (Marron, 2007). This methodology allows us to test the single hypothesis that mice with the +SINE haplotype are behaviorally different from -SINE mice. All of the behavioral data from both cohorts of mice were used in single analyses in both male and female mice. This technique does not assign a *P-value* to individual behavioral assays, and contributions from each behavioral assay are visualized by distance weighted discrimination (DWD) plots. After the data is plotted, hypothesis testing then confirms the impressions gained from the visualization of the data. This can be done without the loss of information entailed by classical dimensionality reduction, using a Direction Projection Permutation hypothesis test (DiProPerm) (Benito *et al.*, 2004, Hu *et al.*, 2006, Marron, 2007).

DWD focuses on two-class discrimination in multi-dimensional space formed by the data. The objective is to find a direction, a loading vector, which best separates the two classes. The variables are the 11 behavioral test scores for all of the individual animals. The length of a bar corresponds to the importance in separating the two classes and a positive loading value indicates that the -SINE haplotype tends to have a higher level of the corresponding variable than the

+SINE haplotype, while the negative loading value means the opposite.

The second step projects all behavioral test scores from the +SINE and -SINE haplotypes in a DWD direction to obtain a pair-wise t-statistic. The data projection plots a cloud of data points from each of the two classes, with the Gaussian distribution of both classes under the data points. The Gaussian distribution of all data points is represented above the two curves of +SINE and -SINE Gaussian distribution. A pair-wise t-statistic was then obtained.

The DiProPerm test is used to assess the significance of the t-statistic. All of the data from each behavioral test and each mouse was randomly re-labeled into two classes. This permutation was performed 100 times, and each time there was a new t-statistic. The empirical p-value corresponds to the proportion of the t-statistics of the permutated data at or above the t-statistic (http://www.stat.colostate.edu/~chihoon/FDA_ratPMdata.pdf).

Genetic Correlation Analysis with Nociception Assays. To determine if the absence of the SINE element is genetically related to sensitivity in pain models of several fundamental nociceptive modalities, *Comt1* SINE status was compared to sensitivity in 22 nociception and hypersensitivity assays previously collected in twelve inbred mouse strains. Six of the strains had the SINE element: A/J, AKR/J, BALB/cJ, C57BL/6J, C57BL/10J and SM/J. Six of the strains did not: 129P3/J, C3H/HeJ, C58/J, CBA/J, DBA/2J and RIIIS/J. Brief descriptions of the assays are found in Table 2.3, with greater detail available on The Jackson Laboratory's Mouse Phenome Database website (http://www.jax.org/phenome) and in the original reports (Lariviere *et al.*, 2002, Mogil *et al.*, 1999a, Mogil *et al.*,

1999b). Multivariate statistical analyses were used as previously described (Lariviere *et al.*, 2002) to simultaneously assess the genetic correlations between absence of the SINE element in standard inbred strains and their sensitivity in: six inflammatory, six thermal and one mechanical nociception assay; one mechanical sensitivity assay; and eight mechanical, thermal and afferent-dependent hypersensitivity assays (see Table 2.3). Pearson product-moment correlation coefficients were calculated between the strain means for each assay and the SINE status of the strain, with 1 = absence and 0 = presence due to the expectation of a negative correlation with pain sensitivity, and with strain means corrected by multiplication by -1 so that higher numbers indicated greater sensitivity. As such, a positive correlation indicates that absence of the SINE element is observed in strains more sensitive in the particular assay. Multidimensional scaling (MDS) and principal components analysis (PCA) were used to visualize all pairwise correlations simultaneously (Systat 13, Chicago, IL, USA). Briefly, in MDS, coordinates in two-dimensional space are reiteratively computed for a set of points representing SINE status and the assays to fit as closely as possible the measured similarities of Pearson correlations using a Kruskal loss function with monotonic regression. High positive correlations are represented as small distances between points, and high negative correlations are represented as large distances between points. Uncorrelated points have intermediate distances between them. In PCA, two linear combinations of the points are constructed, and the weights of the linear combinations are plotted in a two-dimensional space to produce a vector for each point. Highly positively

correlated points are represented with vectors with angles close to 0° between them, and high negative correlations as angles close to 180° between vectors. The results can also be viewed in three dimensions to determine if the same groupings are observed as in the two-dimensional representation.

RESULTS

Expression QTL (eQTL) analysis of microarray data reveals cis-regulation of Comt1

The use of gene expression as a quantitative phenotype for SNP haplotype mapping allows for identification of genomic regions that control gene expression (eQTL). The correlation of differential gene expression for a specific gene with the haplotype pattern at its own chromosomal location indicates that the gene is cis-regulated - meaning that a difference at or near the gene influences its expression. *Comt1* gene expression (intensity scores) for all strains was used as a quantitative phenotype for haplotype association mapping analysis. A genome-wide association plot for *Comt1* gene expression from pituitary (Affymetrix probeset 1418701_at) using the SNPster algorithm shows an eQTL peak with a -LogP score of 6 on chromosome 16 (Figure 2.1a) near the physical location of the *Comt1* gene, indicating that *Comt1* is cis-regulated. Analyses of Comt1 expression for other brain regions, (nucleus accumbens, cortex, hippocampus, amygdala and striatum) also demonstrate cis-regulation (data not shown).

More detailed investigation of the Chr 16 region identified only 6 SNPs that define the 2.5MB haplotype interval immediately surrounding *Comt1* (Figure 2.1b). The other SNPs in the interval that show no association are non-

informative for the strains included here. The genomic location of each SNP is indicated with its association score on the Y-axis. The SNP with the maximal -LogP score of 6, rs4165252, is at genomic location 20650976. We sequenced coding regions of *Comt1* in brain and liver cDNA in several +SINE and -SINE strains and did not discover new SNPs, confirming earlier reports of identity by descent (IBD) in this region (Yang *et al.*, 2007). HAM analysis uses a 3 SNP window to define haplotypes and for the surveyed strains, there were three distinct haplotypes in this SNP position: AGT, AAC, and AAT (Figure 2.1c). We did not include the wild-derived strains CZECHII/EiJ, CAST/EiJ, MOLF/EiJ or PWD/PhJ in the original survey, but note: these strains exhibit an additional haplotype at this position, GGC.

A B2 SINE element defines haplotype

We discovered the SINE insertion by aligning BAC clone sequence from 129/SvEvTac with C57BL6/J. C57BL6/J had an insertion of roughly 240 bp in the 3'UTR. RepeatMasker identified the inserted sequence as a B2 SINE element (http://www.repeatmasker.org). Although we found no other polymorphisms within *Comt1*, the HAM analysis pointed us toward this insertion as the cis-element contributing to regulation of *Comt1.*

A PCR to detect the presence or absence of the SINE element was developed to assess the status of the insertion among mouse strains (Figure 2.1d and e). Almost all of the -SINE strains are haplotype AGT, and almost all of the +SINE strains are haplotype AAT, except for A/J, PL/J, and SM/J. We included a single 129 strain, 129S1/SvImJ in our analysis, but included

129X1/SvJ in our SINE element PCR assay. Although both these 129 sub-strains have the haplotype that exhibit -SINE, these two strains are +SINE. We examined a third 129 strain, 129P3/J, and found this 129 parental strain to be a -SINE strain; 129/SvEvTac, is also a -SINE strain (data not shown).

Expression QTL (eQTL) analysis of microarray data reveals significant effect of SINE haplotype on Comt1 expression

ANOVA identified a significant main effect of both SINE element status and sex for all brain regions examined. Overall, +SINE strains had higher *Comt1* expression and males showed higher expression levels than females (see Table 2.1). A significant SINE by sex interaction effect was also observed for expression levels in the nucleus accumbens ($F_{(1,55)}$=24.4;P<0.0001), prefrontal cortex ($F_{(1,57)}$=8.2;P<0.01), amygdala ($F_{(1,57)}$=18.0;P<0.0001) and striatum ($F_{(1,51)}$=9.9;P<0.01). Posthoc analyses indicate that female mice show increased *Comt1* expression in the striatum and +SINE females have slightly lower *Comt1* expression in the nucleus accumbens in contrast to males (Table 1).

Validation of array data

Typical microarray data is shown for cortex and nucleus accumbens (Figure 2.2). To validate results from the microarray data we developed TaqMAN assays. qPCR of cortex cDNA replicated the array findings (Figure 2.3 a, P<0.01). In 10-week old male mice, the average increase in *Comt1* mRNA is approximately 20% across the surveyed strains. Resultant from increased mRNA presence we expected to find an increase in COMT1 protein levels and developed an ELISA assay to ascertain protein levels. However, we could not show differences

observed in COMT1 protein levels in prefrontal cortex were significant for the strains surveyed (Figure 2.3b).

Comt1 *Enzymatic Activity is higher in brain lysates and cell constructs*

In the absence of determining robust differences in COMT1 protein levels among the strains we investigated whether there was any change in enzymatic activity. We examined this in both *in-vivo* and *in-vitro* assays. The +SINE strains had an average of 20% more activity, mirroring gene expression profiles ($t(8)=-4.4$; $P<0.01$; Figure 2.3c). To validate the hypothesis that the presence of the SINE element was driving the increase in activity, we constructed full-length (cDNA) *Comt1* clones of the NM_001111063 transcript with and without the B2 SINE element. Rat adrenal (PC-12) cells were transiently transfected with each construct. COMT1 enzymatic activity was measured and found to be 5-fold greater in +SINE transcripts (Figure 2.3d).

SINE haplotype has an effect on anxiety and exploratory phenotypes

The DiProPerm analysis showed that +SINE strains have a significantly different behavioral profile than the -SINE strains. Four behaviors had a significant effect in separating the two classes. These were open field rearing and total distance, percent time in the light side of the light/dark arena and total distance in the elevated plus maze (Figure 2.4a). The results were similar for both male and female mice. When viewed in the distance-weighted discrimination (DWD) loading plot, the length of the bar corresponds to its contribution in discriminating between the two haplotypes. A positive loading

value indicates that the -SINE mice have an increased measure of the behavior than the +SINE mice and a negative loading value means the opposite. Based on the DWD results, -SINE mice rear more in the open field assay and spend more time in the lighted area of the LD assay and +SINE mice exhibit greater locomotion in the elevated plus maze and open field. All behavioral data from the DWD loading plot for all strains were plotted on a data projection plot (Figure 2.4b) and this clearly shows discrimination between the absence (black) or presence (grey) of the SINE insertion. The DiProPerm analysis assessed the significance of the t-statistic by a permutation test and found it to be highly significant in both female and male mice (Figure 2.4c and Table 2.2). When individual behavioral tests are analyzed the elevated plus maze contributes a significant effect to the DWD loading plot for males only.

When strain means, rather than individual scores, for combined tests were analyzed, distance in the elevated plus maze was no longer significantly different in +SINE vs –SINE mice. Open field distance and rearing were significant in females ($t=2.6;P<0.05$) but only exhibited borderline significance in males ($t=2.3$; $P=0.07$). Percent time spent in the lighted area of the LD assay was significant in both males ($t=2.2;P<0.05$) and females ($t=2.2;P<0.05$).

Strains without the SINE insertion are more sensitive to spontaneous inflammatory nociception.

Strains without the SINE insertion are more sensitive to spontaneous inflammatory nociception. Absence of the SINE insertion is positively and significantly correlated with increased pain sensitivity of inbred strains of mice in

spontaneous inflammatory nociception assays. These include assays of subcutaneous injection of the inflammatory irritants bee venom, capsaicin or formalin to evoke paw licking, and intraperitoneal injection of acetic acid or magnesium sulfate to evoke abdominal constrictions or writhes (see Table 2.3 for statistical significance; (Lariviere *et al.*, 2002 for more details of the assays) for more details of the assays). Thermal nociception was also positively and significantly correlated with absence of the SINE haplotype in two of six assays, with the majority of assays showing no relation to SINE haplotype (Table 2.3). There was no consistent relationship of SINE haplotype with mechanical sensation or nociception in the von Frey and tail clip tests, respectively, or with a range of hypersensitivity assays tested with thermal or mechanical stimuli including hypersensitivity evoked by inflammatory irritants or nerve injury (Table 2.3). Multivariate analyses and the MDS and PCA plots in Figure 2.5 confirm these individual findings and demonstrate graphically that absence of SINE haplotype is most genetically related to increased sensitivity to spontaneous inflammatory nociception. Note that the clustering of SINE status with spontaneous inflammatory nociception assays in the PCA plot was preserved when viewed in three dimensions (with 0.65 of the total variation accounted for), and more closely matched the correlations reported in Table 2.3 (e.g. strong correlation of absence of SINE element with Hargreaves' test of thermal nociception).

DISCUSSION

Commonly used inbred strains of mice exhibit broad phenotypic and

genotypic variation. We measured behavioral phenotypes and gene expression variation across 29 inbred mouse strains and identified *Comt1* as being one of a number of genes that exhibit differential expression among inbred strains of mice. A cis-regulated pattern of gene expression was observed for all brain regions we examined. We have linked this gene expression difference to the insertion of a B2 SINE element in the 3'UTR of the gene such that mice with an insertion of the SINE element show increased expression and increased COMT1 enzymatic activity. Using a distance-weighted discrimination technique, we identified four behavioral phenotypes that contributed most strongly to discrimination of the status of the *Comt1* haplotype. Our results indicate that mouse strains with the SINE element display increased locomotor activity, decreased rearing behavior and exhibit an increased anxiety response in the light/dark assay.

The SINE element insertion is a recent event in inbred strains

The use of gene expression data as a quantitative trait has been successful for identification of eQTL (Chen *et al.*, 2008, Wu *et al.*, 2008). The actual polymorphism responsible for cis-regulation of gene expression, however, can often be difficult to identify. In mouse, *Comt1* is located in a genomic region for which most strains share common haplotypes. We identified very few polymorphisms in the *Comt1* region within the common inbred strains (6 SNPs within 2.5 Mb). More extensive resequencing data (Frazer *et al.*, 2007) shows polymorphic variance only for wild-derived inbred strains and a similar pattern of two major haplotypes for laboratory inbred strains. *Comt1* itself exhibits no

coding sequence polymorphisms. In an attempt to identify non-coding regulatory polymorphisms we aligned sequence from BACs of two strains that were in different inferred haplotypes (C57BL/6J, 129/SvEvTac). A SINE element was discovered in the 3'UTR of *Comt1*. The SINE element insertion is likely to be of recent origin within the inbred strains as it is not found in wild-derived strains and it is not present in all C57 or 129-derived strains.

Insertion of a B2 SINE element increases COMT1 enzymatic activity

Since *Comt1* mRNA expression correlated to the presence or absence of the SINE insertion we predicted that we would detect concomitant changes in COMT1 protein levels. Our data did not reveal that protein levels correlated in a robust and consistent manner with SINE element status and although this could be due to secondary compensatory mechanisms it is more likely resultant from assay variability. However, our cell-based studies established that the presence of the SINE element does impact enzyme activity levels. It is not clear how a SINE element insertion can functionally cause a variation in the amount of measurable (mRNA) *Comt1* and how this translates to variable enzyme activity and changes in protein levels. It is plausible that insertion of this SINE element affects mRNA secondary structure leading to alteration in mRNA degradation rate and protein folding. Protein folding may in turn affect protein stability, enzymatic activity or post-translational modification efficiency. Recently, the COMT enzyme has been shown to be phosphorylated and N-acetylated in rats (Overbye & Seglen, 2009) indicating that post-translational alterations of the protein are also important and might be more mechanistically relevant

considering the requirement for rapid action of COMT1 for catecholamine modulation. The exact mechanism by which the SINE element alters COMT1 enzymatic function will require further investigation.

Behavioral effects of COMT enzymatic activity in inbred strains

The COMT protein is involved in catecholamine regulation, a pathway that has been implicated in behavioral function in both humans and animal models. Human COMT has been implicated in phenotypes related to pain, stress, anxiety and ADHD (reviewed by (Andersen & Skorpen, 2009, Harrison & Tunbridge, 2008, Lachman, 2008). In humans, a non-synonymous G→A base pair substitution results in a valine→methionine substitution at position 158. The Met^{158} amino acid substitution results in a less active form of the enzyme (Chen *et al.*, 2004) thereby resulting in higher brain concentrations of dopamine. Presence of the Met^{158} allele of *COMT* has been associated with poor emotional regulation for anxiety-related traits (Domschke *et al.*, 2004, Enoch *et al.*, 2003) and low sensation seeking (Stein *et al.*, 2005). However, it should be noted that the role of COMT in these behaviors in humans has not been consistent across all studies.

Animal models have also been useful for studying the role of COMT on behavior. Examination of *Comt1* knockout (KO) and transgenic (Tg) mice has addressed anxiety-related behaviors. Female *Comt1* KO mice show increased anxiety as measured by latency to emerge from the dark quadrant in the light/dark assay (Gogos *et al.*, 1998) and Tg mice carrying the human Val^{158}

allele exhibit decreased anxiety in the elevated plus maze (Papaleo *et al.*, 2008). The results from these animal studies concur with human studies linking increased enzymatic activity to decreased anxiety.

Based on the data observed in humans and animal models, one would expect that +SINE mice that have increased enzymatic activity, would exhibit decreased anxiety rather than increased anxiety as indicated by the observation that +SINE mice spend less time in the lighted quadrant of the light/dark arena in comparison with -SINE mice. However, +SINE mice also exhibit increased locomotor activation in a novel environment (the open field) and increased locomotion in response to novelty is believed to reflect decreased anxiety or emotionality (Fujita *et al.*, 1994, Kabbaj *et al.*, 2000). This theory is supported by the observation that some anxiolytics, particularly benzodiazepines like diazepam and chlordiazepoxide at moderate doses, increase locomotor activity in anxiety-related assays in mice (Choleris *et al.*, 2001, Vlainic & Pericic, 2009). Interestingly, female *Comt1* KO mice also display significantly less ambulatory activity than wild-type animals in the lighted quadrant of the light/dark arena (Gogos *et al.*, 1998) although we did not observe this difference among the inbred strains. The observation of increased locomotor response to novelty in +SINE mouse strains does seem to concur with the human observation that increased COMT enzymatic activity is associated with decreased anxiety. The seemingly disparate results from two behavioral measures of anxiety may not be surprising since different anxiety assays often do not correlate and may measure different components of anxiety-related behavior (Lister, 1990).

Exploratory activity in novel environments has also been described as an animal model for novelty seeking (Piazza *et al.*, 1989). Novelty and sensation seeking traits are correlated in human studies (McCourt *et al.*, 1993). A decrease in novelty-induced locomotion in mice with decreased COMT1 enzymatic activity corresponds with human studies that link the Met^{158} allele of COMT with a decrease in sensation-seeking behavior (Lang *et al.*, 2007, Stein *et al.*, 2005).

+SINE mice also exhibit decreased rearing behavior in the open field. Rearing behavior in a novel environment has been described as both a measure of exploratory behavior and an indicator of anxiety (Crusio *et al.*, 1989a, Crusio *et al.*, 1989b). However, previous studies in our laboratory and by others indicate that rearing behavior might also represent a distinct class of movements based on the lack of correlation between rearing behavior and anxiety- and locomotor-related behavior in common rodent tests for anxiety (Bailey *et al.*, 2008, Fernandez, 1997, Henderson *et al.*, 2004). Various studies have reported that anxiolytics cause a decrease (Crabbe *et al.*, 1998, Fahey *et al.*, 2001, Gray & McNaughton, 2000, Hughes, 1993, McNaughton, 1985), an increase (Crabbe *et al.*, 1998) or have no effect on rearing (Choleris *et al.*, 2001, Czech *et al.*, 2003). Some of these differences may reflect differences in the animal model (rat vs. mice), anxiolytic, dose or behavioral assay. Based on studies that have shown a decrease in rearing behavior in response to anxiolytics, one might hypothesize that the decrease in rearing behavior observed in the +SINE mice is also a reflection of decreased anxiety. However, until the neurobiological and

neurochemical mechanisms that govern rearing behavior and anxiety are more fully understood, such an interpretation is conjecture at this point.

Relevance of the SINE element to pain sensitivity.

In humans, lower levels of COMT activity have been linked to heightened pain perception (Diatchenko *et al.*, 2006a, Diatchenko *et al.*, 2005). *Comt1* KO mice also exhibit increased pain sensitivity (Papaleo *et al.*, 2008) and *Tg* mice carrying the human Val^{158} allele are more resistant to pain. The results of our study are consistent with decreased pain sensitivity in inbred strains with increased COMT activity. Previous reports in both rodents and humans show a stronger relationship of *COMT* genotype with noxious thermal stimuli over pressure stimuli (Diatchenko *et al.*, 2006b) which is consistent with our results indicating a stronger positive association with sensitivity in several thermal nociception assays but not with mechanical nociception. However, in the current study the strongest relationship between *Comt1* genotype was with inflammatory nociception – an assay that has not been assessed with regard to COMT activity in humans. This novel finding suggests specific relationship of *Comt1* genotype with the immediate effects of and spontaneous responses to nociceptive inflammatory insults, but not with the more prolonged consequences of inflammation- or nerve injury-induced hypersensitivity (Table 2.3). It is currently unknown how this specificity arises, but because *COMT* genotype differences are likely to be mediated via β-2 and β--3 adrenergic receptors, a stronger positive association with sensitivity in several thermal nociception assays but not with mechanical nociception (Nackley *et al.*, 2007) is consistent with our results.

Specific hypotheses regarding heritable differences in the effects of modulation of adrenergic receptor activity and relative specificity for inflammatory pain over other pain types should be tested in both humans and animal models.

Acknowledgements. This work is funded by a grant from the NIMH, 1R01MH077251. Gene expression analysis was provided by The Genomics Institute of the Novartis Research Foundation.

Notes: This manuscript was submitted January 17, 2010; accepted July 19, 2010, and will be published in *Genes, Brain and Behavior.* Electronic publication is ahead of print; article currently available online through PubMed.

References

Andersen, S. & Skorpen, F. (2009) Variation in the COMT gene: implications for pain perception and pain treatment. *Pharmacogenomics,* **10,** 669-684.

Axelrod, J. & Tomchick, R. (1958) Enzymatic O-methylation of epinephrine and other catechols. *J Biol Chem,* **233,** 702-705.

Bailey, J.S., Grabowski-Boase, L., Steffy, B.M., Wiltshire, T., Churchill, G.A. & Tarantino, L.M. (2008) Identification of QTL for locomotor activation and anxiety using closely-related inbred strains. *Genes Brain Behav*.

Benito, M., Parker, J., Du, Q., Wu, J., Xiang, D., Perou, C.M. & Marron, J.S. (2004) Adjustment of systematic microarray data biases. *Bioinformatics,* **20,** 105-114.

Chen, J., Lipska, B.K., Halim, N., Ma, Q.D., Matsumoto, M., Melhem, S., Kolachana, B.S., Hyde, T.M., Herman, M.M., Apud, J., Egan, M.F., Kleinman, J.E. & Weinberger, D.R. (2004) Functional analysis of genetic variation in catechol-O-methyltransferase (COMT): effects on mRNA, protein, and enzyme activity in postmortem human brain. *Am J Hum Genet,* **75,** 807-821.

Chen, Y., Zhu, J., Lum, P.Y., Yang, X., Pinto, S., MacNeil, D.J., Zhang, C., Lamb, J., Edwards, S., Sieberts, S.K., Leonardson, A., Castellini, L.W., Wang, S., Champy, M.F., Zhang, B., Emilsson, V., Doss, S., Ghazalpour, A., Horvath, S., Drake, T.A., Lusis, A.J. & Schadt, E.E. (2008) Variations in DNA elucidate molecular networks that cause disease. *Nature,* **452,** 429-435.

Choleris, E., Thomas, A.W., Kavaliers, M. & Prato, F.S. (2001) A detailed ethological analysis of the mouse open field test: effects of diazepam, chlordiazepoxide and an extremely low frequency pulsed magnetic field. *Neurosci Biobehav Rev,* **25,** 235-260.

Crabbe, J.C., Gallaher, E.J., Cross, S.J. & Belknap, J.K. (1998) Genetic determinants of sensitivity to diazepam in inbred mice. *Behav Neurosci,* **112,** 668-677.

Crusio, W.E., Schwegler, H., Brust, I. & Van Abeelen, J.H. (1989a) Genetic selection for novelty-induced rearing behavior in mice produces changes in hippocampal mossy fiber distributions. *J Neurogenet,* **5,** 87-93.

Crusio, W.E., Schwegler, H. & van Abeelen, J.H. (1989b) Behavioral responses to novelty and structural variation of the hippocampus in mice.

I.Quantitative-genetic analysis of behavior in the open-field. *Behav Brain Res,* **32,** 75-80.

Czech, D.A., Jacobson, E.B., LeSueur-Reed, K.T. & Kazel, M.R. (2003) Putative anxiety-linked effects of the nitric oxide synthase inhibitor L-NAME in three murine exploratory behavior models. *Pharmacol Biochem Behav,* **75,** 741-748.

DeYoung, C.G., Getchell, M., Koposov, R.A., Yrigollen, C.M., Haeffel, G.J., af Klinteberg, B., Oreland, L., Ruchkin, V.V., Pakstis, A.J. & Grigorenko, E.L. (2010) Variation in the catechol-O-methyltransferase Val 158 Met polymorphism associated with conduct disorder and ADHD symptoms, among adolescent male delinquents. *Psychiatr Genet,* **20,** 20-24.

Diatchenko, L., Nackley, A.G., Slade, G.D., Bhalang, K., Belfer, I., Max, M.B., Goldman, D. & Maixner, W. (2006a) Catechol-O-methyltransferase gene polymorphisms are associated with multiple pain-evoking stimuli. *Pain,* **125,** 216-224.

Diatchenko, L., Nackley, A.G., Slade, G.D., Fillingim, R.B. & Maixner, W. (2006b) Idiopathic pain disorders--pathways of vulnerability. *Pain,* **123,** 226-230.

Diatchenko, L., Slade, G.D., Nackley, A.G., Bhalang, K., Sigurdsson, A., Belfer, I., Goldman, D., Xu, K., Shabalina, S.A., Shagin, D., Max, M.B., Makarov, S.S. & Maixner, W. (2005) Genetic basis for individual variations in pain perception and the development of a chronic pain condition. *Hum Mol Genet,* **14,** 135-143.

Domschke, K., Deckert, J., O'Donovan M, C. & Glatt, S.J. (2007) Meta-analysis of COMT val158met in panic disorder: ethnic heterogeneity and gender specificity. *Am J Med Genet B Neuropsychiatr Genet,* **144B,** 667-673.

Domschke, K., Freitag, C.M., Kuhlenbaumer, G., Schirmacher, A., Sand, P., Nyhuis, P., Jacob, C., Fritze, J., Franke, P., Rietschel, M., Garritsen, H.S., Fimmers, R., Nothen, M.M., Lesch, K.P., Stogbauer, F. & Deckert, J. (2004) Association of the functional V158M catechol-O-methyl-transferase polymorphism with panic disorder in women. *Int J Neuropsychopharmacol,* **7,** 183-188.

Eisener-Dorman, A.F., Grabowski-Boase, L., Steffy, B.M., Wiltshire, T. & Tarantino, L.M. Quantitative trait locus and haplotype mapping in closely related inbred strains identifies a locus for open field behavior. *Mamm Genome*.

Eleftheriou, B.E. (1975) Regional brain catechol-O-methyl transferase: age related differences in the mouse. *Exp Aging Res,* **1,** 99-103.

Emin Erdal, M., Herken, H., Yilmaz, M. & Bayazit, Y.A. (2001) Significance of the catechol-O-methyltransferase gene polymorphism in migraine. *Brain Res Mol Brain Res,* **94,** 193-196.

Enoch, M.A., Xu, K., Ferro, E., Harris, C.R. & Goldman, D. (2003) Genetic origins of anxiety in women: a role for a functional catechol-O-methyltransferase polymorphism. *Psychiatr Genet,* **13,** 33-41.

Evans, J., Xu, K., Heron, J., Enoch, M.A., Araya, R., Lewis, G., Timpson, N., Davies, S., Nutt, D. & Goldman, D. (2009) Emotional symptoms in children: The effect of maternal depression, life events, and COMT genotype. *Am J Med Genet B Neuropsychiatr Genet,* **150B,** 209-218.

Fahey, J.M., Pritchard, G.A., Grassi, J.M., Pratt, J.S., Shader, R.I. & Greenblatt, D.J. (2001) Pharmacodynamic and receptor binding changes during chronic lorazepam administration. *Pharmacol Biochem Behav,* **69,** 1-8.

Fernandez, E.E. (1997) Structure of the mouse behaviour on the elevated plus-maze test of anxiety. *Behav Brain Res,* **86,** 105-112.

Frazer, K.A., Eskin, E., Kang, H.M., Bogue, M.A., Hinds, D.A., Beilharz, E.J., Gupta, R.V., Montgomery, J., Morenzoni, M.M., Nilsen, G.B., Pethiyagoda, C.L., Stuve, L.L., Johnson, F.M., Daly, M.J., Wade, C.M. & Cox, D.R. (2007) A sequence-based variation map of 8.27 million SNPs in inbred mouse strains. *Nature,* **448,** 1050-1053.

Fujita, O., Annen, Y. & Kitaoka, A. (1994) Tsukuba high- and low-emotional strains of rats (Rattus norvegicus): an overview. *Behav Genet,* **24,** 389-415.

Gogos, J.A., Morgan, M., Luine, V., Santha, M., Ogawa, S., Pfaff, D. & Karayiorgou, M. (1998) Catechol-O-methyltransferase-deficient mice exhibit sexually dimorphic changes in catecholamine levels and behavior. *Proc Natl Acad Sci U S A,* **95,** 9991-9996.

Gray, J. & McNaughton, N. (2000) *The neuropsychology of anxiety,* Oxford University Press, Oxford.

Guyton, A.C. (1991) Textbook of Medical Physiology. In Wonsiewicz, M.J. (ed), W.B. Saunders Company, Philidelphia, p. 676.

Harrison, P.J. & Tunbridge, E.M. (2008) Catechol-O-methyltransferase (COMT): a gene contributing to sex differences in brain function, and to sexual dimorphism in the predisposition to psychiatric disorders. *Neuropsychopharmacology,* **33,** 3037-3045.

Henderson, N.D., Turri, M.G., DeFries, J.C. & Flint, J. (2004) QTL analysis of multiple behavioral measures of anxiety in mice. *Behav Genet,* **34,** 267-293.

Hu, Z., Fan, C., Oh, D.S., Marron, J.S., He, X., Qaqish, B.F., Livasy, C., Carey, L.A., Reynolds, E., Dressler, L., Nobel, A., Parker, J., Ewend, M.G., Sawyer, L.R., Wu, J., Liu, Y., Nanda, R., Tretiakova, M., Ruiz Orrico, A., Dreher, D., Palazzo, J.P., Perreard, L., Nelson, E., Mone, M., Hansen, H., Mullins, M., Quackenbush, J.F., Ellis, M.J., Olopade, O.I., Bernard, P.S. & Perou, C.M. (2006) The molecular portraits of breast tumors are conserved across microarray platforms. *BMC Genomics,* **7,** 96.

Hughes, R.N. (1993) Effects on open-field behavior of diazepam and buspirone alone and in combination with chronic caffeine. *Life Sci,* **53,** 1217-1225.

Kabbaj, M., Devine, D.P., Savage, V.R. & Akil, H. (2000) Neurobiological correlates of individual differences in novelty-seeking behavior in the rat: differential expression of stress-related molecules. *J Neurosci,* **20,** 6983-6988.

Lachman, H.M. (2008) Does COMT val158met affect behavioral phenotypes: yes, no, maybe? *Neuropsychopharmacology,* **33,** 3027-3029.

Lang, U.E., Bajbouj, M., Sander, T. & Gallinat, J. (2007) Gender-dependent association of the functional catechol-O-methyltransferase Val158Met genotype with sensation seeking personality trait. *Neuropsychopharmacology,* **32,** 1950-1955.

Lariviere, W.R., Wilson, S.G., Laughlin, T.M., Kokayeff, A., West, E.E., Adhikari, S.M., Wan, Y. & Mogil, J.S. (2002) Heritability of nociception. III. Genetic relationships among commonly used assays of nociception and hypersensitivity. *Pain,* **97,** 75-86.

Lister, R.G. (1990) Ethologically-based animal models of anxiety disorders. *Pharmacol Ther,* **46,** 321-340.

Marron, J.S., Todd, M.J. , Ahn, J. (2007) Distance-Weighted Discrimination. *Journal of the American Statistical Association,* **102,** 1267-1271.

McClurg, P., Janes, J., Wu, C., Delano, D.L., Walker, J.R., Batalov, S., Takahashi, J.S., Shimomura, K., Kohsaka, A., Bass, J., Wiltshire, T. & Su, A.I. (2007) Genomewide association analysis in diverse inbred mice: power and population structure. *Genetics,* **176,** 675-683.

McClurg, P., Pletcher, M.T., Wiltshire, T. & Su, A.I. (2006) Comparative analysis of haplotype association mapping algorithms. *BMC Bioinformatics,* **7,** 61.

McCourt, W.F., Gurrera, R.J. & Cutter, H.S. (1993) Sensation seeking and novelty seeking. Are they the same? *J Nerv Ment Dis,* **181,** 309-312.

McNaughton, N. (1985) The effects of systemic and intraseptal injections of sodium amylobarbitone on rearing and ambulation in rats. *Australian Journal of Psychology,* **37,** 15-27.

Mogil, J.S., Wilson, S.G., Bon, K., Lee, S.E., Chung, K., Raber, P., Pieper, J.O., Hain, H.S., Belknap, J.K., Hubert, L., Elmer, G.I., Chung, J.M. & Devor, M. (1999a) Heritability of nociception I: responses of 11 inbred mouse strains on 12 measures of nociception. *Pain,* **80,** 67-82.

Mogil, J.S., Wilson, S.G., Bon, K., Lee, S.E., Chung, K., Raber, P., Pieper, J.O., Hain, H.S., Belknap, J.K., Hubert, L., Elmer, G.I., Chung, J.M. & Devor, M. (1999b) Heritability of nociception II. 'Types' of nociception revealed by genetic correlation analysis. *Pain,* **80,** 83-93.

Nackley, A.G. & Diatchenko, L.(2010) Assessing potential functionality of catechol-O-methyltransferase (COMT) polymorphisms associated with pain sensitivity and temporomandibular joint disorders. *Methods Mol Biol,* **617,** 375-393.

Nackley, A.G., Shabalina, S.A., Tchivileva, I.E., Satterfield, K., Korchynskyi, O., Makarov, S.S., Maixner, W. & Diatchenko, L. (2006) Human catechol-O-methyltransferase haplotypes modulate protein expression by altering mRNA secondary structure. *Science,* **314,** 1930-1933.

Nackley, A.G., Tan, K.S., Fecho, K., Flood, P., Diatchenko, L. & Maixner, W. (2007) Catechol-O-methyltransferase inhibition increases pain sensitivity through activation of both beta2- and beta3-adrenergic receptors. *Pain,* **128,** 199-208.

Overbye, A. & Seglen, P.O. (2009) Phosphorylated and non-phosphorylated forms of catechol O-methyltransferase in rat liver, brain and other tissues. *Biochem J,* **417,** 535-545.

Palmason, H., Moser, D., Sigmund, J., Vogler, C., Hanig, S., Schneider, A., Seitz, C., Marcus, A., Meyer, J. & Freitag, C.M. (2009) Attention-deficit/hyperactivity disorder phenotype is influenced by a functional catechol-O-methyltransferase variant. *J Neural Transm*.

Papaleo, F., Crawley, J.N., Song, J., Lipska, B.K., Pickel, J., Weinberger, D.R. & Chen, J. (2008) Genetic dissection of the role of catechol-O-

methyltransferase in cognition and stress reactivity in mice. *J Neurosci,* **28,** 8709-8723.

Piazza, P.V., Deminiere, J.M., Le Moal, M. & Simon, H. (1989) Factors that predict individual vulnerability to amphetamine self-administration. *Science,* **245,** 1511-1513.

Pletcher, M.T., McClurg, P., Batalov, S., Su, A.I., Barnes, S.W., Lagler, E., Korstanje, R., Wang, X., Nusskern, D., Bogue, M.A., Mural, R.J., Paigen, B. & Wiltshire, T. (2004) Use of a dense single nucleotide polymorphism map for in silico mapping in the mouse. *PLoS Biol,* **2,** e393.

Pooley, E.C., Fineberg, N. & Harrison, P.J. (2007) The met(158) allele of catechol-O-methyltransferase (COMT) is associated with obsessive-compulsive disorder in men: case-control study and meta-analysis. *Mol Psychiatry,* **12,** 556-561.

Qian, Q., Wang, Y., Zhou, R., Li, J., Wang, B., Glatt, S. & Faraone, S.V. (2003) Family-based and case-control association studies of catechol-O-methyltransferase in attention deficit hyperactivity disorder suggest genetic sexual dimorphism. *Am J Med Genet B Neuropsychiatr Genet,* **118B,** 103-109.

Stein, M.B., Fallin, M.D., Schork, N.J. & Gelernter, J. (2005) COMT polymorphisms and anxiety-related personality traits. *Neuropsychopharmacology,* **30,** 2092-2102.

Su, A.I., Wiltshire, T., Batalov, S., Lapp, H., Ching, K.A., Block, D., Zhang, J., Soden, R., Hayakawa, M., Kreiman, G., Cooke, M.P., Walker, J.R. & Hogenesch, J.B. (2004) A gene atlas of the mouse and human protein-encoding transcriptomes. *Proc Natl Acad Sci U S A,* **101,** 6062-6067.

Vlainic, J. & Pericic, D. (2009) Effects of acute and repeated zolpidem treatment on pentylenetetrazole-induced seizure threshold and on locomotor activity: comparison with diazepam. *Neuropharmacology,* **56,** 1124-1130.

Wu, C., Delano, D.L., Mitro, N., Su, S.V., Janes, J., McClurg, P., Batalov, S., Welch, G.L., Zhang, J., Orth, A.P., Walker, J.R., Glynne, R.J., Cooke, M.P., Takahashi, J.S., Shimomura, K., Kohsaka, A., Bass, J., Saez, E., Wiltshire, T. & Su, A.I. (2008) Gene set enrichment in eQTL data identifies novel annotations and pathway regulators. *PLoS Genet,* **4,** e1000070.

Yang, H., Bell, T.A., Churchill, G.A. & Pardo-Manuel de Villena, F. (2007) On the subspecific origin of the laboratory mouse. *Nat Genet,* **39,** 1100-1107.

Zubieta, J.K., Heitzeg, M.M., Smith, Y.R., Bueller, J.A., Xu, K., Xu, Y., Koeppe, R.A., Stohler, C.S. & Goldman, D. (2003) COMT val158met genotype affects mu-opioid neurotransmitter responses to a pain stressor. *Science,* **299,** 1240-1243.

Figure 2.1 Identification of *Comt1* as a cis-regulated gene. **a**. Genome wide association analysis (HAM) of *Comt1* RNA expression levels for probe set 1418701_at in male pituitary across 29 strains. The genomic position of SNPs is displayed on the X axis in cumulative position in the genome. Chromosomes are sequentially colored (1-19 and X). The Y axis displays the association score (-LogP) for association of between strain gene expression patterns with each inferred haplotype. The highest association on Chr. 16 has a maximal score, -LogP = 6. **b.** Expanded view of the 4 MB region surrounding the *Comt1* locus. Eight SNPs with –LogP=0 are non-informative for these strains, thus producing a break in the QTL locus. The red markers below zero on the Yaxis define all Affymetrix 430v2 probe sets in their correct genomic location. **c**. SNP allele calls for 29 inbred mouse strains at this locus define at least four distinct haplotypes. However, there are two major haplotype groups and all strains in this interval are also characterized by the presence (grey) or absence of a SINE element in the 3'UTR of *Comt1.* **d.** The presence of the B2 SINE element is demonstrated by PCR. Strains are aligned in the same order. **e.** cDNA structure of *Comt1* illustrating exons, position of the SINE insertion, Affymetrix and TaqMAN probe sets, diagnostic PCR primers and coding exons.

Figure 2.1

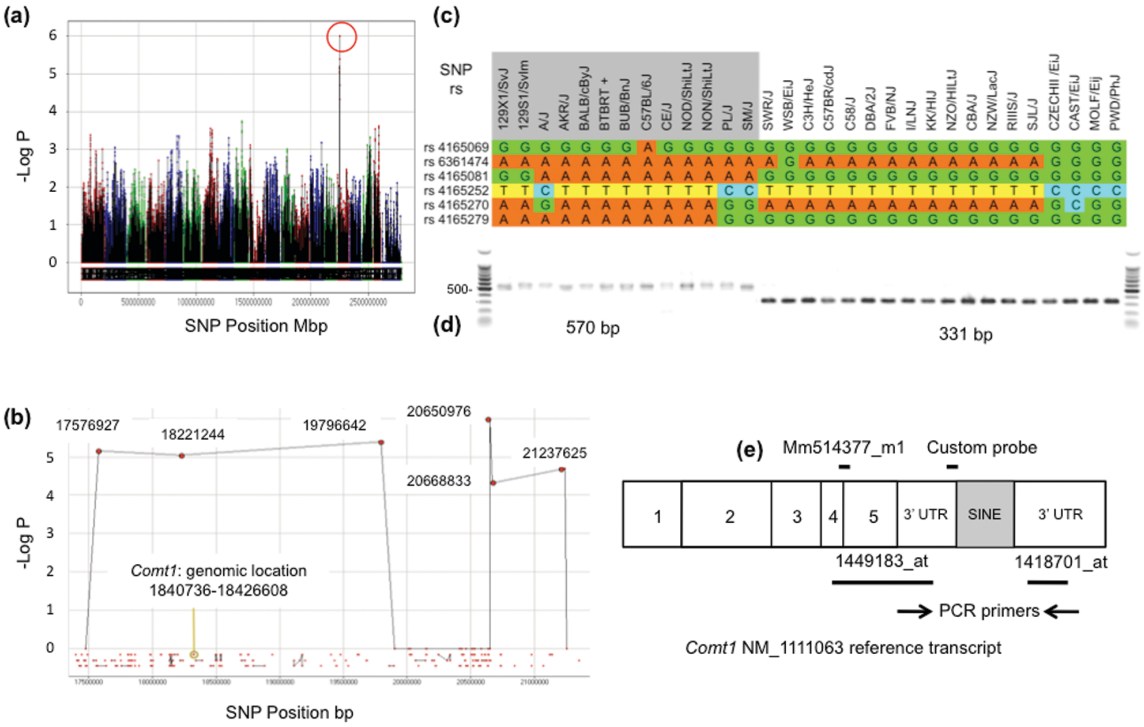
(a)
-Log P
SNP Position Mbp
(c)
SNP
rs
129X1/SvJ
129S1/SvIm
A/J
AKR/J
BALB/cByJ
BTBRT +
BUB/BnJ
C57BL/6J
CE/J
NOD/ShiLtJ
NON/ShiLtJ
PL/J
SM/J
SWR/J
WSB/EiJ
C3H/HeJ
C57BR/cdJ
C58/J
DBA/2J
FVB/NJ
I/LNJ
KK/HiJ
NZO/HlLtJ
CBA/J
NZW/LacJ
RIIS/J
SJL/J
CZECHII /EiJ
CAST/EiJ
MOLF/EiJ
PWD/PhJ
rs 4165069
rs 6361474
rs 4165081
rs 4165252
rs 4165270
rs 4165279
500-
(d)
570 bp
331 bp
(b)
17576927
18221244
19796642
20650976
21237625
20668833
-Log P
Comt1: genomic location
1840736-18426608
SNP Position bp
(e)
Mm514377_m1
Custom probe
1
2
3
4
5
3' UTR
SINE
3' UTR
1449183_at
1418701_at
PCR primers
Comt1 NM_1111063 reference transcript

Figure 2.2 Gene expression values for *Comt1* (Affymetrix probe 1449183_at) in: **a.** prefrontal cortex (27 strains) and **b**. nucleus accumbens (29 strains). Three male animals were pooled from each strain. Each result is also characterized by the presence (grey) or absence of a SINE element in the 3'UTR of *Comt1.*

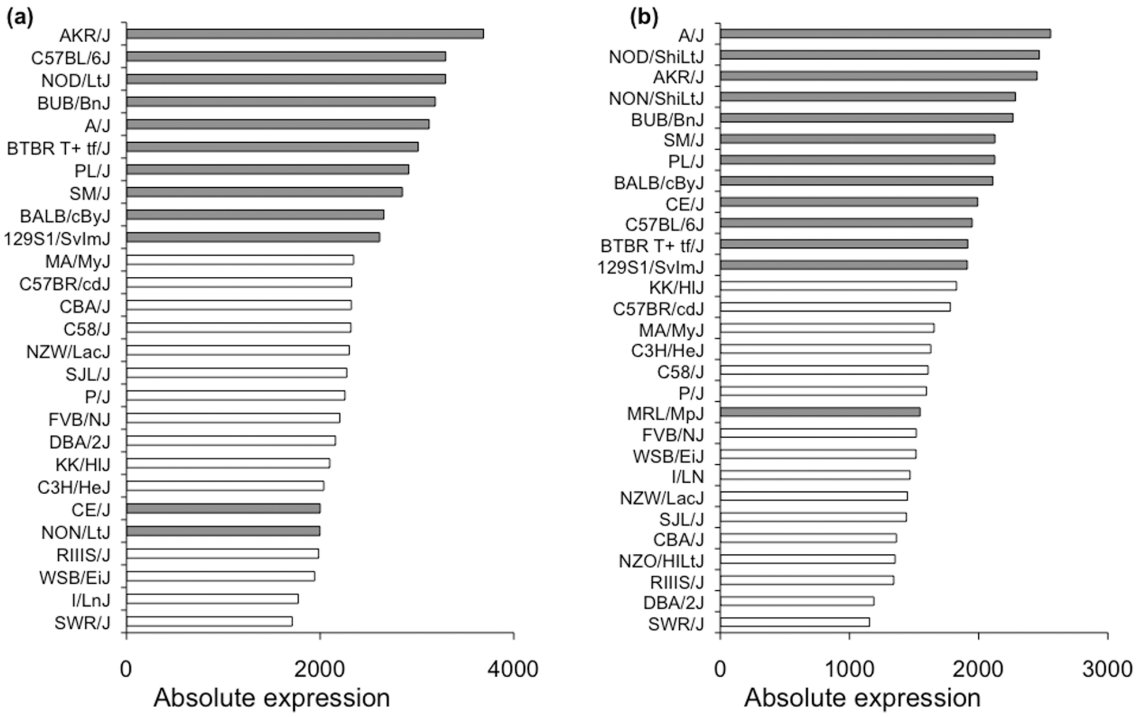

Figure 2.3 Functional analysis of *Comt1* variants. Microarray gene expression results were validated using TaqMan assays. **a.** Array data for Affymetrix probe 1449183_at and qPCR (grey) from prefrontal cortex RNA: 4 strains, 4 male animals per strain demonstrate reproducible values between q-PCR and array data. Data normalized to C3H/HeJ; error bars are S.E. **P<0.01, 1-tailed paired t-test. **b.** An ELISA assay was developed to assess COMT1 protein levels. COMT1 protein levels in prefrontal cortex were measured for male animals in 8 strains, (+SINE grey) error bars are S.E. **c.** Enzymatic activity of COMT1 protein was measured using a Normetanephrine ELISA assay. Prefrontal cortex lysates from 2 to 4 male animals per strain were collected. Ten strains were assayed: 6 +SINE (grey), and 4 –SINE. Data normalized to C3H/HeJ and then analyzed by 1-tailed Mann Whitney test, **P < 0.01 **d.** Full length cDNA constructs of both +SINE and -SINE haplotypes were prepared and transiently transfected into PC12 cells. Cell lysates were tested for enzymatic activity in the same manner as brain tissue samples.

Figure 2.3

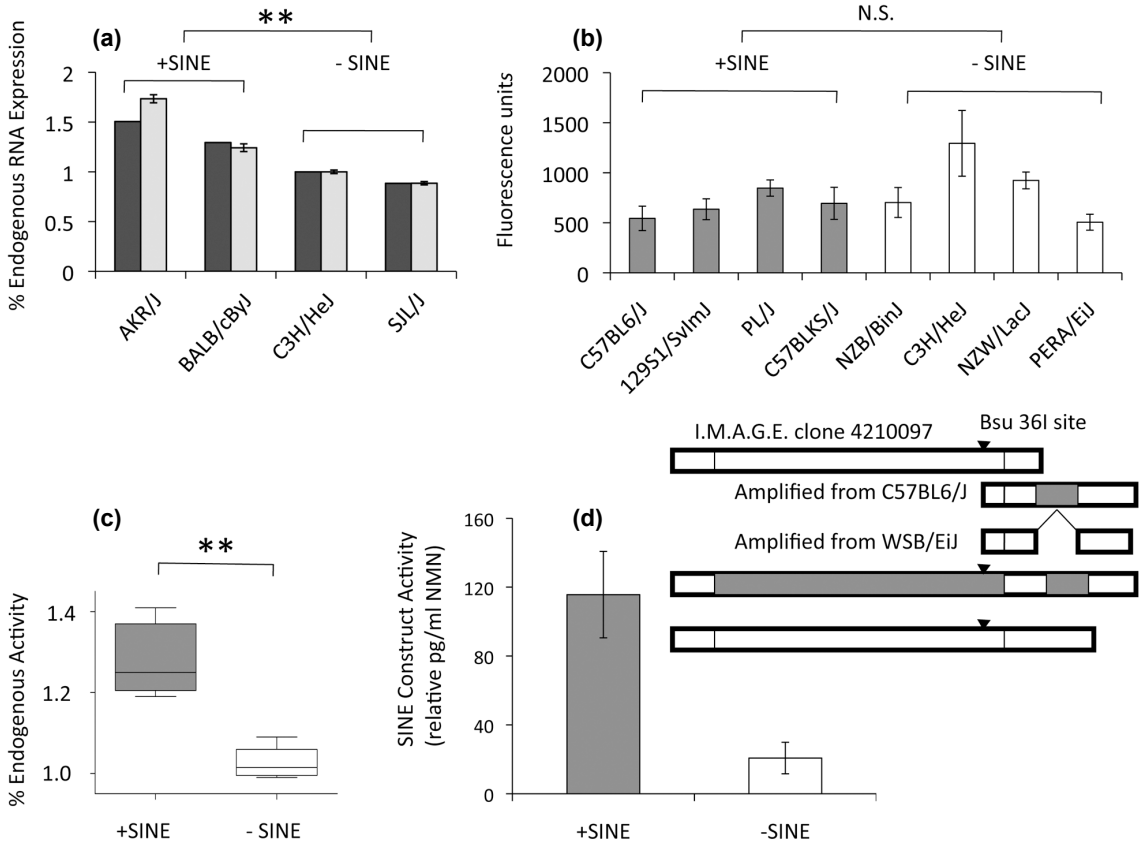
(a)
**
+SINE
- SINE
% Endogenous RNA Expression
2
1.5
1
0.5
0
AKR/J
BALB/cByJ
C3H/HeJ
SJL/J
(b)
N.S.
+SINE
- SINE
Fluorescence units
2000
1500
1000
500
0
C57BL6/J
129S1/SvImJ
PL/J
C57BLKS/J
NZB/BinJ
C3H/HeJ
NZW/LacJ
PERA/EiJ
(c)
**
% Endogenous Activity
1.4
1.2
1.0
+SINE
- SINE
(d)
SINE Construct Activity (relative pg/ml NMN)
160
120
80
40
0
+SINE
-SINE
I.M.A.G.E. clone 4210097
Bsu 36I site
Amplified from C57BL6/J
Amplified from WSB/EiJ

Figure 2.4 Behavioral assays from individual animals are correlated with the presence or absence of the SINE element in *Comt1.* Males were tested in two separate groups depending on assay. **a.** The four most significant behaviors that discriminate for the presence or absence of the SINE element in *Comt1* are shown on a DWD loading plot (male) *OFR* - open field, rearing, *LDB* - Light/Dark Box, % time in light, *OFD* - Open Field, total distance, *EPM* - Elevated Plus Maze, total distance. **b.** Data projection plot on DWD direction of contributing behavioral assays, grey points indicate scores from +SINE haplotype, black from -SINE. **c.** DiProPerm plot of t-statistics. The DiProPerm test plot depicts the 100 t-statistics as 100 black dots under a Gaussian peak. The t-statistic for the DWD direction plot is depicted as a black line. Similar scores are seen for female mice.

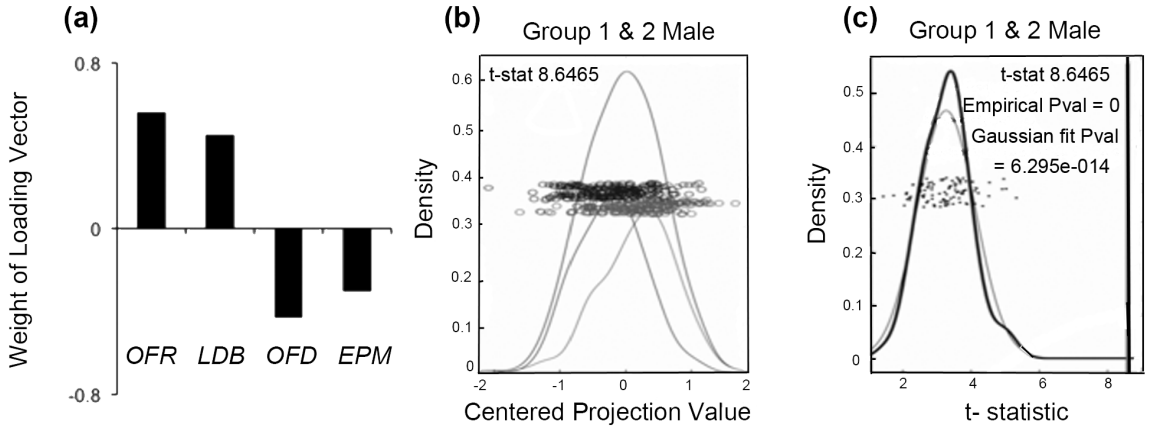

Figure 2.5 Multivariate analyses of cross-correlations between negative SINE status of inbred mouse strains and strain means for 22 assays of sensation, nociception and hypersensitivity (corrected for sensitivity; see Table 2.2 for abbreviations). MDS (**a**) and PCA (**b**) plots show that strains without a SINE element have increased sensitivity to spontaneous inflammatory nociception assays. In the MDS plot, the Euclidean distances between the point for *Comt1* SINE status and the points for sensitivity in the pain models are representative of their Pearson product-moment correlations; points for traits with higher positive correlations are closer (see text). Using a Kruskal loss function with monotonic regression, the final stress was 0.21. The proportion of total variance accounted for is 0.81. In the PCA plot, the angles between rays projecting to the points are representative of the correlations between the two traits (see text). The proportion of total variance accounted for is 0.53. Circles indicate the set of all spontaneous inflammatory nociception assays and demonstrate the overall proximity and strong genetic correlation of negative SINE status with this type of nociception.

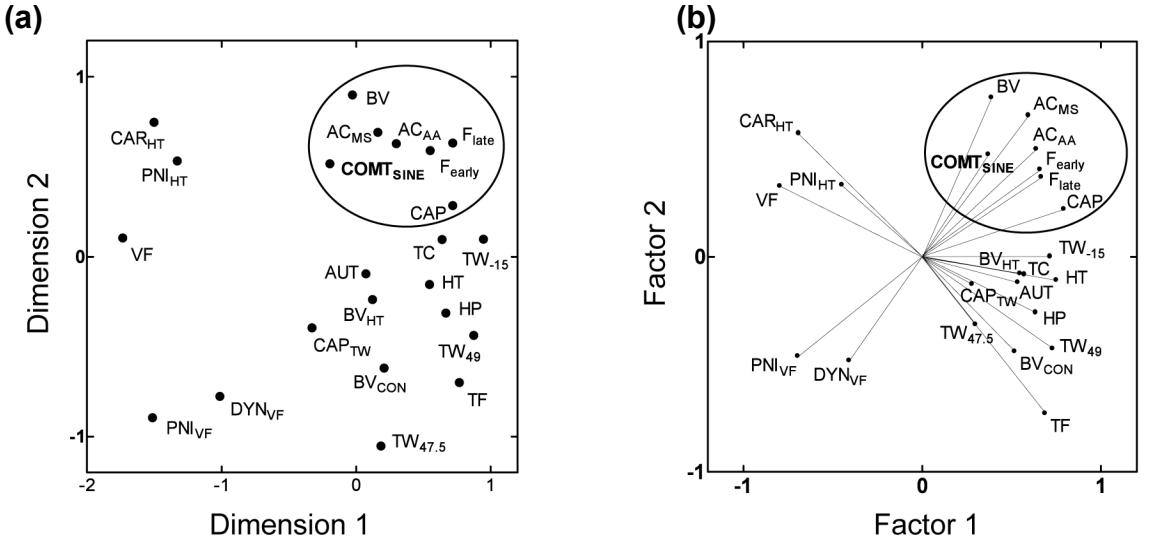

Table 2.1: Association of the presence or absence of the SINE element with gene expression of *Comt1* in seven brain regions.

	Female						
	- SINE Haplotype			+ SINE Haplotype			
Brain Region	N	Mean	Std Err	N	Mean	Std Err	P value
Z-score	16	-5.86	0.15	13	-2.47	0.36	P<0.0001
Nucleus Accumbens	16	1141	72.9	13	1072	38.5	P=0.437
Prefrontal Cortex	16	791.4	15.08	13	1134	57.98	P<0.0001
Amygdala	16	320.8	7.78	13	458.6	13.03	P<0.0001
Hypothalamus	16	789.8	13.89	13	1267	48.72	P<0.0001
Hippocampus	16	737.8	18.3	13	1027	28.13	P<0.0001
Striatum	16	893.1	25.15	13	1371	65.46	P<0.0001
Pituitary	15	805.7	33.25	13	814	38.87	P=0.872
	Male						
Z-score	16	2.24	0.37	13	6.94	0.52	P<0.0001
Nucleus Accumbens	15	2136	53.28	12	2887	146.84	P<0.0001
Prefrontal Cortex	16	1493	47.29	13	2131	77.2	P<0.0001
Amygdala	16	1507	34.76	13	1888	44.39	P<0.0001
Hypothalamus	16	1310	104.5	13	1852	129.18	P<0.01
Hippocampus	15	2370	139.2	13	2690	96.5	P<0.05
Striatum	11	508.2	19.91	12	718.5	43.25	P<0.0001
Pituitary	16	2444	59.28	13	2679	89.93	P<0.05

Table 2.2 Behavioral scores that best discriminate the +SINE/-SINE haplotypes

	Female	Male
Behavioral phenotype	*OFR, LDB, OFD, EPM*	*OFR, LDB, OFD, EPM*
DiProPerm t-statistic	10.501	8.6465
P value	P<0.0001	P<0.0001

Table 2.3 Correlations between negative SINE status and strain means for 22 assays of sensation, nociception and hypersensitivity (corrected for sensitivity; positive correlation indicates absence of SINE haplotype associated with increased sensitivity in the assay).

Abbreviation	Description of pain model	Pearson Correlation (Strains in Common)
Spontaneous inflammatory nociception		
AC_{AA}	Abdominal constriction (writhing) test – acetic acid	0.46 (11)
AC_{MS}	Abdominal constriction (writhing) test – magnesium sulfate	0.61* (11)
BV	Bee venom-induced spontaneous pain behavior (licking)	0.55* (12)
CAP	Capsaicin-induced spontaneous pain behavior (licking)	0.27 (12)
F_{early}	Early/acute phase of formalin test	0.64* (11)
F_{late}	Late/tonic phase of formalin test	0.35 (11)
Thermal nociception		
TW_{-15}	Tail withdrawal from -15°C ethanol	0.05 (12)
HP	Hot-plate test	0.41 (11)
HT	Hargreaves et al.'s thermal paw-withdrawal test	0.60* (11)
TF	Tail-flick from radiant heat source	-0.21 (10)
$TW_{47.5}$	Tail withdrawal from 47.5°C water	-0.28 (12)
TW_{49}	Tail withdrawal from 49°C water	-0.20 (11)

Mechanical nociception			
TC	Tail-clip test	0.33	(12)
Mechanical sensitivity			
VF	von Frey monofilament test	-0.01	(11)
Mechanical hypersensitivity			
DYN_{VF}	Dynorphin-induced mechanical hypersensitivity assessed with von Frey monofilament test	0.29	(7)
PNI_{VF}	Peripheral nerve injury-induced mechanical hypersensitivity assessed with von Frey monofilament test	-0.23	(11)
Thermal and afferent-dependent hypersensitivities			
AUT	Autotomy following sciatic and saphenous nerve transection	0.00	(11)
BV_{HT}	Bee venom-induced thermal hypersensitivity assessed with Hargreaves' test (ipsilateral)	0.31	(12)
BV_{CON}	Contralateral bee venom-induced thermal hypersensitivity assessed with Hargreaves' test	0.14	(12)
CAP_{TW}	Capsaicin-induced thermal hypersensitivity assessed with tail-withdrawal test , 47°C water	0.20	(12)
CAR_{HT}	Carrageenan-induced thermal hypersensitivity assessed with Hargreaves' test	-0.09	(11)
PNI_{HT}	Peripheral nerve injury-induced thermal hypersensitivity assessed with Hargreaves' test	-0.08	(11)

*Statistically significant ($P < 0.05$, one-tailed test, uncorrected).

Table 2.4: Mean strain values for four behavioral measurements most important in separating the +SINE and -SINE haplotypes by DWD analysis. Standard Deviation is noted as s.d.

		OFR : Open Field, Mean Rearing						*LDB* : Light/Dark Box, Mean % time in Light					
Strain	SINE Haplo-type	Male	N	s.d.	Female	N	s.d.	Male	N	s.d.	Female	N	s.d.
129S1/ SvImJ	+	8.1	14	10.4	1.0	14	1.5	4.7	8	4.9	0.2	8	0.4
A/J	+	11.4	14	13.6	8.0	14	13.6	0.0	8	0.0	0.3	8	0.2
AKR/J	+	77.6	14	27.0	54.4	16	22.4	3.0	8	4.3	1.6	8	1.6
BALB/cByJ	+	59.7	14	31.8	52.7	13	31.2	0.3	8	0.4	0.2	8	0.6
BTBR T+ tf/J	+	55.5	14	23.2	46.9	16	17.9						
BUB/BnJ	+	69.3	16	26.8	49.0	12	15.9	6.2	4	5.3	6.4	4	4.4
C3H/HeJ	-	93.5	7	34.7	83.5	15	38.3	36.1	4	7.0	24.4	4	8.2
C57BL/6J	+	95.1	15	36.4	69.4	27	24.3	9.6	4	4.8	6.4	4	1.9
C57BR/cdJ	-	116.1	16	32.2	93.8	15	25.0	21.5	4	4.1	20.0	4	6.0
C58/J	-	83.4	14	27.7	63.4	16	24.7	6.5	4	5.4	7.4	4	4.7
CBA/J	-	54.1	16	40.2	57.1	15	45.3	5.1	3	3.0	33.6	4	34.5
CE/J	+	84.4	15	22.9	78.0	4	57.2	20.0	4	14.1	19.6	2	1.3
DBA2/J	-	79.5	8	33.4	78.0	14	25.7	4.5	4	3.5	2.2	4	1.8
FVB/NJ	-	173.0	14	47.6	153.6	14	24.5	18.2	7	11.2	22.6	8	6.9
I/LnJ	-	87.5	14	13.9	83.3	4	42.9						
KK/HIJ	-	44.1	8	18.5	48.5	12	24.7						

		OFR : Open Field, Mean Rearing						*LDB* : Light/Dark Box, Mean % time in Light					
Strain	SINE Haplo-type	Male	N	s.d.	Female	N	s.d.	Male	N	s.d.	Female	N	s.d.
LG/J	+	75.3	17	29.5	116.8	12	35.1	1.3	4	2.6	0.3	4	0.5
LP/J	+	24.6	12	15.6	21.1	10	10.3						
MA/MyJ	-	178.7	10	39.7	148.3	8	37.3	17.6	4	12.1	18.3	4	8.5
MRL/MpJ	+	45.1	14	17.7	47.3	14	25.3	3.6	8	10.0	5.4	8	13.2
NOD/LtJ	+	144.5	17	28.9	133.9	18	46.9	9.6	8	10.0	4.7	8	5.1
NON/LtJ	+	137.1	16	53.3	134.6	16	44.8	4.7	4	3.2	6.4	3	5.7
NZB/BINJ	-	28.5	14	16.9	26.9	10	20.0						
NZO/HILtJ	-	51.3	11	24.9	43.4	11	15.7	2.1	4	2.7	2.3	4	1.9
NZW/LacJ	-				54.7	13	15.8	29.3	4	11.0	16.8	4	6.7
P/J	-	174.3	3	33.5	49.3	2	10.6	10.9	2	15.0	3.5	4	4.7
PL/J	+	115.3	18	26.3	135.1	18	24.7	26.6	4	6.4	25.1	4	10.8
PWD/Ph	-	61.0	10	33.6	32.3	10	30.1						
RIIIS/J	-	121.2	15	20.1	109.0	12	34.6						
SJL/J	-	147.9	16	39.8	109.9	16	34.6	8.7	4	9.5	7.4	4	3.7
SM/J	+	68.2	14	38.2	49.4	14	47.4	15.9	4	11.1	13.2	4	6.2
SWR/J	-	178.4	17	32.2	166.0	15	47.6	21.7	3	5.9	15.6	4	7.3
WSB/EiJ	-	70.2	10	36.7	52.7	10	24.9	16.6	4	9.6	19.0	4	6.8

		OFD : Open Field, Mean Distance Traveled (cm)					
Strain	SINE Haplotype	Male	N	s.d.	Female	N	s.d.
129S1/SvImJ	+	1652.8	14	720.0	1023.6	14	730.2
A/J	+	531.8	14	224.6	601.0	14	409.7
AKR/J	+	3798.4	14	634.6	4031.0	16	1398.2
BALB/cByJ	+	2383.4	14	638.9	2441.6	13	427.4
BTBR T+ tf/J	+	4164.3	16	914.6	3562.3	16	994.7
BUB/BnJ	+	2348.5	7	503.6	2710.2	12	606.3
C3H/HeJ	-	1807.8	15	346.8	2171.6	15	545.1
C57BL/6J	+	3005.9	16	589.3	3311.4	27	772.9
C57BR/cdJ	-	4245.8	14	812.9	3347.4	15	1075.5
C58/J	-	4289.3	16	1719.8	3774.1	16	2054.0
CBA/J	-	1824.1	15	392.0	2302.0	15	344.7
CE/J	+	2950.8	8	481.9	5289.6	14	2253.8
DBA2/J	-	2053.6	14	405.9	2063.6	14	473.1
FVB/NJ	-	3763.7	14	479.7	3868.6	14	815.6
I/LnJ	-	4027.9	8	857.8	4166.1	4	1155.3
KK/HIJ	-	1751.9	17	656.1	1715.2	12	538.6
LG/J	+	2808.4	12	455.9	3403.4	12	596.4
LP/J	+	1474.7	10	669.1	1248.1	10	589.2
MA/MyJ	-	4771.8	9	1062.3	5069.7	8	822.0
MRL/MpJ	+	2381.7	14	526.8	2747.6	14	714.4
NOD/LtJ	+	4124.7	17	859.4	4068.2	18	1086.7
NON/LtJ	+	3775.6	16	545.1	3570.1	16	684.3

		OFD : Open Field, Mean Distance Traveled (cm)					
Strain	SINE Haplotype	Male	N	s.d.	Female	N	s.d.
NZO/HILtJ	-	1190.9	11	185.1	1231.0	11	259.2
NZW/LacJ	-				2400.3	13	453.7
P/J	-	3267.9	3	783.5	3015.8	2	843.0
PL/J	+	3812.9	18	866.4	3936.0	18	1002.6
PWD/Ph	-	1808.9	10	326.5	1802.9	10	509.5
RIIIS/J	-	2732.8	15	428.1	2968.3	12	624.6
SJL/J	-	2486.4	16	548.4	2494.9	16	468.2
SM/J	+	3196.5	14	1018.0	3047.2	14	1116.0
SWR/J	-	2769.7	17	478.6	2657.8	15	497.4
WSB/EiJ	-	3282.5	10	697.5	4228.4	10	912.8

		EPM : Elevated Plus Maze, Mean Distance Traveled, (cm)					
Strain	SINE Haplotype	Male	N	s.d.	Female	N	s.d.
129S1/SvImJ	+	1047.9	7	589.3	1068.2	8	463.7
A/J	+	1452.3	6	163.9	997.7	6	300.5
AKR/J	+	2091.7	6	401.1	1866.7	8	257.8
BALB/cByJ	+	1616.7	8	447.0	2082.0	8	515.5
BUB/BnJ	+	2225.1	4	381.9	2121.2	4	203.0
C3H/HeJ	-	777.1	4	249.4	928.3	3	142.9
C57BL/6J	+	1568.0	4	175.7	937.4	4	316.1
C57BR/cdJ	-	1505.3	4	98.3	1630.6	4	102.7
C58/J	-	1395.0	4	278.0	989.6	4	339.1
CBA/J	-	800.7	4	101.3	717.2	4	242.5
CE/J	+	1089.4	4	189.6	1676.2	2	62.4
DBA2/J	-	902.7	3	188.1	848.4	4	140.1
FVB/NJ	-	2276.4	8	383.2	2580.7	6	336.2
LG/J	+	1957.7	4	171.2	1984.6	4	374.3
MA/MyJ	-	1379.8	3	668.8	1708.4	4	131.1
MRL/MpJ	+	2046.6	6	394.3	1825.6	8	369.8
NOD/LtJ	+	2275.9	8	340.1	2367.7	8	409.1
NON/LtJ	+	1994.3	4	584.4	1717.8	2	332.6
NZO/HILtJ	-	661.0	4	364.0	468.9	4	99.1
NZW/LacJ	-	1825.6	4	101.2	2014.1	4	114.5
P/J	-	1148.2	2	362.4	961.9	4	204.9

		EPM : Elevated Plus Maze, Mean Distance Traveled, (cm)					
Strain	SINE Haplotype	Male	N	s.d.	Female	N	s.d.
PL/J	+	1988.3	4	296.4	2351.3	4	255.3
SJL/J	-	1873.6	4	478.9	1933.2	4	367.8
SM/J	+	648.6	2	195.3	1202.1	4	496.3
SWR/J	-	1752.8	2	150.4	2391.9	2	371.4

CHAPTER 3: MOLECULAR CHARACTERIZATION OF THE 3'UTR B2 SINE ELEMENT IN *COMT1*

SK Segall[1], T Wiltshire[2], AG Nackley[1], C Santos[2] , B Steffy[2] , J Gauthier[1], PL Deininger[3], G Slade[1] , L Diatchenko[1]

Center for Neurosensory Disorders[1], Eshelman School of Pharmacy[2] , University of North Carolina, Chapel Hill, NC, USA

Tulane Cancer Center, Tulane School of Public Health and Tropical Medicine, New Orleans, LA, USA[3]

[*]corresponding authors

Abstract

Recently, a functional haplotype of *Catechol-O-Methyltransferase (Comt1*) was discovered in inbred strains of mice defined by a B2 short interspersed repeat element (SINE) insertion in the 3'untranslated region (UTR) (Kember *et.al.,* 2010, Mulligan *et.al.,* 2010, Segall *et. al.,* 2010). The strains of this haplotype, *Comt1*^{B2i}, have increased *Comt1* transcript 5' to and decreased transcript 3' of the insertion in the majority of tissues surveyed. COMT1 enzymatic activity was increased in male mice of *Comt1*^{B2i} strains in several

brain regions (Kember *et.al.,* 2010, Li *et.al.,* 2010, Segall *et. al.,* 2010). We demonstrated that the B2 insertion results in two transcripts of *Comt1*^{B2i}, a truncated form, which ends right after the B2 element, and a full transcript, which include B2 element. The full transcript is expressed at lower frequency in both cell construct experiments and tissue from *Comt1*^{B2i} animals. From preliminary cell construct experiments, the *Comt1*^{B2i} transcript is more stable, and leads to increased protein levels and increased enzymatic activity in cell construct experiments (Chapter 2, Figure 2.3). We propose several molecular mechanisms which could cause this result: more stable mRNA 2^{o} structure, and/or an early polyadenylation signal, which truncates the 3' UTR, leading to more stable RNA, more protein and more activity. Future experiments will determine if it is the loss of the most distal 3'UTR which causes the truncated *Comt1*^{B2i} transcript to become more stable, or the presence of the B2 sequence itself is responsible for the increased stability of *Comt1*^{B2i} transcript.

INTRODUCTION

SINE Elements in Mouse and Human Genomes

As we will show in this work, we have identified a molecular mechanism that could explain some phenotypic data for behavior and pain response in inbred strains of mice. Short interspersed nucleotide elements (SINEs) are found in all inbred strains of mice, and in this case is the source of this *Comt1* haplotype in classic inbred strains. SINE elements are sequences of small nuclear RNAs, such as tRNA and rRNA, which have been reverse-transcribed and integrated into the genome (Dieninger 1989, Goodier & Kazazian 2008).

SINE elements are 80-400 bp in length and are distributed throughout eukaryotic genomes (Jagadeeswaran *et. al.* 1981, Rogers 1985). Table 3.1 lists the two main classes of SINE elements both originate from RNA Polymerase III transcribed genes (reviewed by Okada 1991). The first class is derived form the 7SL RNA genes, the RNA component of the signal recognition particle (Krayev & Kramerov 1980, Ullu & Tschudi 1984). The human SINE element is termed Alu, for an internal *Alu I* restriction site (Houck *et al.*, 1979). In mouse, the analogous SINE element is termed B1 (Krayev *et. al.,* 1980). B1 elements are preferred methylation targets, found in GC rich regions, and have a high correlation with orthologous areas of the human genome.

Mice have a second class of SINE elements which do not have human orthologs: B2, ID, and B4 SINE elements comprise this class. These elements have been found in three rodent species: Chinese hamster (Haynes & Jelinek 1981), rat (den Dunnen & Schoenmakers 1987) and mouse (Kramerov *et.al.,* 1979, Krayev *et.al.,* 1982). These SINE elements are derived from tRNAs (Daniels & Deininger 1985, Sakamoto & Okada 1985, Ohshima *et.al.*,1993). The 5' end of these SINEs have approximately 70% similarity with a $tRNA^{Lys}$ or a $tRNA^{Gly}$ (usually 70 bp). The remaining 100-200 bp do not share sequence homology between the families. The 3' ends have an A-rich motif (reviewed by Serdobova & Kramerov 1997). Mice have on the order of 1×10^5 copies of B2 elements within their genomes (Serdobova & Kramerov 1998).

Alu Repeats and Gene Disruption

SINE elements may be stable within a genome, but are sources of

mutation if they transpose into a gene. The best characterized SINE element is the Alu element as most SINE research to date has primarily focused on diseases or syndromes generated by human Alus. Alu elements are ubiquitous in the human genome; they account for over ten percept of our total sequence (reviewed by Deininger & Batzer 1999). They can be found in every location within a gene except where the insertion disrupts essential gene function. *De novo* Alu insertions into the genome commonly result in negative outcomes (Batzer & Deininger 2002). An overview of molecular mechanisms disrupted by SINE insertions is listed in Table 3.2. Genes may be truncated, alternatively spliced, re-arranged or suppressed (reviewed by Häsler & Strub 2006). Human mRNA sequence may have full or partial *Alu* elements sequence in coding regions of mRNA (Nekrutenko *et. al.,* 2001), through a process termed exonization, where intronic sequences are recruited into the coding regions. A recent study found the majority of Alu-containing exons within coding regions caused premature termination signal or frame shift, with probable loss of gene function (Sorek *et. al.,* 2002). In addition to changing the coding portion of a gene, an *Alu* element may decrease translation. Several studies have found an *Alu* element within the 5'UTR to decrease mRNA translation efficiency, possibly through a more stable mRNA secondary structure (Landry *et. al.,* 2001, Sobczak & Krzyzosiak 2002).

B2 SINE Elements and Gene Disruption

The contribution of SINEs to alterations in gene function has not been as well characterized in mouse. It is estimated that 37.5% of the mouse genome is

transposable elements (SINEs, LINEs, and other interspersed repeat elements) and 1% is specifically SINE elements (Deininger 1989). The B2 SINE element has been extensively studied, with publications listing its effects of transcription, alternative splicing and evolution (reviewed by Brosius 1999). Table 3.3 lists consequences of SINE activity in the mouse genome.

A recent study by Chernova *et. al.,* 2008, described the effect of a B2 SINE insertion in the 5'UTR of Aminolevulinic acid synthase 1 (*Alas1*). When comparing microarray expression profiles of C57BL/6J and DBA2/J mice, *Alas1* level was markedly lower in DBA2/J. Q-PCR confirmed a greater than five-fold difference between the strains, and sequence for *Alas1* revealed the B2 insertion. To test how a 5'UTR B2 SINE insertion repressed transcription, two constructs with and without the B2 insertion were made and analyzed for promoter activity using a luciferase reporting system. Additionally, 10 deletion mutants were made across the B2 sequence in the DBA construct. Promoter activity in the cellular system showed the entire B2 SINE element was required to inhibit transcription. Among several theories, the authors postulate the local RNA structures of B2 insertion may be more stable, and thus, less able to be transcribed. While these few papers describe the deleterious effects of SINE insertions, other papers show how SINE insertions have provided a source of evolutionary diversity (reviewed by Goodier & Kazazian 2008).

Proposed mechanism of the B2 SINE element in *Comt1*

Predicted B2 consensus RNA secondary structure folds into an ordered RNA structure (Bladon *et.al.,* 1990). The t-RNA derived region folds into a

specific structure, which suggests a role in function and stability (Kass *et.al.,* 1997). Indeed, previous reports of B2 SINE insertions show reduced gene expression when the insertion is located in the 5'UTR (Chernova *et. al.,* 2008), into intronic sequence (Zheng *et.al.,* 1992), or near promoter sequence (Arranz *et.al.,* 1994). A 3'UTR insertion of a B2 SINE element has been shown to cause alternative mRNA species by early polyadenylation in five studies (Kress *et.al.,* 1984, Maichele *et.al.,* 1993, Michel *et.al.*,1997, Ryskov *et.al.,* 1984, Rothkopf, *et.al.,* 1986, Maichele *et.al.,* 1993).

SINE elements as Natural Phylogenetic Markers

Both human and mouse SINEs depend on other mobile elements for propagation as they lack sequence for protein. Long interspersed repeat elements (LINES) encode reverse transcriptase and provide factors for SINE element amplification and mobilization. However, once a SINE element appears at a location within the genome, there is no mechanism to remove the SINE from the new location (Deininger 1989). In other words, while a SINE element can be copied and inserted in a new genomic location, it cannot not mobilize itself *out* of this position on the chromosome. A SINE insertion in an ancestral species will be present in all subsequent species. Additionally, there have been no reported cases of identical tRNA-related SINE families present in unrelated taxa. Therefore, SINE insertions can be used as molecular phylogenetic markers for tracing ancestry.

It is estimated that a new SINE family remains in a genome for more than 10^7 years (Serdobova & Kramerov 1997). To find the consensus sequence of a

SINE family, sequences from many family members are aligned to find the most common nucleotide at each position (Deininger 1989). The more ancient the SINE element is believed to be, the more SNPs accumulate in what is considered the consensus sequence from the ancestral sequence (Roy *et. al. ,* 1998).

Estimation of the age of the B2 insertion into *Comt1*

The origin of new insertions of B2 elements are from currently "active" B2 master gene(s) (Roy *et. al.,* 1998). The average sequence divergence between copies of a B2 element (within a species) is around 10% (Rogers *et. al.,* 1985). A recent B2 element insertion was discovered in intron 4 of the murine β-glucuronidase gene (*Gus-s*) in the strain BALB/cByJ (Roy *et. al.,* 1998). Compared to the 182 bp consensus sequence in the B2 element of the mouse subfamily II, the intronic B2 in *Gus-s* contained three SNPs and one nucleotide deletion, for a sequence divergence of approximately 2%. Since this *Gus-s* B2 element insertion only occurs in the BALB/cByJ strain, it is likely that the mutation occurred recently when the initial laboratory colony was formed.

MATERIALS AND METHODS

Animal Husbandry

Details may be found on page 33.

Inbred Strains

Details may be found on page 34.

B2 Analysis

Details on original identification of B2 element found on page 40. The original

analysis generated by www.repeatmasker.org classified the insertion as a B2-B4 SINE element. To determine what portion of the insertion was B4, we registered with www.girinst.org for access to B2 and B4 consensus sequence. Using the Sequencher program (Build 3768, Gene Codes Corporation, Ann Arbor, MI, USA) we were able to align B2 and B4 consensus sequence to a reference transcript for *Comt1* in C57BL/6J, NM1111063. Further characterization was conducted by Professor PL Deininger, who kindly provided details through correspondence.

Gene Expression Studies

Primer sequences are listed in Table 3.4. For semi-quantitative PCR, the reaction was halted at 30 cycles with no extention. qPCR was conducted by the SYBR green method in accordance with manufactor's recommendation (FastStart SYBR Green Master Mix, Cat. 04673484001, Roche).

COMT ELISA assay

Details may be found on page 40.

Enzymatic analysis of brain lysates

Sample preparation.

Details may be found on page 42.

Enzymatic assay.

Details may be found on page 42.

Cell Constructs

Comt1^{B2i} and Comt1^{+}

Details may be found on page 43.

Transient transfection of* Comt1 *cDNA clones.

Details may be found on page 44.

Analysis of cell constructs

Sample preparation and enzymatic assay.

Details may be found on page 44.

Transfection efficiency

The amount of control plasmid for transfection activity (SEAP, Clonetech, Mountain View, CA, USA) was kept at 0.2 μg per well of a 35 mm 6-well plate. Parallel transfection with the pCMV-Sport6 lacking an insert was conducted for each experiment. Cell lysates collected 24 hours post-transfection. COMT1 activity was normalized for transfection efficiency by measuring amount of SEAP transcript in q-PCR.

Western blot

This assay has been described previously (Nackley *et.al.,* 2006). Centrifuged lysates, after normalization for protein content using a BCA assay, were run on a 10% Novex Tris-Glycine gels (Invitrogen) and transferred to nitrocellulose membranes (Whatman, Florham Oak, NJ, USA). Blots were blocked with 5% non-fat milk made in 1X PBST for 1 hour at room temperature, and then incubated with COMT polyclonal 1° antibody, (Chemicon, Temecula, CA, USA) (1:10,000; USA) overnight at 4° C, washed with PBST 3X and then incubated with Goat Anti-Rabbit IgG HRP polyclonal 2° antibody (1:5000) for 1 hr at room temperature. Blots then were washed with PBST for 10 minutes at room temperature, exposed to chemiluminescence reagent (Pierce, Milwaukee,

WI, USA), and developed.

Assessment of mRNA degradation rates

This assay has been described previously (Nackley *et.al.,* 2006, Nackley & Diatchenko 2010). A time course of mRNA degradation was measured after actinomyocin D (act D; Sigma) was added to media. Twenty-four hours after transfections of *Comt1*^{B2i}, *Comt1*$^{+}$*,* and SEAP plasmids, cells were treated with actD (10μg/ml) to stop transcription and collected 0,2,4,and 8 hours post treatment. RNA was isolated using Trizol and processed for real time PCR.

RESULTS

Analysis of the B2 insertion

The *Comt1*^{B2i} insertion has seven SNPs, approximately 4% sequence divergence (Figure 3.1). Uncharacteristically, the sequence for this particular B2 insertion is found in one other place in C57BL6/J genome, on Chromosome 5 (Deininger, personal communication). The B2 sequence in *Comt1*^{B2i} has several polyadenylation signals, including the most common and strongest motif in mouse, AATAAA (Tian *et.al.,* 2010) (Figure 3.2 a). The more distal polyadenylation signal is ATTAAA, although it should be noted that this signal is also 5' of the B2 insertion.

Array reveals bimodal expression patterns in coding versus 3'UTR probes

In Chapter 2, we discussed the significant effect of both *Comt1* haplotype and sex for all brain regions examined. Overall, *Comt1*^{B2i} strains had higher *Comt1* gene expression, and males had higher expression than females (Segall *et.al.,* 2010), which is consistent with suppression of COMT expression by

estrogen (Xie *et.al.,* 1999). The Affymetrix array has two coding probes for *Comt1,* 1449183_at in the coding regions, and 1418701_at in the 3'UTR region (Figure 3.3). All seven regions of brain in both male and female showed lower signal for *Comt1*^{B2i} strains in the 3'UTR probe set 1418701_at, while expression was usually approximately 20% higher in the coding regions (Figure 3.4 a-g). Hypothalamus in the male survey was an outlier as four strains appear to have "switched" expression profiles: A/J, C57BL/6J, SJL/J, and C3H/HeJ (Figure 3.4 c). In nucleus accumbens and pituitary, female *Comt1*^{B2i} strains do not show a statistically significant effect of the B2 insert in the coding region (Figure 3.4 d, e and Table 2.1). Females had less *Comt1* gene expression than males in all surveyed regions except for striatum (Table 2.1). When all brain regions are considered, a *Z*-score by sex and by haplotype, showed males to have significantly more *Comt1* gene expression than females, and the *Comt1*^{B2i} haplotype to have more RNA than *Comt1*$^{+}$ in both males and females (Figure 3.5).

Validation of array data by qPCR, protein ELISA and enzymatic assay

To validate results from the microarray data we developed a TaqMAN assay. The positions of the TaqMAN probe are in Figure 3.3. qPCR of pooled prefrontal cortex, pooled striatum/nucleus accumbens, and pooled hippocampus/hypothalamus/amygdala tissue from two male animals per strain replicated array findings that showed the strains of the *Comt1*^{B2i} haplotype to have more *Comt1* transcript in the coding region (Figure 3.6a: $P<0.01$ and $P<0.001$). Resultant from increased mRNA presence we expected to find an

increase in COMT1 protein levels and developed an ELISA assay to ascertain protein levels. However, the *Comt1*$^{+}$ strains statistically showed more protein in the cortex and Nucleus Accumbens/Striatum tissue (P<0.05) and no difference in the Hippocampus/Hypothalamus/Amygdala tissue (Figure 3.6b).

The same samples used in the protein ELISA were used in an enzymatic assay (Figure 3.6c). In the enzymatic assay, the strains of the *Comt1*^{B2i} haplotype samples had significantly more enzymatic activity in cortex and Nucleus Accumbens/ striatum regions (P<0.01, P<0,001). The enzymatic assay was not conducted on Hippocampus/Hypothalamus/Amygdala samples.

The *Comt1*^{B2i} transcript leads to more protein expression in cell construct experiments

Preliminary western blot results show that COMT1 protein is made in the cell construct experiment and apparently more protein in the *Comt1*^{B2i} construct as compared to *Comt1*$^{+}$ construct (Figure 3.6d). Endogenous COMT from rat is seen faintly in the two controls of empty vector and no DNA added.

Semi-quantitative and quantitative analysis of transcript

Semi-quantitative and quantitative PCR of cell construct and tissue samples showed a pattern of expression similar but exaggerated of array findings. PCR product surrounding the B2 insertion had extremely low product from cDNA made from tissue of animals of the *Comt1*^{B2i} haplotype (Figure 3.7a). In contrast, PCR from tissue of animals of the *Comt1*$^{+}$ haplotype had robust amplification from liver and kidney cDNA, and in cortex, a faint amplification compared to no amplification in *Comt1*^{B2i} cortex. Transfection experiments also

showed less PCR product surrounding the B2 insertion in the *Comt1*^{B2i} transfections, although *two* products are made, with the longer and expected product more abundant (Fig.3.7, arrow). PCR in the region within the 1418701_at array probe had similar results, with weak amplification of *Comt1* cDNA in samples of the *Comt1*^{B2i} haplotype (Figure 3.7b).

qPCR with SYBR-green had mixed results, possibly due to variability in developmental age in the mice of the *Comt1* haplotypes. (Figure 3.7c). qPCR amplimer which spans several exons in the coding region was present at 20 times the amount of transcript in this region in *Comt1*^{B2i} cortex compared to *Comt1*$^{+}$ cortex. Unexpectedly, a *Comt1*^{B2i} liver had only half the amount of qPCR transcript of coding region compared to a *Comt1*$^{+}$ liver. Cells transfected with *Comt1*^{B2i} construct showed twice the amount of qPCR transcript in the coding region in comparison to *Comt1*$^{+}$ cell construct transfection.

To confirm the *Comt1*^{B2i} transcript included B2 sequence, the qPCR primers had the forward primer 5' of the insert and the reverse primer within the B2 insert. *Comt1*^{B2i} cortex and liver and *Comt1*^{B2i} expression construct had abundantly more qPCR product when the internal primer was within the B2 element. As B2 elements are abundantly expressed throughout the genome, we were not sure if the reverse primer would be quenched by other B2 elements, which are present in cDNA from liver or cortex. qPCR which surrounds the B2 insertion (same primers as in Figure 3.7a) showed again very little product is made in *Comt1*^{B2i} cortex and liver through the B2 element. The transfection experiment showed roughly a 75% reduction in signal for *Comt1*^{B2i} cell construct

in qPCR, which surrounds the B2 insertion in comparison with the wild type construct.

The *Comt1*^{B2i} transcript is more stable.

In chapter two, cell construct experiments of both haplotypes showed the *Comt1*^{B2i} construct to have greater enzymatic activity. In order to identify how the construct has greater activity, transcript stability experiments were conducted with actinomyocin D, an inhibitor of transcription. Transfections on separate days showed the *Comt1*^{B2i} transcript to be more stable than the *Comt1*$^{+}$ transcript as measured by qPCR in the coding region, Figure 3.8.

DISCUSSION

De novo insertions of repeat elements into the human genome commonly result in negative outcomes (Batzer & Deininger 2002). The contribution of repeat elements to alterations in gene function has not been as well characterized in mouse. From our review of the literature, the B2 insertion into *Comt1* is the first description of a repeat element increasing gene function in mouse. In other organisms, we were not able to find any comparable examples of repeat elements increasing gene function. Therefore, we believe the B2 insertion into the 3'UTR of *Comt1* is the first example of a repeat element increasing gene function in any organism.

Additionally, the B2 insertion in *Comt1* is unusual in another regard: Chromosome 5 contains the sequence for this particular B2 insertion in the C57BL6/J genome (Deininger, personal communication). Therefore, either one B2 insertion gave rise to the other B2 insertion or they both arose from another

common source in the population (Deininger, personal communication). The B2 element in *Comt1* is also the first time a perfect match in B2 sequence has been found in two regions of the genome, and warrants further characterization for the study of B2 elements (Deininger, personal communication).

From our data, the strains of the B2 insertion had significantly less protein in cortex and striatum/nucleus accumbens tissue, but a recent report by Li *et.al.* found the short isoform associated with increased protein expression relative to the longer ancestral isoforms in several brain regions (Li *et.al.,* 2010). It may be possible that our ELISA was not able to detect small changes in protein abundance. We did find greater protein expression in cell transfection experiments (see Future Experiments, Chapter 6).

Semiquantitiative and qPCR results support our hypothesis that the B2 element causes an early polyadenylation signal. From various tissues of the *Comt1*^{B2i} haplotype, very little transcript is made 3' of the B2 insert in array, PCR and qPCR results. What is interesting is the unusual high signal from PCR product within the B2 insertion. The objective of the qPCR experiments within the B2 element was to find out if transcript was made into the B2 sequence, or if the B2 sequence was not generated. The cortex and liver samples presumably have an abundance of B2 transcript in cDNA, so it would be expected that the reverse primer would have been quenched by annealing to other transcripts. However, there is more than a hundred fold difference compared to the wild type *Comt1.* In the cell transfection experiments, the only mouse B2 sequence is from cDNA made from the transfected vector, and the difference between

Comt1^{B2i} and *Comt1*$^{+}$ is nearly 5000 fold. When the reverse primer is 3' of the B2 element, the *Comt1*^{B2i} signal drops ~75%. Therefore, it is reasonable to speculate that the polyadenylation signal within the B2 element causes an early polyadenylation, and that very little transcript is made through the polyadenylation signal. Because we did not obtain PCR product from control samples, which were DNAsed but not reverse transcribed, we should exclude possibility that this longer PCR product is derived from untranscribed vector itself.

The translation from highly efficient CMV promoter may mask degradation rates of *Comt1* isoforms, as transcript is made at an artificially inflated rate. Therefore, we measured transcript degradation in a time course series in the presence of actinomyocin D (actD), a nonspecific inhibitor of transcription. The rate of degradation in the coding region of *Comt1*^{B2i} was less than *Comt1*$^{+}$ in two separate experiments. Two subsequent transfection experiments with actD over a longer time course (10 hours) have been conducted and will be quantified. The maximal differences occurred at 6 and 8 hours following actD treatment: ~ 25% more mRNA remained for the *Comt1*^{B2i} transcript, which corresponds with the amount of increased enzymatic activity in brain lysates from animals of the *Comt1*^{B2i} haplotype.

In conclusion, we have learned some facts and have some suggestions as to how the insertion of the B2 SINE element leads to greater enzymatic activity to the ancestral *Comt1*$^{+}$ transcript. From our cell construct experiment and the results by Li *et.al.,* 2010, more protein is made by the *Comt1*^{B2i} transcript. We

have demonstrated the *Comt1*^{B2i} transcript is more stable in actD experiments. Very little transcript is produced 3' of the B2 insertion in tissue and construct experiments. It may be the region 3' of the B2 insertion has an important regulatory element, and an early polyadenylation signal removes the regulatory sequence that promote RNA degradation.

A B1 SINE insertion is in this region (Figure 3.2). It is tempting to speculate if the B1 element is involved in regulation through miRNA. The corresponding SINE element to B1 is termed Alu in humans and has been implicated in transcript degradation. A recent bioinformatic study of nearly 30 human miRNAs show high complementarity to a specific site within conserved Alu elements in 3'UTR (Smalheiser *et.al.,* 2006). We do not know if miRNAs exist for B1 elements in mouse. The molecular mechanism for the stability of *Comt1*^{B2i} will be explored in future experiments, detailed in Chapter 6.

Notes: This chapter will the basis of our next manuscript. Further experiments will be conducted in the Laboratory of Luda Diatchenko.

References

Arranz, V., Kress, M. & Ernoult-Lange, M. (1994) The gene encoding the MOK-2 zinc-finger protein: characterization of its promoter and negative regulation by mouse Alu type-2 repetitive elements. *Gene,* **149,** 293-298.

Batzer, M.A. & Deininger, P.L. (2002) Alu repeats and human genomic diversity. *Nat Rev Genet,* **3,** 370-379.

Bladon, T.S., Fregeau, C.J. & McBurney, M.W. (1990) Synthesis and processing of small B2 transcripts in mouse embryonal carcinoma cells. *Mol Cell Biol,* **10,** 4058-4067.

Brosius, J. (1999) RNAs from all categories generate retrosequences that may be exapted as novel genes or regulatory elements. *Gene,* **238,** 115-134.

Chen, J.M., Masson, E., Macek, M., Jr., Raguenes, O., Piskackova, T., Fercot, B., Fila, L., Cooper, D.N., Audrezet, M.P. & Ferec, C. (2008) Detection of two Alu insertions in the CFTR gene. *J Cyst Fibros,* **7,** 37-43.

Chernova, T., Higginson, F.M., Davies, R. & Smith, A.G. (2008) B2 SINE retrotransposon causes polymorphic expression of mouse 5-aminolevulinic acid synthase 1 gene. *Biochem Biophys Res Commun,* **377,** 515-520.

Clark, R.M., Dalgliesh, G.L., Endres, D., Gomez, M., Taylor, J. & Bidichandani, S.I. (2004) Expansion of GAA triplet repeats in the human genome: unique origin of the FRDA mutation at the center of an Alu. *Genomics,* **83,** 373-383.

Daniels, G.R. & Deininger, P.L. (1985) Integration site preferences of the Alu family and similar repetitive DNA sequences. *Nucleic Acids Res,* **13,** 8939-8954.

Deininger, P.L. (1989) SINEs: Short Interspersed Repeat Elements in Higher Eucaryotes. In Howe, D.E.B.M.M. (ed), *Mobile DNA.* American Society of Microbiolgy, Washington DC, pp. 619-636.

Deininger, P.L. & Batzer, M.A. (1999) Alu repeats and human disease. *Mol Genet Metab,* **67,** 183-193.

den Dunnen, J.T. & Schoenmakers, J.G. (1987) Consensus sequences of the Rattus norvegicus B1- and B2 repeats. *Nucleic Acids Res,* **15,** 2772.

Diatchenko, L., Nackley, A.G., Slade, G.D., Bhalang, K., Belfer, I., Max, M.B., Goldman, D. & Maixner, W. (2006) Catechol-O-methyltransferase gene

polymorphisms are associated with multiple pain-evoking stimuli. *Pain,* **125,** 216-224.

Dussault, A.A. & Pouliot, M. (2006) Rapid and simple comparison of messenger RNA levels using real-time PCR. *Biol Proced Online,* **8,** 1-10.

Goodier, J.L. & Kazazian, H.H., Jr. (2008) Retrotransposons revisited: the restraint and rehabilitation of parasites. *Cell,* **135,** 23-35.

Hasler, J. & Strub, K. (2006) Alu elements as regulators of gene expression. *Nucleic Acids Res,* **34,** 5491-5497.

Haynes, S.R. & Jelinek, W.R. (1981) Low molecular weight RNAs transcribed in vitro by RNA polymerase III from Alu-type dispersed repeats in Chinese hamster DNA are also found in vivo. *Proc Natl Acad Sci U S A,* **78,** 6130-6134.

Houck, C.M., Rinehart, F.P. & Schmid, C.W. (1979) A ubiquitous family of repeated DNA sequences in the human genome. *J Mol Biol,* **132,** 289-306.

Jagadeeswaran, P., Forget, B.G. & Weissman, S.M. (1981) Short interspersed repetitive DNA elements in eucaryotes: transposable DNA elements generated by reverse transcription of RNA pol III transcripts? *Cell,* **26,** 141-142.

Kass, D.H., Kim, J., Rao, A. & Deininger, P.L. (1997) Evolution of B2 repeats: the muroid explosion. *Genetica,* **99,** 1-13.

Kember, R.L., Fernandes, C., Tunbridge, E.M., Liu, L., Paya-Cano, J.L., Parsons, M.J. & Schalkwyk, L.C. (2010) A B2 SINE insertion in the Comt1 gene (Comt1(B21)) results in an overexpressing, behavior modifying allele present in classical inbred mouse strains. *Genes Brain Behav*.

Kim, J. & Deininger, P.L. (1996) Recent amplification of rat ID sequences. *J Mol Biol,* **261,** 322-327.

Knebelmann, B., Forestier, L., Drouot, L., Quinones, S., Chuet, C., Benessy, F., Saus, J. & Antignac, C. (1995) Splice-mediated insertion of an Alu sequence in the COL4A3 mRNA causing autosomal recessive Alport syndrome. *Hum Mol Genet,* **4,** 675-679.

Kramerov, D.A., Grigoryan, A.A., Ryskov, A.P. & Georgiev, G.P. (1979) Long double-stranded sequences (dsRNA-B) of nuclear pre-mRNA consist of a few highly abundant classes of sequences: evidence from DNA cloning experiments. *Nucleic Acids Res,* **6,** 697-713.

Krayev, A.S., Kramerov, D.A., Skryabin, K.G., Ryskov, A.P., Bayev, A.A. & Georgiev, G.P. (1980) The nucleotide sequence of the ubiquitous repetitive DNA sequence B1 complementary to the most abundant class of mouse fold-back RNA. *Nucleic Acids Res,* **8,** 1201-1215.

Krayev, A.S., Markusheva, T.V., Kramerov, D.A., Ryskov, A.P., Skryabin, K.G., Bayev, A.A. & Georgiev, G.P. (1982) Ubiquitous transposon-like repeats B1 and B2 of the mouse genome: B2 sequencing. *Nucleic Acids Res,* **10,** 7461-7475.

Kress, M., Barra, Y., Seidman, J.G., Khoury, G. & Jay, G. (1984) Functional insertion of an Alu type 2 (B2 SINE) repetitive sequence in murine class I genes. *Science,* **226,** 974-977.

Landry, J.R., Medstrand, P. & Mager, D.L. (2001) Repetitive elements in the 5' untranslated region of a human zinc-finger gene modulate transcription and translation efficiency. *Genomics,* **76,** 110-116.

Li, Z., Mulligan, M.K., Wang, X., Miles. M., Lu, L., Williams, R.W. (2010) A Transposon in Comt Generates mRNA Variants and Causes Widespread Expression and Behavioral Differences among Mice. *PLOS One,* **5,** 1-11.

Maichele, A.J., Farwell, N.J. & Chamberlain, J.S. (1993) A B2 repeat insertion generates alternate structures of the mouse muscle gamma-phosphorylase kinase gene. *Genomics,* **16,** 139-149.

Markert, M.L., Hutton, J.J., Wiginton, D.A., States, J.C. & Kaufman, R.E. (1988) Adenosine deaminase (ADA) deficiency due to deletion of the ADA gene promoter and first exon by homologous recombination between two Alu elements. *J Clin Invest,* **81,** 1323-1327.

Michel, D., Chatelain, G., Mauduit, C., Benahmed, M. & Brun, G. (1997) Recent evolutionary acquisition of alternative pre-mRNA splicing and 3' processing regulations induced by intronic B2 SINE insertion. *Nucleic Acids Res,* **25,** 3228-3234.

Mustajoki, S., Ahola, H., Mustajoki, P. & Kauppinen, R. (1999) Insertion of Alu element responsible for acute intermittent porphyria. *Hum Mutat,* **13,** 431-438.

Myerowitz, R. & Hogikyan, N.D. (1987) A deletion involving Alu sequences in the beta-hexosaminidase alpha-chain gene of French Canadians with Tay-Sachs disease. *J Biol Chem,* **262,** 15396-15399.

Nackley, A.G., Shabalina, S.A., Tchivileva, I.E., Satterfield, K., Korchynskyi, O.,

Makarov, S.S., Maixner, W. & Diatchenko, L. (2006) Human catechol-O-methyltransferase haplotypes modulate protein expression by altering mRNA secondary structure. *Science,* **314,** 1930-1933.

Nekrutenko, A. & Li, W.H. (2001) Transposable elements are found in a large number of human protein-coding genes. *Trends Genet,* **17,** 619-621.

Ohshima, K., Koishi, R., Matsuo, M. & Okada, N. (1993) Several short interspersed repetitive elements (SINEs) in distant species may have originated from a common ancestral retrovirus: characterization of a squid SINE and a possible mechanism for generation of tRNA-derived retroposons. *Proc Natl Acad Sci U S A,* **90,** 6260-6264.

Okada, N. (1991) SINEs. *Curr Opin Genet Dev,* **1,** 498-504.

Rogers, J.H. (1985) The origin and evolution of retroposons. *Int Rev Cytol,* **93,** 187-279.

Roman, A.C., Benitez, D.A., Carvajal-Gonzalez, J.M. & Fernandez-Salguero, P.M. (2008) Genome-wide B1 retrotransposon binds the transcription factors dioxin receptor and Slug and regulates gene expression in vivo. *Proc Natl Acad Sci U S A,* **105,** 1632-1637.

Rothkopf, G.S., Telakowski-Hopkins, C.A., Stotish, R.L. & Pickett, C.B. (1986) Multiplicity of glutathione S-transferase genes in the rat and association with a type 2 Alu repetitive element. *Biochemistry,* **25,** 993-1002.

Roy, A.M., Gong, C., Kass, D.H. & Deininger, P.L. (1998) Recent B2 element insertions in the mouse genome. *DNA Seq,* **8,** 343-348.

Ryskov, A.P., Ivanov, P.L., Kramerov, D.A. & Georgiev, G.P. (1984) [Universal orientation and 3'-terminal localization of repeated sequences in the B2 family of mRNA]. *Mol Biol (Mosk),* **18,** 92-103.

Sakamoto, K. & Okada, N. (1985) Rodent type 2 Alu family, rat identifier sequence, rabbit C family, and bovine or goat 73-bp repeat may have evolved from tRNA genes. *J Mol Evol,* **22,** 134-140.

Schichman, S.A., Caligiuri, M.A., Strout, M.P., Carter, S.L., Gu, Y., Canaani, E., Bloomfield, C.D. & Croce, C.M. (1994) ALL-1 tandem duplication in acute myeloid leukemia with a normal karyotype involves homologous recombination between Alu elements. *Cancer Res,* **54,** 4277-4280.

Segall, S.N., AG; Diatchenko, L; Lariviere, W; Lu, X; Marron, J; Grabowski-Boase, L; Walker, J: Slade, G; Bailey, JS; Gauthier, J; Steffy, BM; Maynard, T; Tarantino, L; Wiltshire, T (2010) Comt1 Genotype and

Expression Predicts Anxiety and Nociceptive Sensitivity in Inbred Strains of Mice. *Genes, Brain and Behavior*.

Serdobova, I.M. & Kramerov, D.A. (1998) Short retroposons of the B2 superfamily: evolution and application for the study of rodent phylogeny. *J Mol Evol,* **46,** 202-214.

Smalheiser, N.R. & Torvik, V.I. (2006) Alu elements within human mRNAs are probable microRNA targets. *Trends Genet,* **22,** 532-536.

Smit , A.F. (2005) B2_Mm1t - a subfamily of SINEs from mouse.

So, C.W., Ma, Z.G., Price, C.M., Dong, S., Chen, S.J., Gu, L.J., So, C.K., Wiedemann, L.M. & Chan, L.C. (1997) MLL self fusion mediated by Alu repeat homologous recombination and prognosis of AML-M4/M5 subtypes. *Cancer Res,* **57,** 117-122.

Sobczak, K. & Krzyzosiak, W.J. (2002) Structural determinants of BRCA1 translational regulation. *J Biol Chem,* **277,** 17349-17358.

Sorek, R., Ast, G. & Graur, D. (2002) Alu-containing exons are alternatively spliced. *Genome Res,* **12,** 1060-1067.

Strout, M.P., Marcucci, G., Bloomfield, C.D. & Caligiuri, M.A. (1998) The partial tandem duplication of ALL1 (MLL) is consistently generated by Alu-mediated homologous recombination in acute myeloid leukemia. *Proc Natl Acad Sci U S A,* **95,** 2390-2395.

Swensen, J., Hoffman, M., Skolnick, M.H. & Neuhausen, S.L. (1997) Identification of a 14 kb deletion involving the promoter region of BRCA1 in a breast cancer family. *Hum Mol Genet,* **6,** 1513-1517.

Teugels, E., De Brakeleer, S., Goelen, G., Lissens, W., Sermijn, E. & De Greve, J. (2005) De novo Alu element insertions targeted to a sequence common to the BRCA1 and BRCA2 genes. *Hum Mutat,* **26,** 284.

Tian, B., Pan, Z. & Lee, J.Y. (2007) Widespread mRNA polyadenylation events in introns indicate dynamic interplay between polyadenylation and splicing. *Genome Res,* **17,** 156-165.

Ullu, E. & Tschudi, C. (1984) Alu sequences are processed 7SL RNA genes. *Nature,* **312,** 171-172.

Xie, T., Ho, S.L. & Ramsden, D. (1999) Characterization and implications of estrogenic down-regulation of human catechol-O-methyltransferase gene transcription. *Mol Pharmacol,* **56,** 31-38.

Zheng, J.H., Natsuume-Sakai, S., Takahashi, M. & Nonaka, M. (1992) Insertion of the B2 sequence into intron 13 is the only defect of the H-2k C4 gene which causes low C4 production. *Nucleic Acids Res,* **20,** 4975-4979.

Figure 3.1 Consensus *Mus Musculus* B2 SINE family sequence and the B2 insertion in the 3'UTR of *Comt1.* SNPs are denoted by highlight and star above. B2 SINE sequence (top) is from a direct submission to Repbase (Smit 2005). Reference (bottom) is from C57BL/6J transcript NM_1111063.

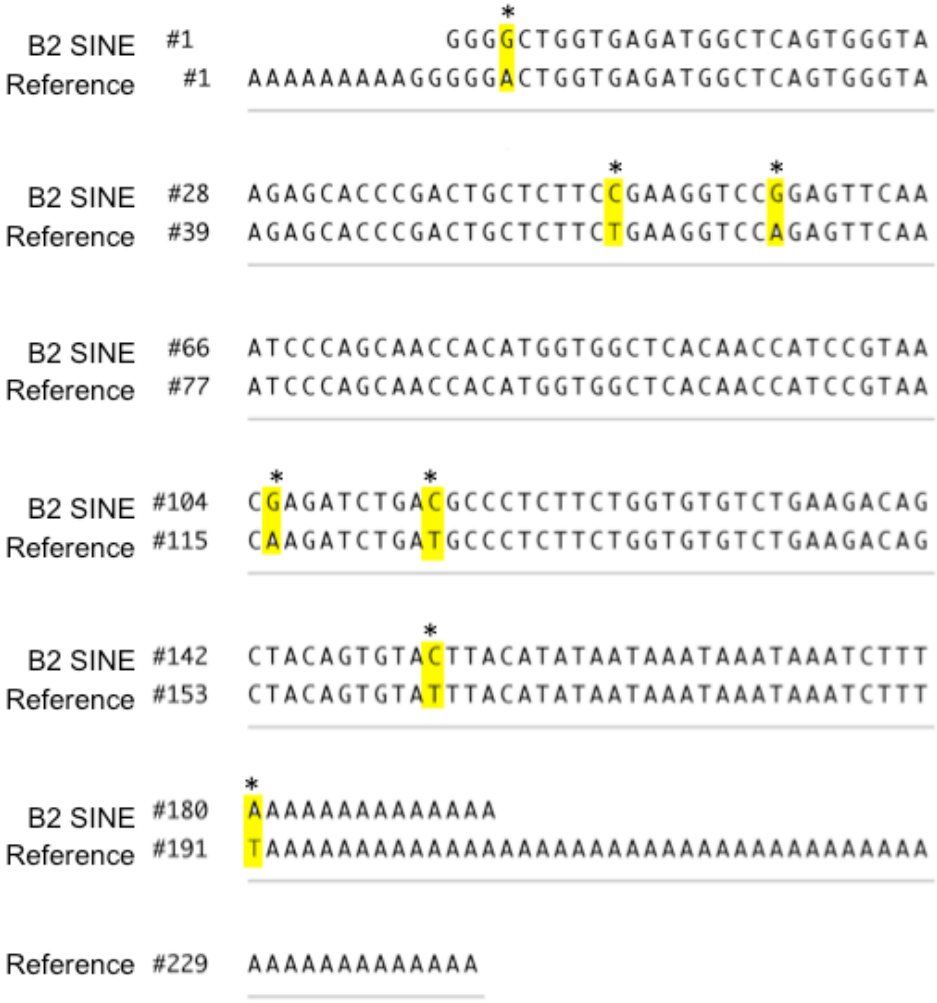

Figure 3.2 Identification of polyadenylation signal in *Comt1*^{B2i}. **a.** Full mRNA sequence of *Comt1*^{B2} from C57BL6/J, NM_0001111063 transcript. B2 SINE insertion is highlighted in pink. **b.** Sequence of polyadenylation hexamers and frequency found in the mouse genome .

(a)

TGGGTATATAAAGGCTCAGGCCCAGTGTGCATGCAGAGTGACCACATGAGCACTCTGCCTTTTGGAAATAGGTGAC
ATGAGTGTGTGGGCTGTAGAGCCTCAGCTTTGAGGTCCCTCTCTTGAGACTATCCTGAAGCAGCCCTCACACCTAG
GGCTTGGACCTGCCTCCTCTAAAGACTCTTCCACAAGCCTTCCCAACCTAGATCAGCACTCTACCCTGGAAGGAACT
ATGCTGTTGGCTGCTGTCTCATTGGGTCTCCTGTTGCTGGCCTTCCTCCTGCTCCTGCGACACCTAGGCTGGGGCT
TGGTGGCTATTGGTTGGTTTGAGTTCGTGCAGCAGCCGGTCCACAACCTGCTCATGGGTGGCACAAAGGAGCAGC
GCATCCTGCGCCATGTGCAGCAACACGCAAAGCCTGGAGACCCCCAGAGCGTCCTGGAGGCCATTGATACCTACT
GCTCAGAGAAGGAGTGGGCCATGAACGTGGGTGACGCAAAAGGCCAAATCATGGATGCAGTGATTCGGGAGTACA
GGCCCTCGCTGGTGCTGGAGCTAGGAGCTTATTGTGGCTACTCAGCCGTGCGAATGGCCCGCCTGCTGCCACCTG
GAGCCAGGCTTCTCACCATGGAGATTAACCCTGACTACGCTGCCATCACCCAGCAAATGCTGGACTTCGCAGGCCT
ACAGGACAAAGTTTCCATCCTCATCGGGGCATCCCAGGACCTTATCCCCCAGCTGAAGAAGAAGTACGATGTGGAC
ACATT**AGACATGGTCTTTCTTGACCACTGGAAAGACCGCTACCTTCCAGACACACTTCTCCTGGAGGAATGTGGC**
CTGCTGCGCAAGGGGACGGTGCTCCTAGCTGACAATGTCATTGTCCCGGGAACCCCTGACTTCCTGGCGTATGTG
AGGGGGAGCAGCAGCTTCGAGTGCACACACTACAGCTCATACCTGGAGTACATGAAAGTGGTGGACGGCTTGGA
GAAGGCAGTCTACCAGGGTCCAGGCAGCAGCCCCGTGAAGTCCTGACCACTCAGCCTGATGAGCTTCCGTCCCAG
CTCCCTTCTGCACGATGACACACACTCACTCTGACCCCCTCTATGCTTCTGGGGCCTTTCCTCAGGGCCTGTGGCT
CCAGATTGTCATACACTGGCACATTAAAGGTAGTGAGCTCACCATGCAAACCACTACAATACCCCTGGAAAACACCT
GTGCATCAAAGGCTGCATTGAGGCCAGAGATGCAGTAGATCACAGTGCGTGCCTGGCACGCAAAACCCCTCACGG
TGAATCCTCTGCACCCAAGAACAAAAAGGGAGATTTAAAAAAAAAAAAAAAAGGGGGACTGGTGAGATGGCTCAGTG
GGTAAGAGCACCCGACTGCTCTTCTGAAGGTCCAGAGTTCAAATCCCAGCAACCACATGGTGGCTCACAACCATCC
GTAACAAGATCTGATGCCCTCTTCTGGTGTGTCTGAAGACAGCTACAGTGTATTTACATATAATAAATAAATAAATCT
TTTAAAAAAAAAAAAAAAAAAAAAAAAAAAAAAAAAAAAAAAAAAAAAAAAAAAAAAAAAAAAAAATC**AAAGCAGGTGTCATCCTGATG**
GCCTCACTAACTGGAAGAGGAGATTTTTTACAAAGTTTCAGTGTGGGATCCCTAGGCACTGCCATCACTCAGCAA
GAAGTCAGGAAACTGAACATATCCAGATACCATTCGGCTGTCACCAATGGCAGCAACGACTCAGACGGTACTGT
CACCAGCAACTCATACCACATTTCATCTTAAGAATGAGTCACAAACTTTTCAGGTATGATGGCGCATGCCTTTAATC
CCAGAATCCAGGAGGCAGAGGCAGATGGATCTGAGTTCTGTGCCAGCCTGGTCTACACAGTGAGTTCCAGGACAG
CCAGGGCTACATAGAAATACTTTGAAAAAAAAAGTCATAATCTCTTTTATATTATAAAAGAAATTAAAGATCTAAATAT
TTGGATATAAAAAAAAAAAAAAAAAAAAAAAAAAAA

1449183_at probe set **1418701_at probe set**

B2 SINE INSERTION, B1 SINE INSERTION (overlap with 1418701_at)

(b) AATAAA 59.16% TATAAA 3.79% TTTAAA 1.08%

ATTAAA 16.11% AAGAAA 3.28%

Figure 3.3. cDNA structure of *Comt1*^{B2i} illustrating exons, positions of B2 insertion, Affymetrix and TaqMAN probe sets, diagnostic PCR primers and coding exons.

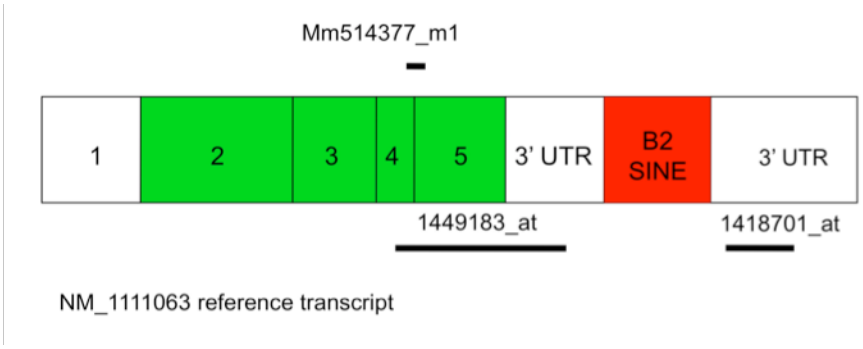

Figure 3.4. (Following pages) Gene expression values for *Comt1* in both coding and UTR regions in seven brain regions of all surveyed strains, male and female. Results are also characterized by the presence (red) or absence (blue) of the B2 SINE element in the 3'UTR of *Comt1.* **a.** amygdala, **b.** hippocampus, **c**. hypothalamus, **d.** nucleus accumbens, **e.** pituitary, **f.** prefrontal cortex, **g.** striatum.

Figure 3.4

(a) Expression in coding region

Expression 3' of B2 element in 3'UTR region

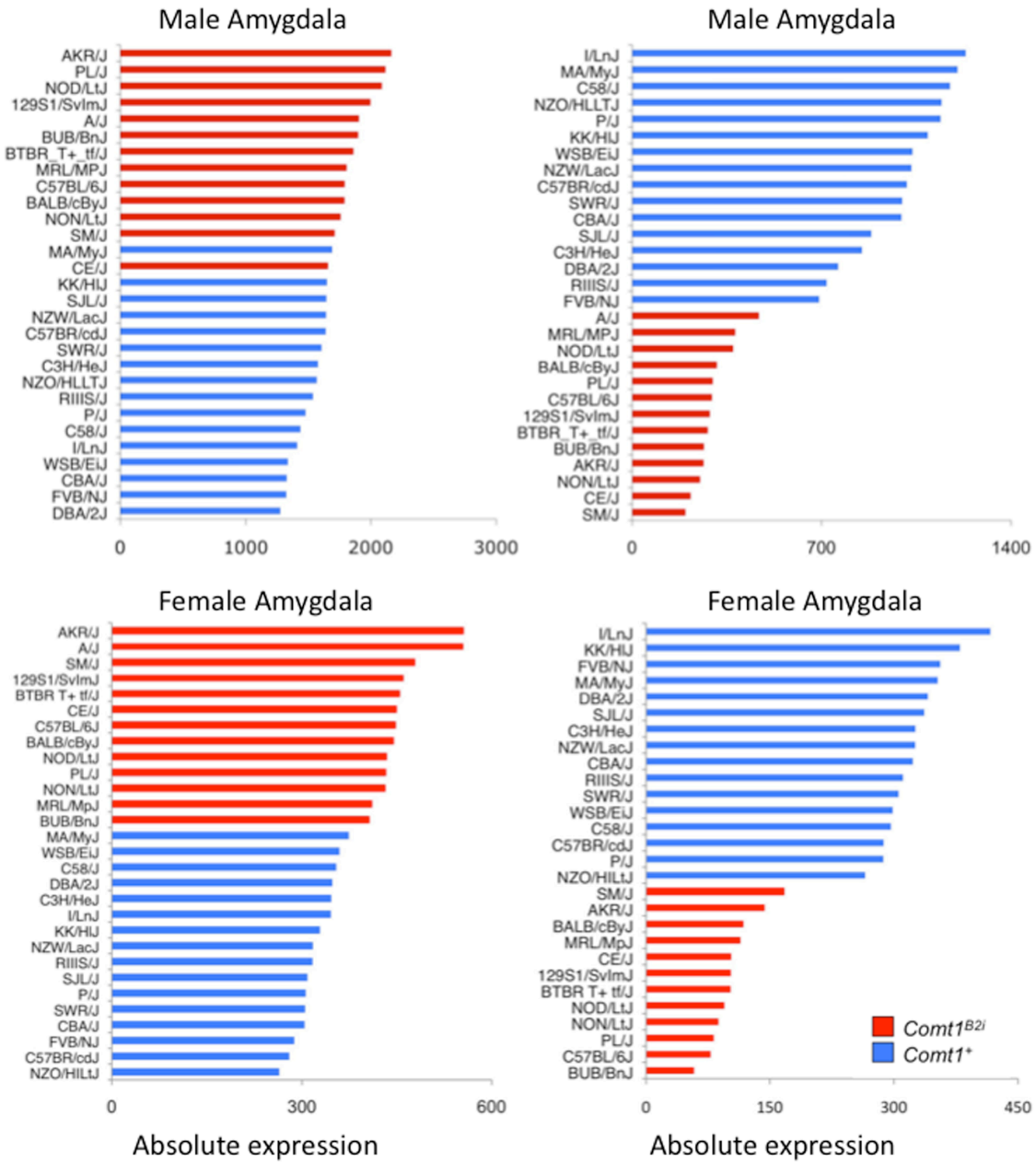

1449183_at probe set

1418701_at probe set

Figure 3.4

(b) Expression in coding region

Expression 3' of B2 element in 3'UTR region

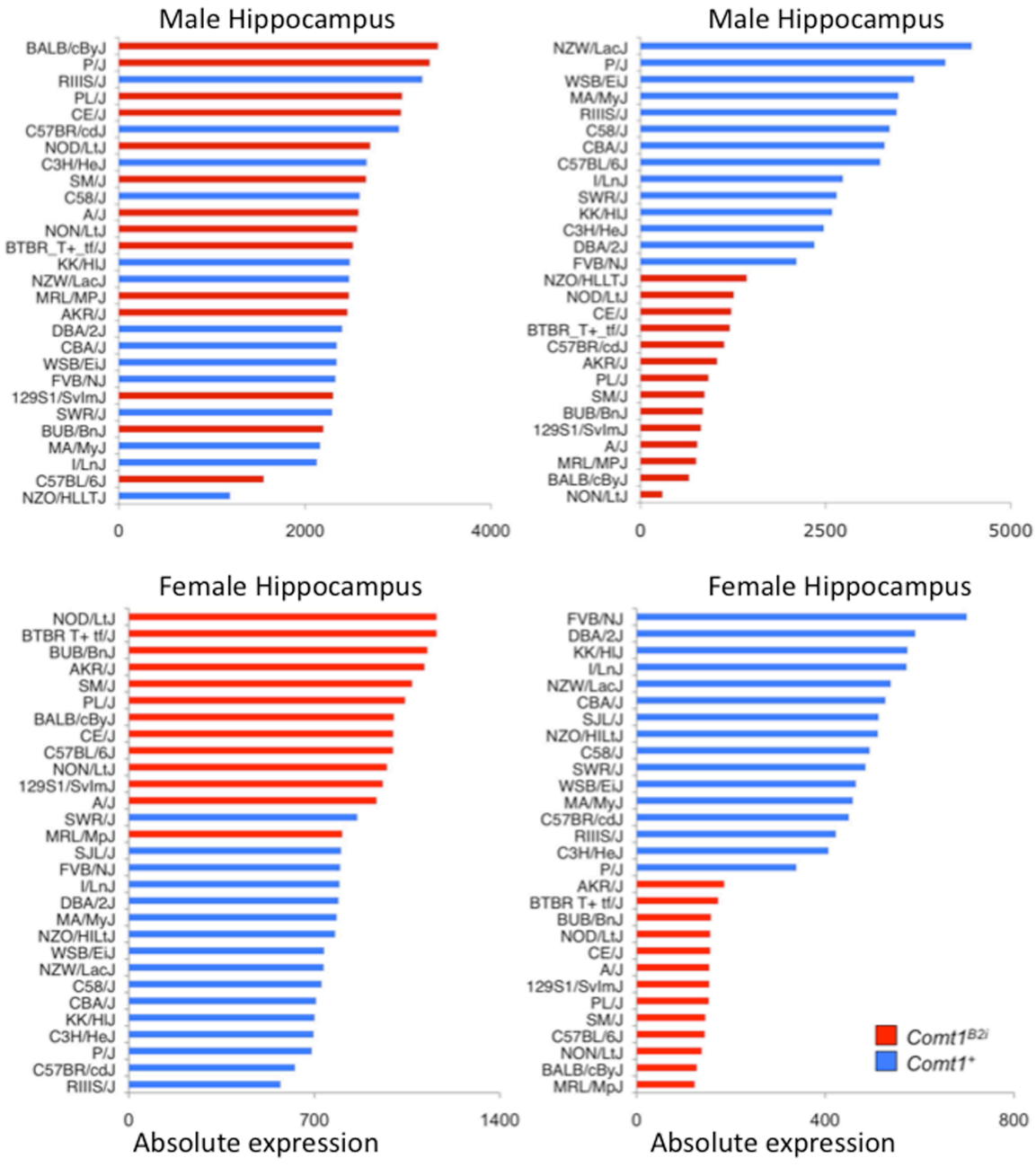

1449183_at probe set

1418701_at probe set

Figure 3.4

(c) Expression in coding region

Expression 3' of B2 element in 3'UTR region

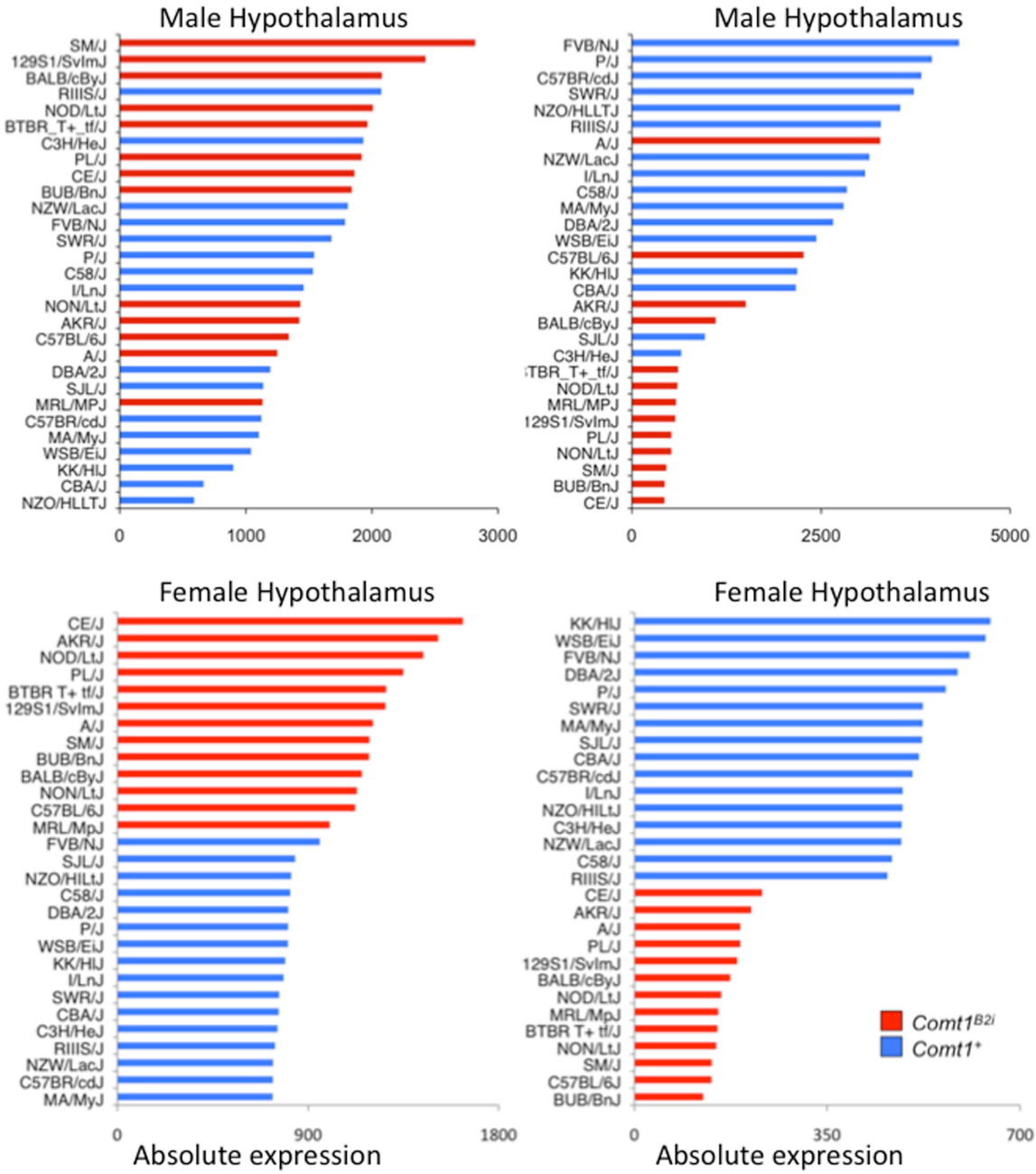

1449183_at probe set

1418701_at probe set

Figure 3.4

(d) Expression in coding region

Expression 3' of B2 element in 3'UTR region

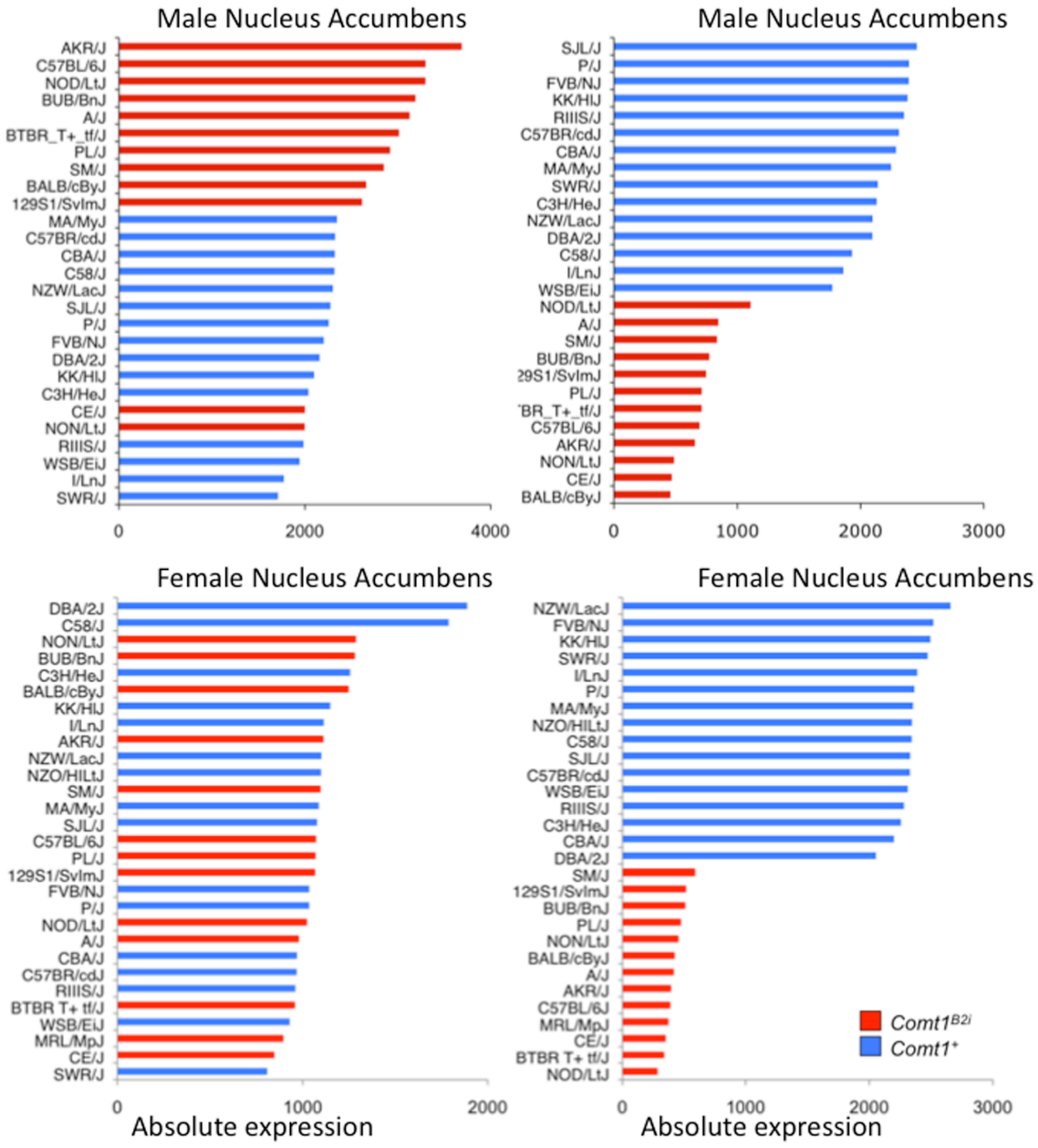

1449183_at probe set

1418701_at probe set

Figure 3.4

(e) Expression in coding region

Expression 3' of B2 element in 3'UTR region

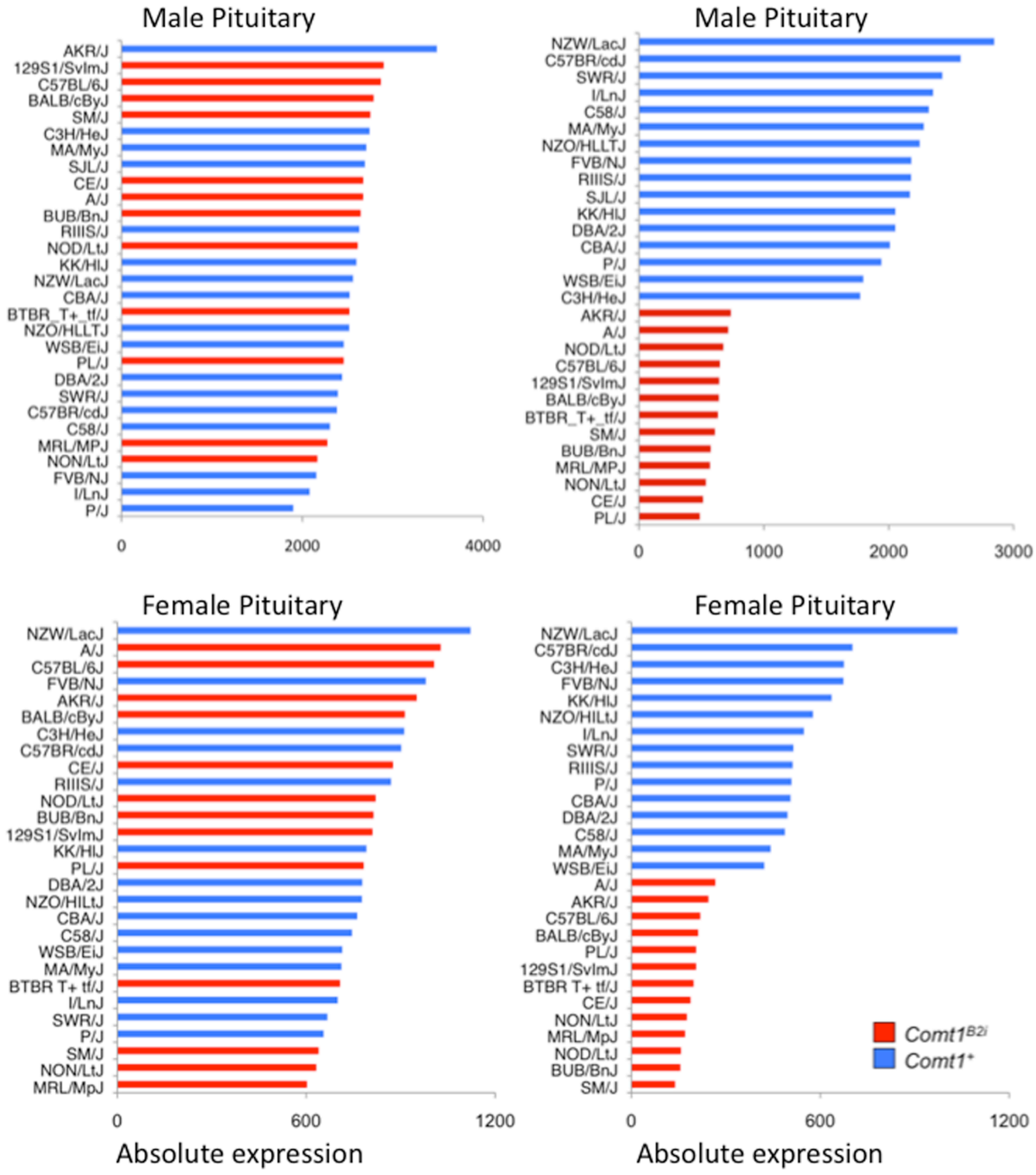

1449183_at probe set

1418701_at probe set

Figure 3.4

(f) Expression in coding region

Expression 3' of B2 element in 3'UTR region

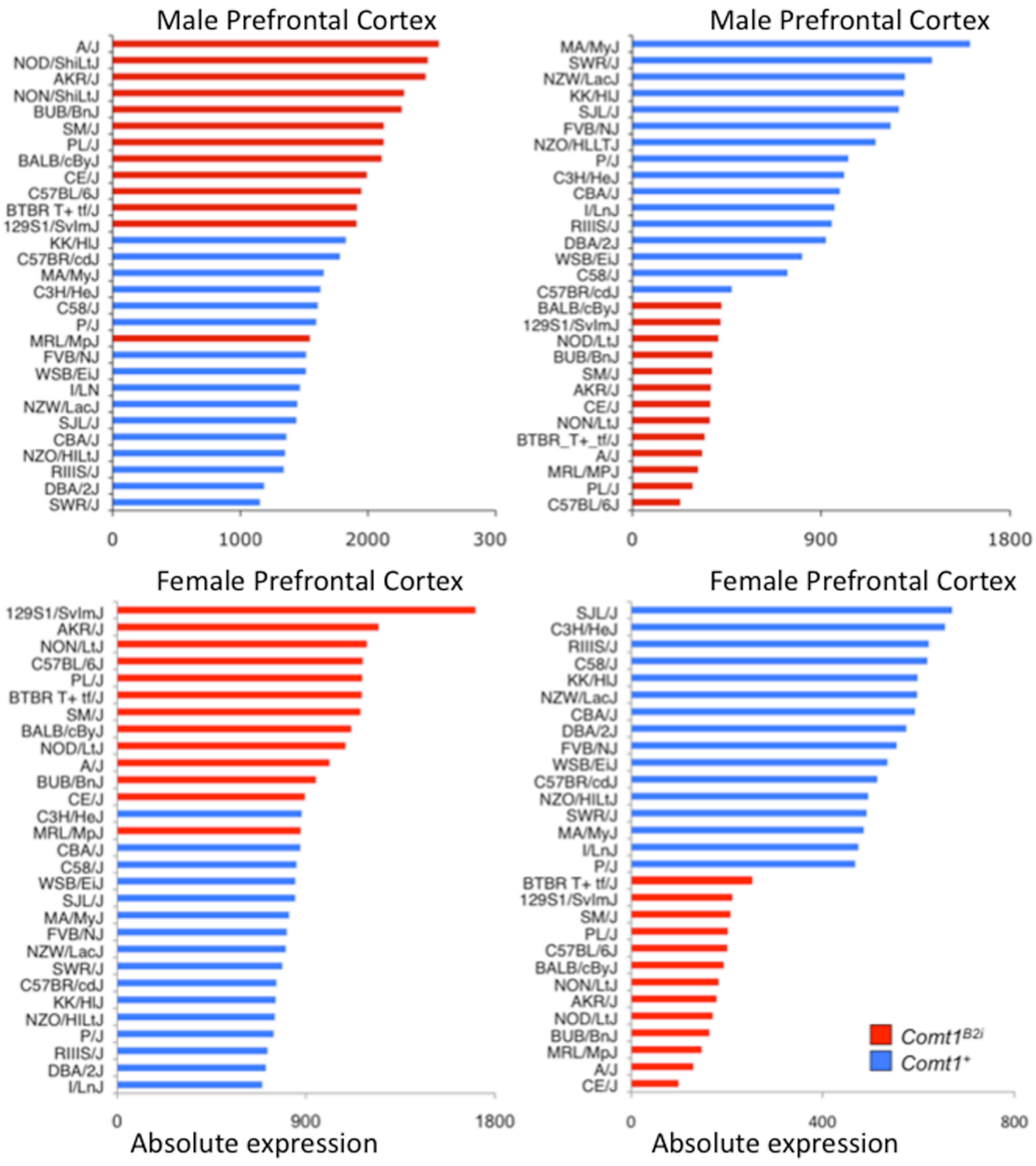

1449183_at probe set

1418701_at probe set

Figure 3.4

(g) Expression in coding region

Expression 3' of B2 element in 3'UTR region

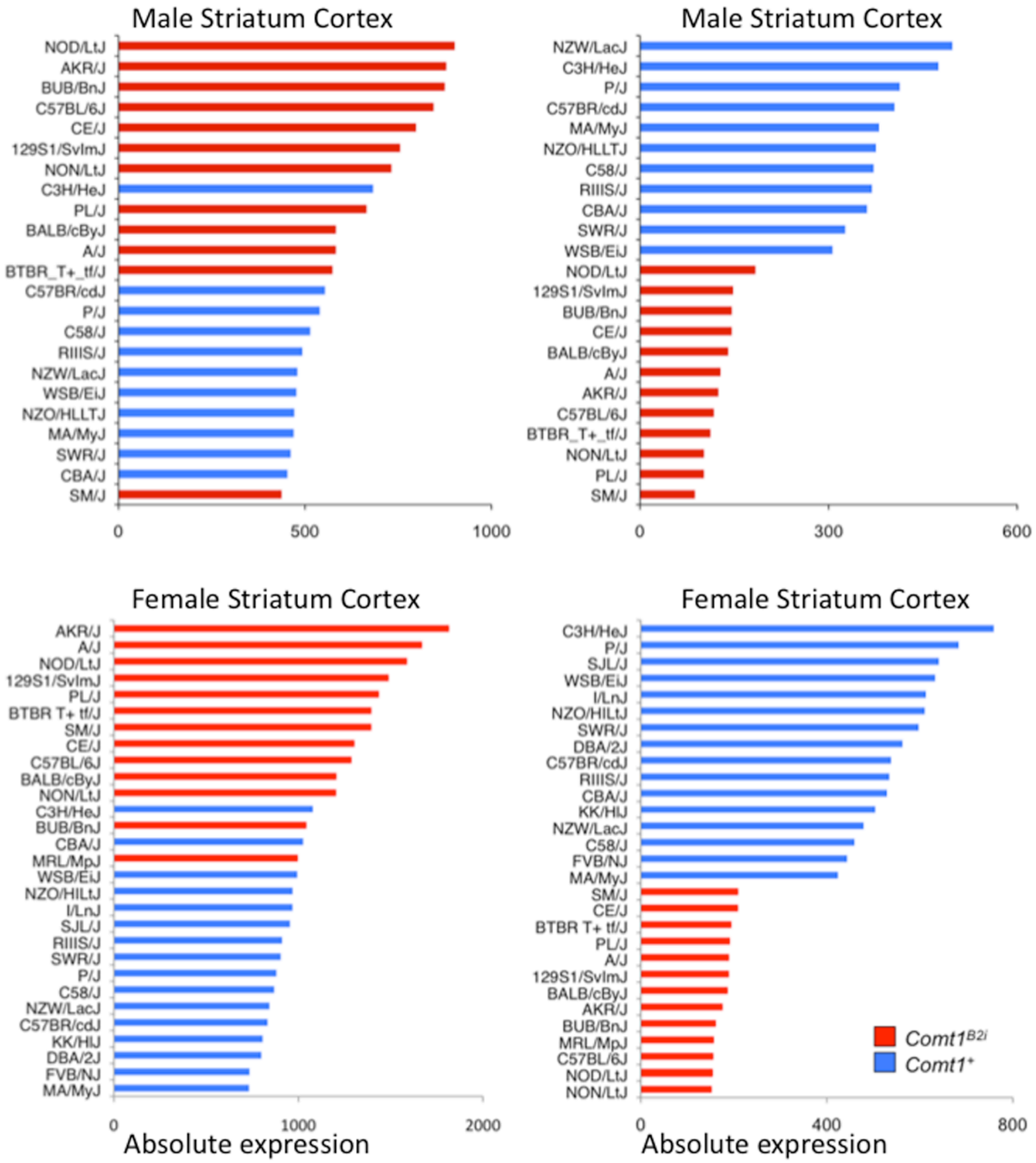

1449183_at probe set

1418701_at probe set

Figure 3.5 Z-score of *Comt1* mRNA in seven brain regions across all surveyed strains. The difference between *Comt1*^{B2i} and *Comt1*$^{+}$ mRNA was significant, P<0.0001. Males have significantly more *Comt1* mRNA than females, P<0.0001. Interaction between B2 SINE status and sex (P=0.0713) shows the difference between *Comt1*^{B2i} and *Comt1*$^{+}$ were similar in both sexes. *** P<0.0001.

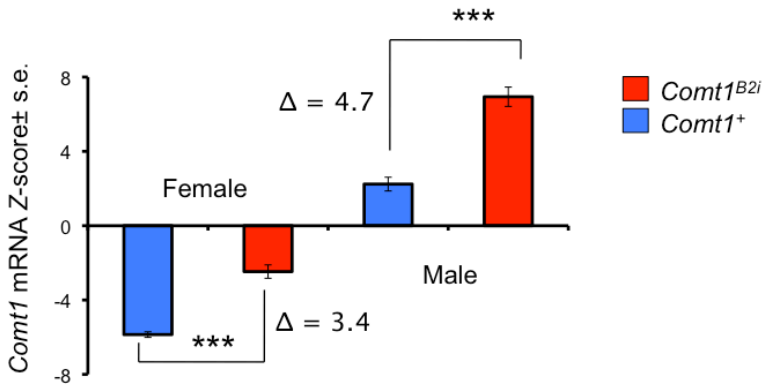

Figure 3.6. Functional analysis of *Comt1* variants. Microarray gene expression results were validated using Taqman assays. **a.** qPCR from RNA: 4 strains, 4 male 10 week old animals per strain, for a total of 16 animals in this analysis. Each animal had a separate qPCR reaction, with three technical replicates. Data normalized to C3H/HeJ and then analyzed by 1-tailed unpaired t-test. **P<0.01, ***P<0.001, *Comt1*^{B2i} more RNA in coding region.

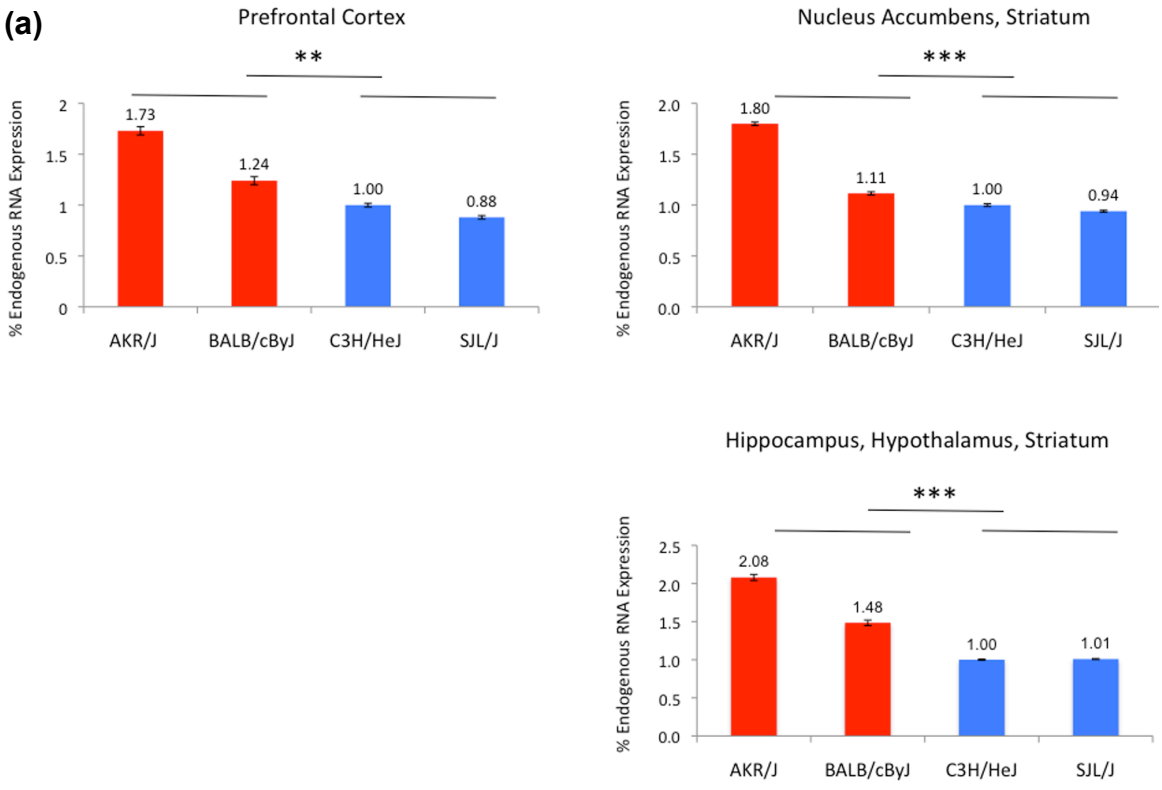

Figure 3.6 b. An ELISA assay was developed to assess COMT1 protein levels. COMT1 protein levels in cortex, nucleus accumbens/striatum, hippocampus/ hypothalamus/amygdala were measured for 10 week old male animals in 7 strains. Tissue was pooled from 2 animals per strain. Error bars are standard deviation in eight technical replicates. Two runs were preformed, and data normalized to C3H/HeJ and then analyzed by strain means in a 1-tailed unpaired t-test with unequal varience, *P<0.05,*Comt1*$^{+}$ more protein. **c.** Enzymatic activity of COMT1 protein was measured using a Normetanephrine ELISA assay. Same samples as used in **a,** cortex and nucleus accumbens/striatum. Error bars are standard deviation in five technical replicates. One run was preformed, and data analyzed by strain means in a 1-tailed unpaired t-test with unequal variance, ***P<0.001, *Comt1*^{B2i} more enzymatic activity. **d.** Western blot of a transfection of cell constructs of both haplotypes.

Figure 3.6: b, c.

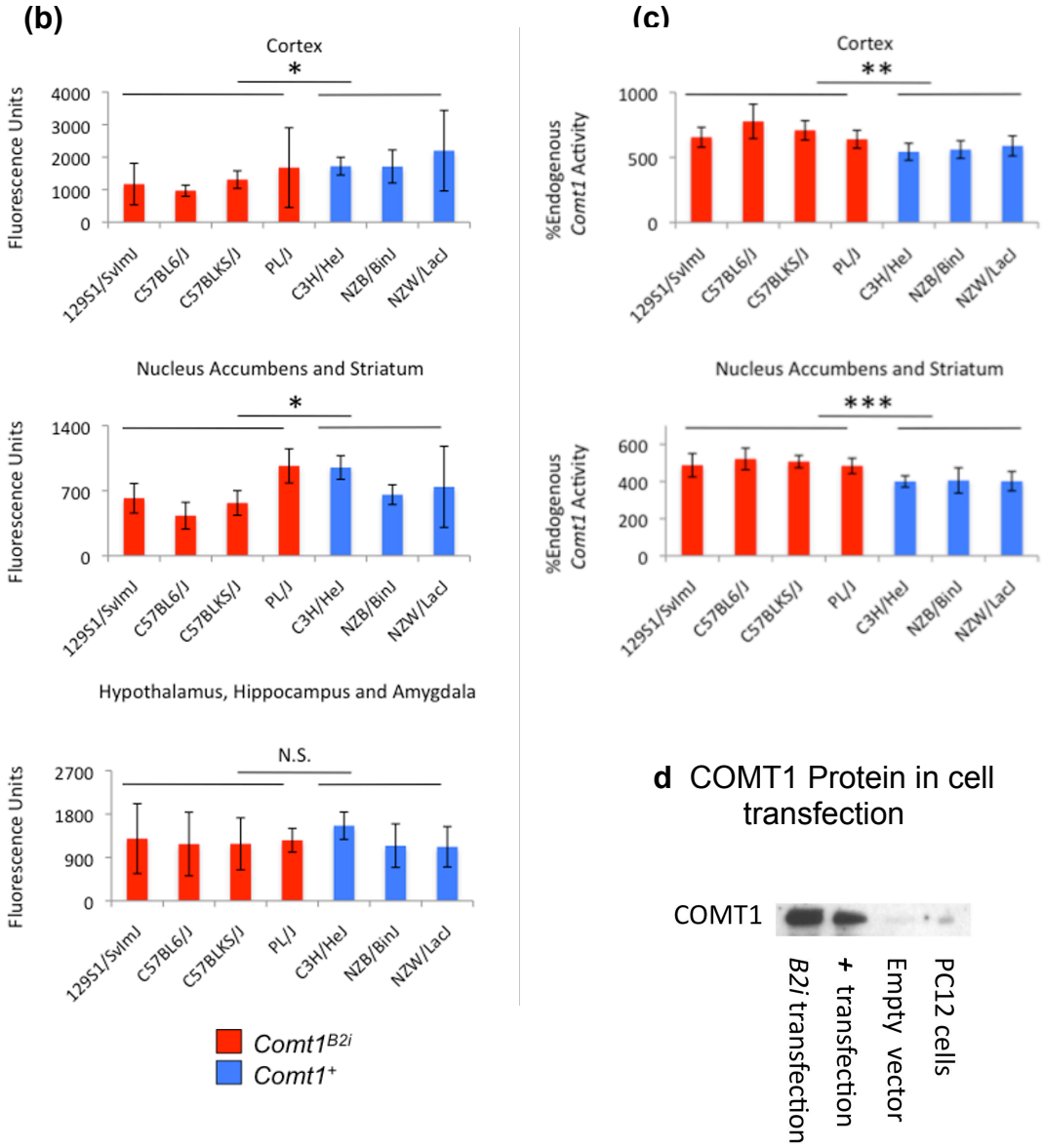
(b)
(c)
Cortex
*
**
Fluorescence Units
%Endogenous Comt1 Activity
4000
3000
2000
1000
0
500
129S1/SvImJ
C57BL6/J
C57BLKS/J
PL/J
C3H/HeJ
NZB/BinJ
NZW/LacJ
Nucleus Accumbens and Striatum
***
1400
700
600
400
200
Hypothalamus, Hippocampus and Amygdala
N.S.
2700
1800
900
Comt1B2i
Comt1+
d COMT1 Protein in cell transfection
COMT1
B2i transfection
+ transfection
Empty vector
PC12 cells

Figure 3.7 Analysis of *Comt1*^{B2i} RNA abundance. Mock cDNA (no reverse transcriptase enzyme added) was run in all experiments. **a.** Semiquantitative PCR using which primers flanking B2 insertion (halted at 30 cycles) showed two products in the cell transfection of the *Comt1*^{B2i} construct. Very little product is produced in this region in tissue samples, while the PCR product without the B2 element is robustly expressed.

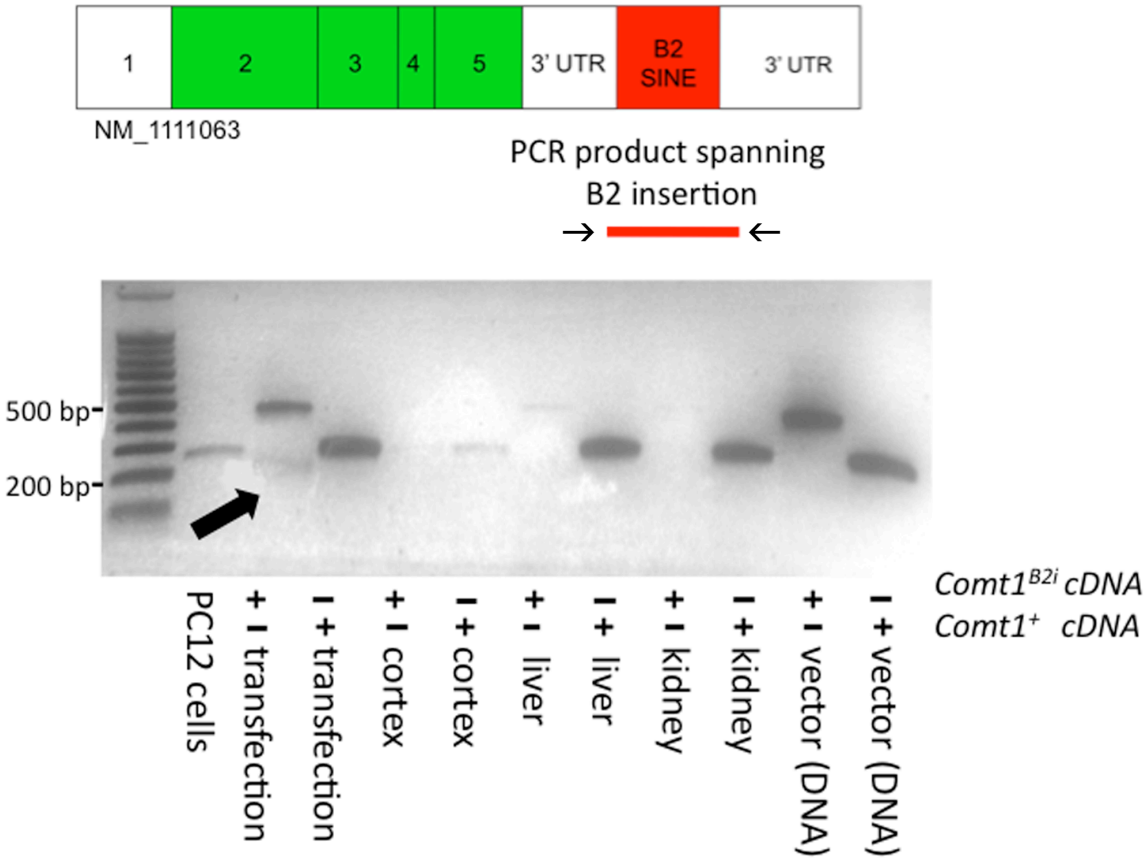

Figure 3.7 b. Semiquantitative PCR using primers amplifying region within 1418701_at probe set. In strains of the B2 insertion, less PCR product is made 3' of the B2 insertion. cDNA was made from an individual animal per strain from Hippocampus/Hypothalamus/Amygdala tissue.

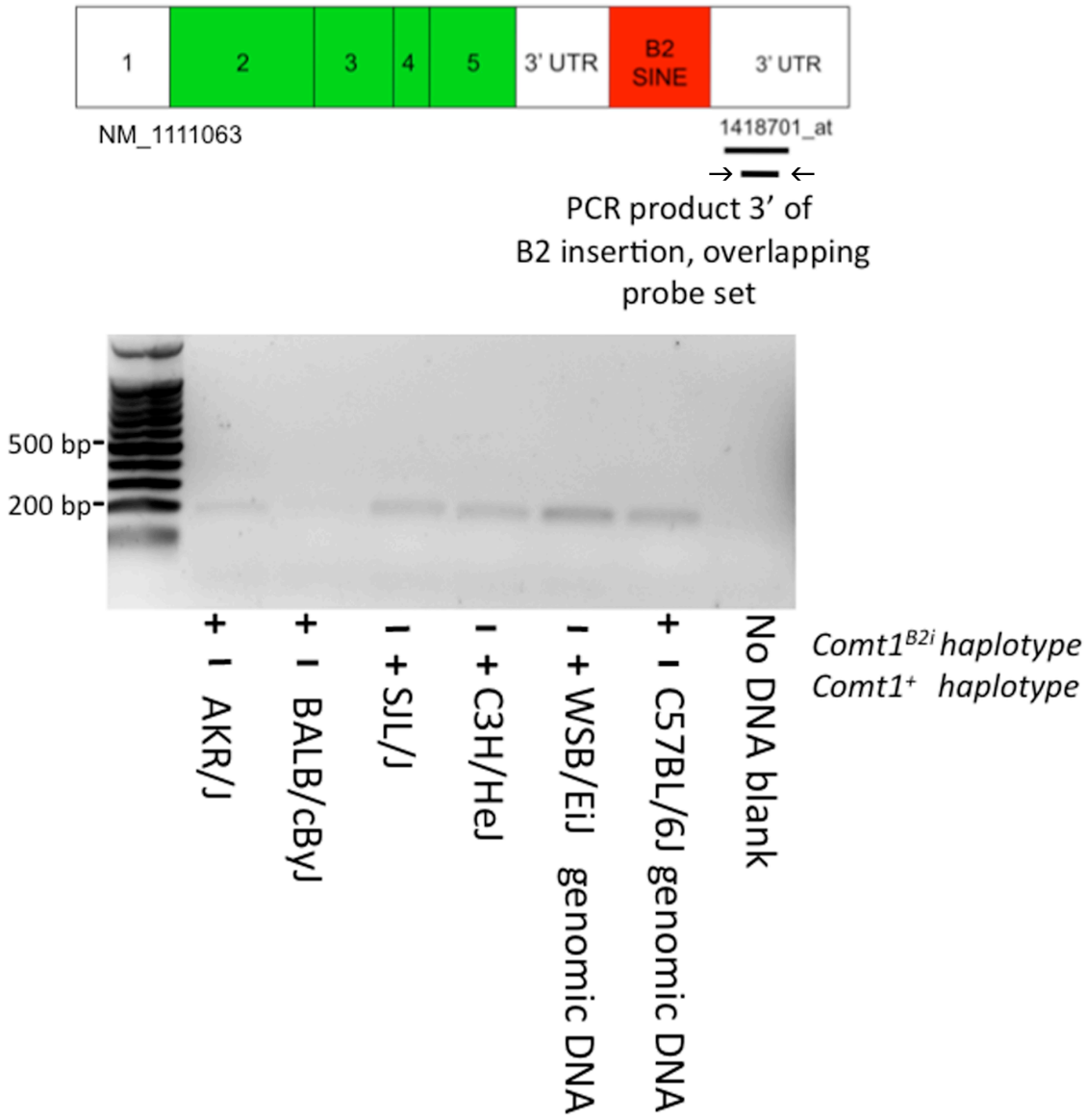

Figure 3.7 c. qPCR throughout the transcript showed variable amounts of coding transcript, a very high amount of transcript within the B2 insertion, and very low expression of transcript 3' of the B2 insertion in cortex, liver and transfection samples in the *Comt1*^{B2i} compared to *Comt1*$^{+}$. Ratio is to ancestral *Comt1*$^{+}$ tissue or construct, using the formula: fold increase = $2^{\wedge_{\Delta\Delta}CT}$ (Dussault & Pouliot 2006).

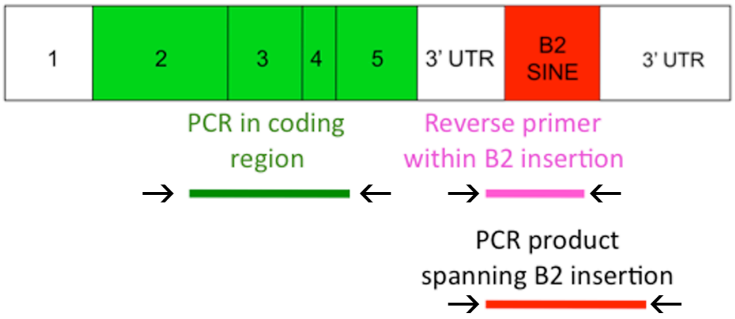

cDNA source	PCR coding CT	PCR within B2 insertion CT	PCR spanning B2 insertion CT	PCR coding ratio	PCR within B2 insertion ratio	PCR spanning B2 insertion ratio
Comt1^{+} cortex	28.89	31.54	29.80	1.00	1.00	1.00
Comt1^{B2i} cortex	23.95	22.68	36.01	19.23	292.60	0.008
Comt1^{+} liver	21.42	30.17	23.97	1.00	1.00	1.00
Comt1^{B2i} liver	21.87	22.25	35.05	0.53	176.49	0.00
Comt1^{+} vector	18.80	30.5	21.50	1.00	1.00	1.00
Comt1^{B2i} vector	16.69	16.91	22.55	1.97	4730.68	0.22

Figure 3.8 Transcript stability in actD assay. Two transfections on separate days of *Comt1*^{B2i} and *Comt1*$^{+}$ constructs had nearly identical degradation rates, as measured by Taqman probe Mm_ 514377 in the coding region.

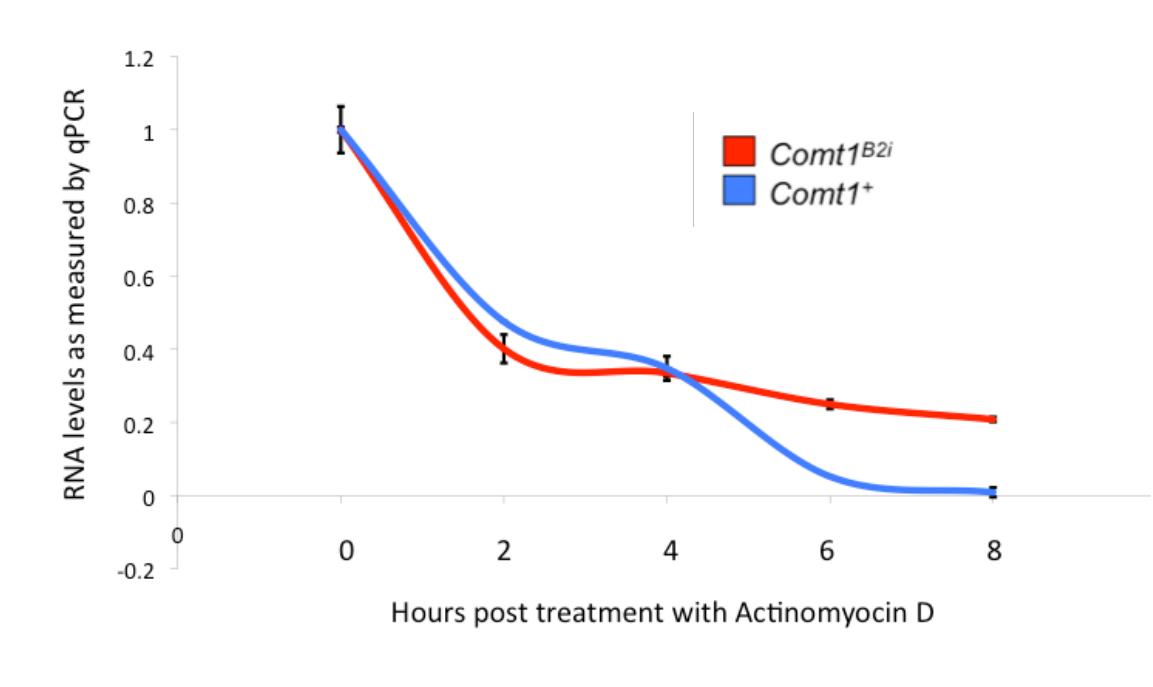

Table 3.1 SINE Repeat Elements in Human and Mouse

	Family	Ancestral sequence	Structure	≈ bp	Component of Genome	Publications
Mouse	B1	7SL RNA gene	monomers with internal 29bp duplication	≈140	2.20%	Krayev e*t. al.,*1980, Ullu & Tschudi, 1984
	B2	$tRNA^{Lys}$ or $tRNA^{Gly}$	5' homology with tRNALys or tRNAGly	≈160	2.00%	Krayev *et. al.,* 1982
	ID	$tRNA^{Ala}$	75bp core region, 10-40bp poly A tail	≈90	0.10%	Kim & Deininger, 1996
	B4	ID and B1	fusion of ID element at 5' end and B1 elements at 3' end	≈150	1.80%	Serdobova & Kramerov, 1998
Human	Alu	7SL RNA gene	dimer, center A-rich region flanked by short intact direct repeats	≈300	10.10%	Houck *et. al.,* 1979

Table 3.2 Consequences of SINE activity in Human Genomes

SINE Family and Mutation Class	Consequence	Mechanism	Change of Gene Function	Publication
de novo Alu insertion	insertional mutagenesis	in frame deletion of exon	breast cancer	Teugels *et. al.,* 2005
	aberrant splicing	insertion of sequence leads to misfolded protein	Cystic Fibrosis	Chen *et.al,* 2008
	truncated protein	frame shift or stop codon, poly (A) signals premature termination	acute intermittent porphyria	Mustajoki *et. al.,* 1999
de novo mutation within Alu insertion	aberrant splicing	Alu elements contain cryptic splice sites. A single nucleotide mutation within the SINE element may cause alternative splicing and/or deletion of sequence critical to gene function.	Alport syndrome	Knebelmann *et. al.,* 1995
	transcription repression	microsatellite expansion	Friedreich ataxia	Clark *et. al.,* 2004
nonallelic homologous recombination between Alu elements	gene duplication	mispairing of SINE sequence and crossing over results in duplication of part of the gene	acute myeloid leukemia	Schichman *et.al*., 1994 So *et.al.,* 1997 Strout *et.al*., 1998
	gene deletion	mispairing of SINE sequence and crossing over results in deletion of part of the gene	* Tay-Sachs ** breast cancer *** adenosine deaminase deficiency	* Myerowitz & Hogikyan, 1987 ** Swensen *et.al.,* 1997 *** Markert *et. al.,* 1988

Table 3.3 Consequences of SINE activity in Mouse Genome

SINE Family and Mutation Class	Mechanism	Change of Gene Function	Publication
B1-X35S	recruit transcription factors Ahr and Slug	B1-X35S containing genes have repressed expression compared to canonical B1 containing genes	Roman *et. al.,* 2008
de novo B2 5'UTR insertion	putative increased stability of mRNA secondary structure	decreased levels of 5-Amino levulinic acid synthase 1	Chernova *et.al.,* 2008
B2 3'UTR insertion	alternative 3' processing and alternative splicing	soluble form of protein synthesized in tissue specific manner; soluble form not found in rat or human	Michel *et. al.,* 1997
	novel polyadenylation signal	generation of new class of genes in the mouse major histocompability class (MHC) class I	Kress *et. al.,* 1984

Table 3.4: Primers for semi-quantitative and quantitative PCR

Primer Pair		Sequence
PCR in coding region	F	5' ATGGGTGGCACAAAGGAGCA 3'
	R	5' GAGGCCATCAGGATGACACC 3'
PCR spanning B2 insertion	F	5' TTTCCTCAGGGCCTGTGGCT 3'
	R	5' GAGGCCATCAGGATGACACC 3'
Reverse primer Within B2 insertion	F	5' TTTCCTCAGGGCCTGTGGCT 3'
	R	5' TCAGAAGAGCAGTCGGGTGC 3'
PCR product 3' of B2 insertion	F	5' CTCACTAACTGGAAGAGGAGATTTTT 3'
	R	5' CATTCTTAAGATGAAATGTGGTATGA 3'

CHAPTER 4: A MORE DETAILED EXAMINATION OF THE EFFECT OF THE B2 INSERTION ON BEHAVIOR, GENE EXPRESSION AND NOCICEPTION

Introduction

There is a large behavioral data set measured in inbred strains of mice which was analyzed for correlations of *Comt1* mRNA levels and behavioral measurements which was not included in our published paper. We also analyzed the effect of the $Comt1^{B2i}$ haplotype for RNA and protein expression of other genes. These data are presented here.

Correlations of *Comt1* RNA Levels and Behavior

As polymorphisms in *COMT* is well known to be involved in human anxiety studies, we initially looked in our RNA expression data across inbred strains and saw a bimodal distribution in one of the Affymetrix *Comt1* probe sets, at_1418701, Figure 3.3. We then used the publicly available SNPster algorithm (http://snpster.gnf.org), which associates phenotype to genotype across a diverse panel of >70 inbred stains. Our phenotype was the expression of the at_1418701 probe set. Our goal was to find a region of the genome where the expression of this probe set correlated with haplotype groups within a gene. The SNPster program revealed the probe set for *Comt1* "mapped back" to itself surrounding the *Comt1* locus, which meant the gene was *cis*-regulated, Figure

2.1. We then considered it likely that a polymorphism within or near the gene was responsible for the difference in expression. Before we identified the source of the polymorphism, we first needed to correlate the difference in expression with a behavioral trait.

The initial approach taken was to take pair-wise correlations of mRNA levels and behavior measurements across the strains and look for P values which passed Bonferroni correction. We defined the Bonferroni correction as $P<0.00069$: a $P<0.05$ divided by eleven behavioral measurements multiplied by seven brain regions. None of our P values reached significance with Bonferroni correction, although three of our behaviors in male mice did correlate with a $P<0.05$ (Table 4.1).

After the B2 insertion was discovered, we then tried to correlate behavior by haplotype, and did not consider RNA levels. In this case, the Bonferroni correction was $P<0.00455$ (0.05 divided by eleven behavioral measurements). We used a one-tailed t-test with unequal variances in Microsoft Excel to calculate significance. With this approach, we still had no significant behaviors with a Bonferroni correction (Table 4.2). If individual animals are considered, we had numerous positive correlations, although this result may be biased as we usually had more *Comt1*^{B2i} animals, and t-tests with individual animals give inflated P values (Professor William Lariviere, personal correspondence).

The analysis conducted with the Directed Projection Permutation (DiProPerm) also used individual animal scores and divided the strains by haplotype. We looked to see if the number of strains or the number of animals

was significantly biased in favor of the *Comt1*^{B2i} haplotype. Two cohorts or groups of animals were used in the original behavioral data gathering. We looked by the number of individual animals: by sex, haplotype and group, and then by the numbers of strains: by sex, haplotype and group for a bias (Figure 4.1). We saw an increase in group 2 of the number of animal behavioral measurements for male and female *Comt1*^{B2i} haplotype. The numbers of animals per strain used in the DiProPerm analysis are listed in Figure 4.2. We were however, fortunate that the strains were chosen before the haplotypes were known and the ratios between the haplotypes were nearly equal.

The DiProPerm analysis did not consider strain means and analyzed all of the behavioral data per group at once. We were not sure what significance we would see if we looked at individual tests or combinations of tests. Therefore, we looked at the subset of the four most important tests which demonstrated a behavioral difference between the two haplotypes and ran the DiProPerm analysis on strain means and individual animal scores for individual tests and for combinations of tests (Table 4.3). As we saw when we analyzed strain means by haplotype in the students' t-test, we had few tests with $P < 0.05$.

What does this mean for the B2 insertion into *Comt1*? As we discussed in Chapter 2, several behavioral assays reached significance for both individuals and for combined tests of strain means. There were several behaviors which were close to significance, but with 29 to 32 strains per assay, significant P values were difficult to obtain. However, one assay was always significant for both males and females when individual animals, strain means, or DiProPerm

was used in analysis: t4, or the Light/Dark box, % Time Spent in Light. We turn now to effects of the B2 insertion less open to interpretation, the effect of haplotype group on protein and gene expression.

Comt1 Haplotype and Biomarkers Expressed in Brain

Part of our overall strategy to find genes involved in anxiety and depression was to quantify biomarkers associated with anxious or depressed phenotypes across the inbred strains. Brain regions were dissected as described in Chapter 2 methods: Development of COMT ELISA assay. One animal was used per strain. Brain samples were sent to a commercial company for quantification of protein levels in a sandwich ELISA (Zeptosens, Basel, Switzerland).

Three biomarkers were examined for correlation to *Comt1* haplotype: Norepinephrine Transporter (NET), Interleukin-6 (IL-6), and Tumor necrosis factor alpha (TNF-α). We were curious if the high COMT1 activity would affect the amount of transporter protein expressed, as theoretically there should be less norepinephrine to transport from the presynaptic cell to the post synaptic cell. We did see significantly less NET protein by $Comt1^{B2i}$ haplotype in all brain regions we examined (Figure 4.3). We could conclude the reason NET protein is expressed at a lower level is because there is no need for the cell to have numerous transporters for low levels of catecholamines (and presumably $Comt1^{B2i}$ strains have low catecholamine levels).

We also saw significantly low levels of two other biomarkers, IL-6 and TNF-α, which may also be due to decreased levels of epinephrine and

norepinephrine. Epinephrine and norepinephrine activate β_2 adrenergic receptors (β_2ARs) (Dohlman *et.al.,* 1991). Activation of β_2ARs up-regulates protein levels of IL-6 in macrophages (with agonist salmeterol, Tan *et.al.,* 2007), cardiac fibroblasts (Yin *et.al.,* 2006), adipose tissue (Mohamed-Ali *et.al.,* 2001), pituicytes (Christensen *et.al.,* 1999), skeletal muscle and myoblasts (Frost *et.al.,* 2004). If the strains of the *Comt1*^{B2i} haplotype have less epinephrine and norepinephrine, then we should see less IL-6 production. In our pooled brain regions, we saw decreased strain mean levels of IL-6 in *Comt1*^{B2i} haplotype, but significance only in the Hippocampus/Hypothalamus/Amygdala region (Figure 4.3b).

Decreased norepinephrine and epinephrine should also decrease protein levels of TNF-α. Norepinephrine inhibits TNF-α and IL-6 production in whole blood and THP-1 cells (van der Poll *et.al.* 1994, Severn *et.al.,* 1992). β_2AR agonists salmeterol and albuterol also reduce TNF-α production in THP-1 cells (Sekut *et.al.,* 1995). Additionally, high levels of TNF-α correlate with pain in temporomandibular joint pain (Shafer *et.al.,* 1994), arthritis (Tak *et.al.,* 1997) and inflammatory neuropathies (Lindenlaub & Sommer 2003). We see TNF-α significantly down regulated in the Nucleus Accumbens/Striatum regions (Figure 4.3 c), although strain means were slightly higher in the two other regions. We could conclude the reason TNF-α and IL-6 protein is expressed at a lower level in strains of the *Comt1*^{B2i} haplotype is because these animals have higher baseline pain thresholds, and lower baseline levels of norepinephrine and epinephrine.

Correlations of *Comt1* Haplotype and Pain Response

An examination of pain data collected in inbred mouse strains (Lariviere *et.al.,* 2002, Mogil *et.al.,*1999 a, b) and deposited in the Jackson Laboratory Phenome Database (http://www.jax.org/phenome) was conducted to determine if the absence of the B2 SINE insertion in inbred mice also influences pain sensitivity. Nociception data was uploaded from the Jax Phenome website (http://www.jax.org/phenome; Project: Mogil1, MPD:22). Five of the strains measured had the B2 SINE insertion: A/J, AKR/J, BALB/cJ, C57BL/6J, SM/J, and five of the strains did not: C3H/HeJ, C58/J, CBA/J, DBA/2J, and RIIIS/J. The data was organized into four types of nociceptive stimulus: chemical, mechanical, thermal, and neuropathic and multiple measures for each modality were available. We tabulated strain means by *Comt1* haplotype, per pain assay, Table 5.4. The strains were divided by $Comt1^{B2i}$ and $Comt1^{+}$ haplotype and analyzed by one-tailed student's t-test on Microsoft Excel, per type of nociceptive stimulus.

In order to derive an overall pain response for each modality, the pain assay data for each individual strain was converted into a *Z*-score as follows: Individual strain z-scores were calculated using the formula where = individual strain mean, = group mean for all strains and = standard deviation across strains. Individual strain z-scores were summed across each measure within a particular modality to generate an overall strain z-score. A t-test of Z-scores by $Comt1^{B2i}$ and $Comt1^{+}$ haplotype was conducted for each type of nociceptive stimulus.

The pain studies conducted by Mogil *et.al.,* preceded the distinction of the 129 sub strains. In 1999, the sub strains 129/SvJ and 129/SvJae were further divided into 17 sub strains (Festing *et.al.,* 1999). Some of the 129s have the B2 SINE element, such as 129X1/SvJ and 129S1/SvImJ, while others do not, such as 129P3/J and 129/SvEvTac. In view of this ambiguity, the pain data for 129/J was not included for the computation of a *Z*-score in Table 5.4. To be noted, when we included 129/J as a $Comt1^{+}$ haplotype, the *Z*- score for chemical data still reached significance with Bonferroni correction, $P<0.01$. When *129/J* was included as a SINE haplotype, the significance with Bonferroni correction remained $P<0.01$.

Although we did not see significance with pain modalities other than chemical induced pain, we looked for trends in the strain means. We saw for chemical pain assays, the $Comt1^{B2i}$ strain means are less sensitive in the majority of assays (Figure 5.3a). In thermal pain: $Comt1^{B2i}$ strain means are less sensitive in assays 1, 2, 3, 4, 7, 9 (Figure 5.3b). $Comt1^{B2i}$ strain means are slightly more sensitive in assay 8. No difference was observed in assays 5, 6. For mechanical pain, $Comt1^{B2i}$ strain means are less sensitive to tail pinch and slightly and (not significantly) more sensitive to von Frey filaments (Figure 4.4c). For neuropathic pain, $Comt1^{B2i}$ strain means are more sensitive in all assays, but the difference is also not significant (Figure 4.4d).

Why do pain sensitivities switch between modalities? Could it be experimental error, or reflect the underlying biology of catecholamine mediated pain?

In a recent Meeting of the American Pain Society, we discussed human LPS/HPS/APS haplotypes and neuropathic pain with colleagues. Our discussions led to a revelation about catecholamine signaling and pain in the spinal chord – a basic premise which has not been articulated in the literature before. We present evidence for this fundamental feature of pain in vertebrate species in our next chapter.

References

Christensen, J.D., Hansen, E.W., Frederiksen, C., Molris, M. & Moesby, L. (1999) Adrenaline influences the release of interleukin-6 from murine pituicytes: role of beta2-adrenoceptors. *Eur J Pharmacol,* **378,** 143-148.

Dohlman, H.G., Thorner, J., Caron, M.G. & Lefkowitz, R.J. (1991) Model systems for the study of seven-transmembrane-segment receptors. *Annu Rev Biochem,* **60,** 653-688.

Festing, M.F., Simpson, E.M., Davisson, M.T. & Mobraaten, L.E. (1999) Revised nomenclature for strain 129 mice. *Mamm Genome,* **10,** 836.

Frost, R.A., Nystrom, G.J. & Lang, C.H. (2004) Epinephrine stimulates IL-6 expression in skeletal muscle and C2C12 myoblasts: role of c-Jun NH2-terminal kinase and histone deacetylase activity. *Am J Physiol Endocrinol Metab,* **286,** E809-817.

Lariviere, W.R., Wilson, S.G., Laughlin, T.M., Kokayeff, A., West, E.E., Adhikari, S.M., Wan, Y. & Mogil, J.S. (2002) Heritability of nociception. III. Genetic relationships among commonly used assays of nociception and hypersensitivity. *Pain,* **97,** 75-86.

Lindenlaub, T. & Sommer, C. (2003) Cytokines in sural nerve biopsies from inflammatory and non-inflammatory neuropathies. *Acta Neuropathol,* **105,** 593-602.

Mogil, J.S., Wilson, S.G., Bon, K., Lee, S.E., Chung, K., Raber, P., Pieper, J.O., Hain, H.S., Belknap, J.K., Hubert, L., Elmer, G.I., Chung, J.M. & Devor, M. (1999) Heritability of nociception II. 'Types' of nociception revealed by genetic correlation analysis. *Pain,* **80,** 83-93.

Mogil, J.S., Wilson, S.G., Bon, K., Lee, S.E., Chung, K., Raber, P., Pieper, J.O., Hain, H.S., Belknap, J.K., Hubert, L., Elmer, G.I., Chung, J.M. & Devor, M. (1999) Heritability of nociception I: responses of 11 inbred mouse strains on 12 measures of nociception. *Pain,* **80,** 67-82.

Mohamed-Ali, V., Flower, L., Sethi, J., Hotamisligil, G., Gray, R., Humphries, S.E., York, D.A. & Pinkney, J. (2001) beta-Adrenergic regulation of IL-6 release from adipose tissue: in vivo and in vitro studies. *J Clin Endocrinol Metab,* **86,** 5864-5869.

Sekut, L., Champion, B.R., Page, K., Menius, J.A., Jr. & Connolly, K.M. (1995)

Anti-inflammatory activity of salmeterol: down-regulation of cytokine production. *Clin Exp Immunol,* **99,** 461-466.

Severn, A., Rapson, N.T., Hunter, C.A. & Liew, F.Y. (1992) Regulation of tumor necrosis factor production by adrenaline and beta-adrenergic agonists. *J Immunol,* **148,** 3441-3445.

Shafer, D.M., Assael, L., White, L.B. & Rossomando, E.F. (1994) Tumor necrosis factor-alpha as a biochemical marker of pain and outcome in temporomandibular joints with internal derangements. *J Oral Maxillofac Surg,* **52,** 786-791; discussion 791-782.

Tak, P.P., Smeets, T.J., Daha, M.R., Kluin, P.M., Meijers, K.A., Brand, R., Meinders, A.E. & Breedveld, F.C. (1997) Analysis of the synovial cell infiltrate in early rheumatoid synovial tissue in relation to local disease activity. *Arthritis Rheum,* **40,** 217-225.

Tan, K.S., Nackley, A.G., Satterfield, K., Maixner, W., Diatchenko, L. & Flood, P.M. (2007) Beta2 adrenergic receptor activation stimulates pro-inflammatory cytokine production in macrophages via PKA- and NF-kappaB-independent mechanisms. *Cell Signal,* **19,** 251-260.

Tchivileva, I.E., Nackley, A.G., Qian, L., Wentworth, S., Conrad, M. & Diatchenko, L.B. (2009) Characterization of NF-kB-mediated inhibition of catechol-O-methyltransferase. *Mol Pain,* **5,** 13.

van der Poll, T., Jansen, J., Endert, E., Sauerwein, H.P. & van Deventer, S.J. (1994) Noradrenaline inhibits lipopolysaccharide-induced tumor necrosis factor and interleukin 6 production in human whole blood. *Infect Immun,* **62,** 2046-2050.

Yin, F., Wang, Y.Y., Du, J.H., Li, C., Lu, Z.Z., Han, C. & Zhang, Y.Y. (2006) Noncanonical cAMP pathway and p38 MAPK mediate beta2-adrenergic receptor-induced IL-6 production in neonatal mouse cardiac fibroblasts. *J Mol Cell Cardiol,* **40,** 384-393.

Figure 4.1 Search for bias in haplotype analysis by SINE status, sex or group. The number of animals or strains are listed above the colored bars in black. **(a)** Group 1 & 2 divided by the total number of animals, by SINE status, by group and as a whole. **(b)** Same analysis as in (a), but by strain.

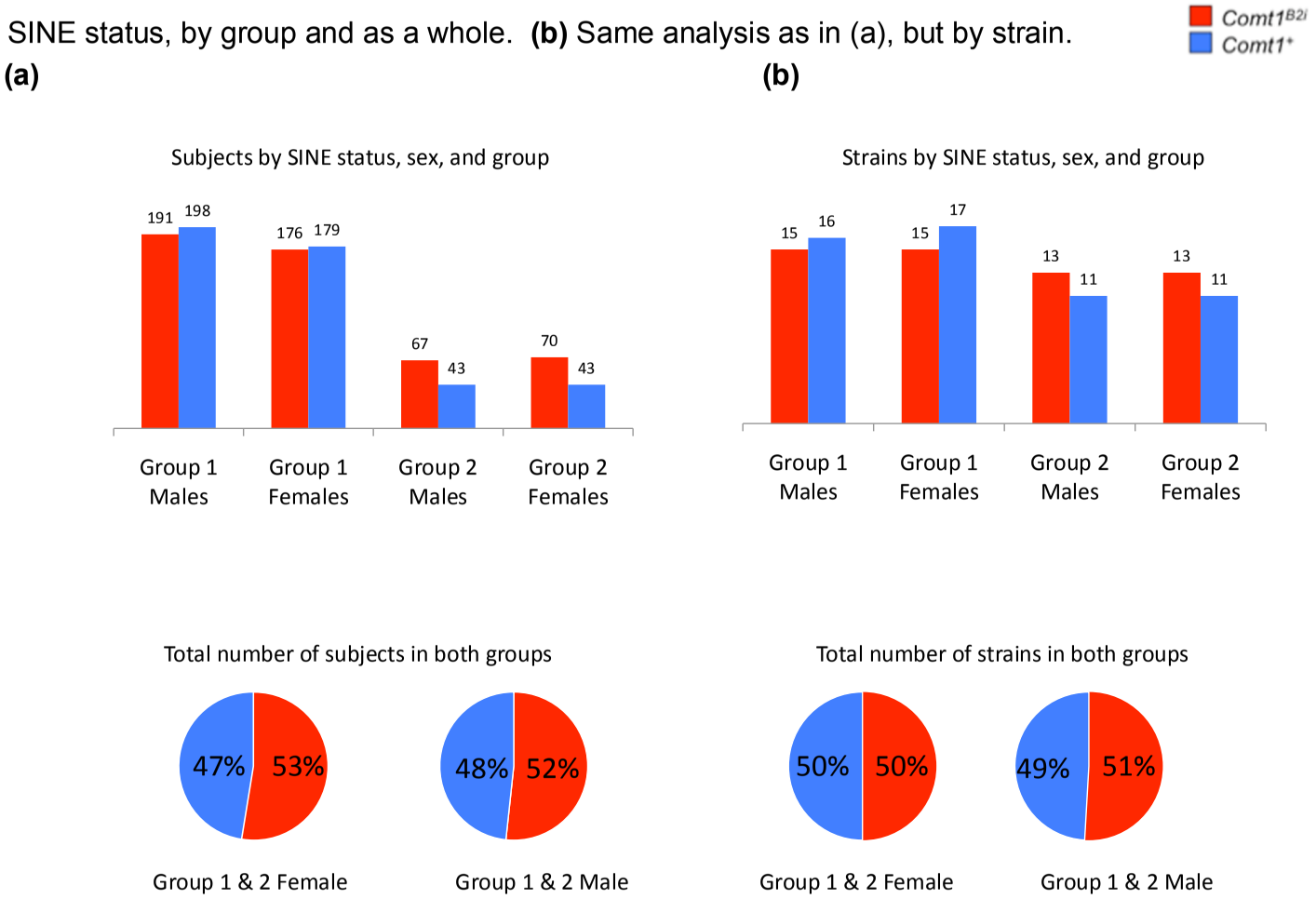

Figure 4.2 Number of subjects by strain & haplotype for group 1 **(a)** and 2 **(b).**

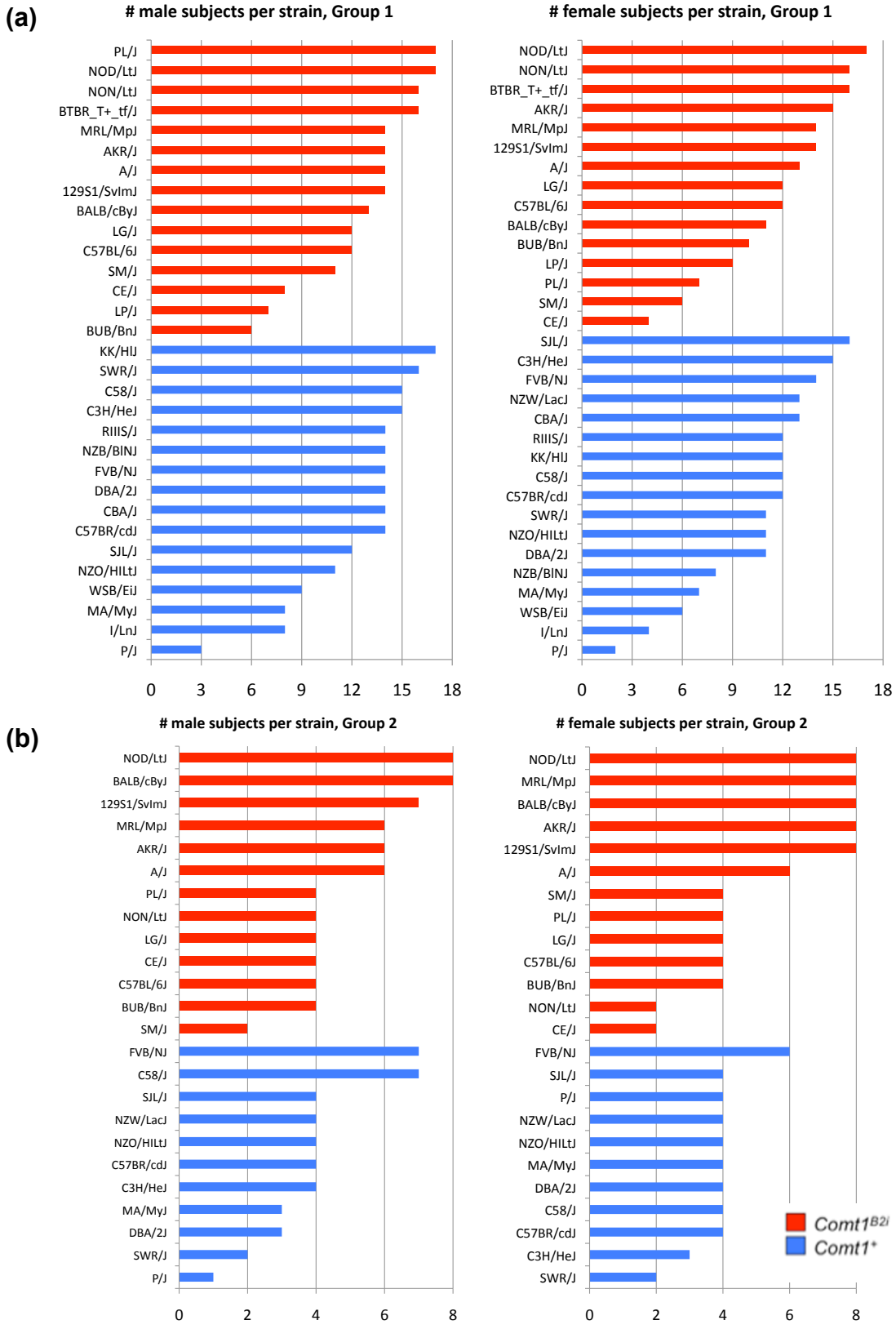

Figure 4.3 ELISA of three biomarkers by pooled brain regions in 22 inbred strains. **a.** Prefrontal cortex **b.** Nucleus Accumbens and striatum **c.** Hippocampus, Hypothalamus and Amygdala. Significance determined using unmatched one-tailed unpaired t-test in Graph Pad Prism, version 5 for IBM.

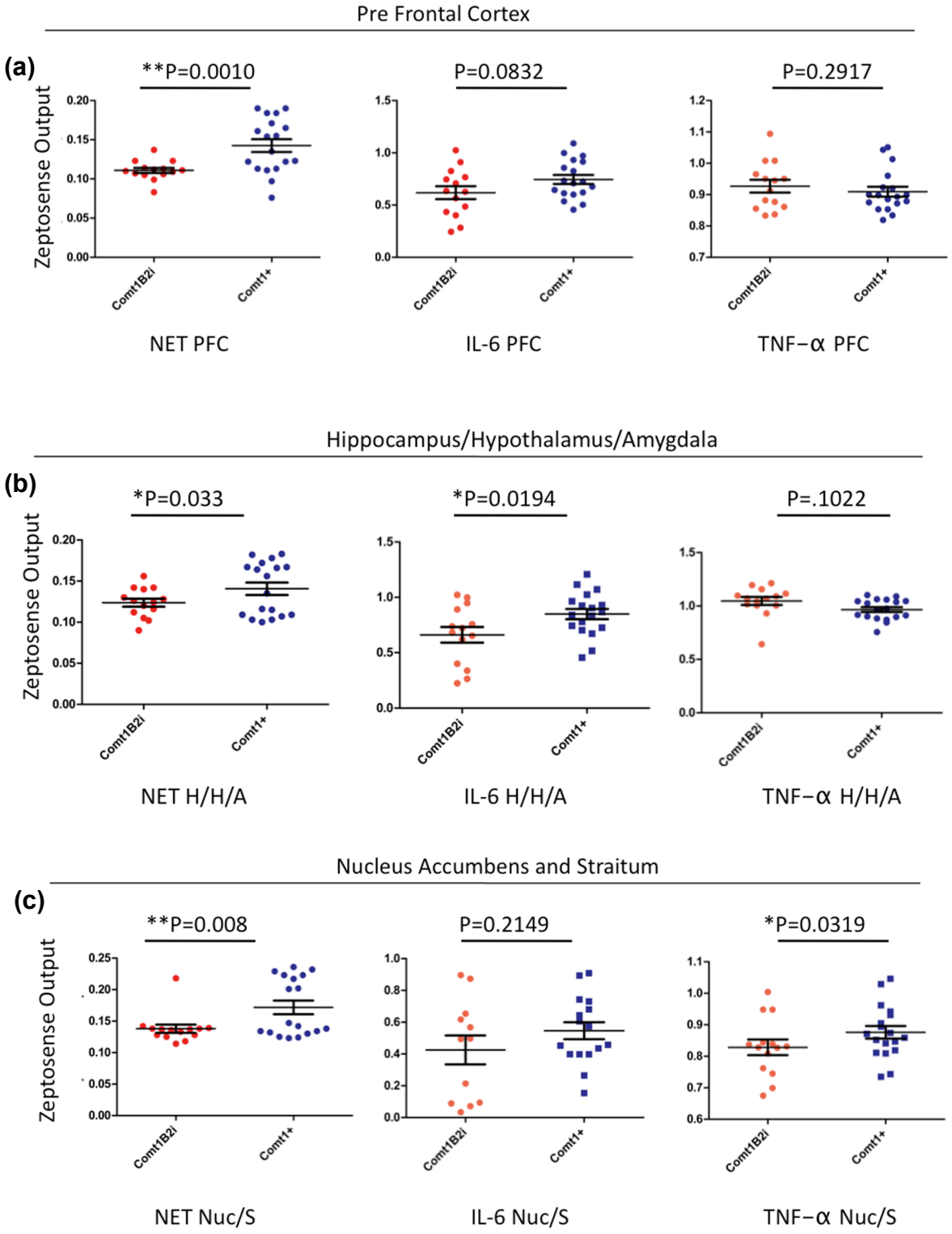

Figure 4.4 Strain means of five *Comt1*^{B2i} and five *Comt1*$^{+}$ haplotypes in assays of chemical-induced nociception, from http://www.jax.org/phenome; Project: MogiI1, MPD:22. The *Comt1*^{B2i} strains were less sensitive in all chemically induced assays.

(a)

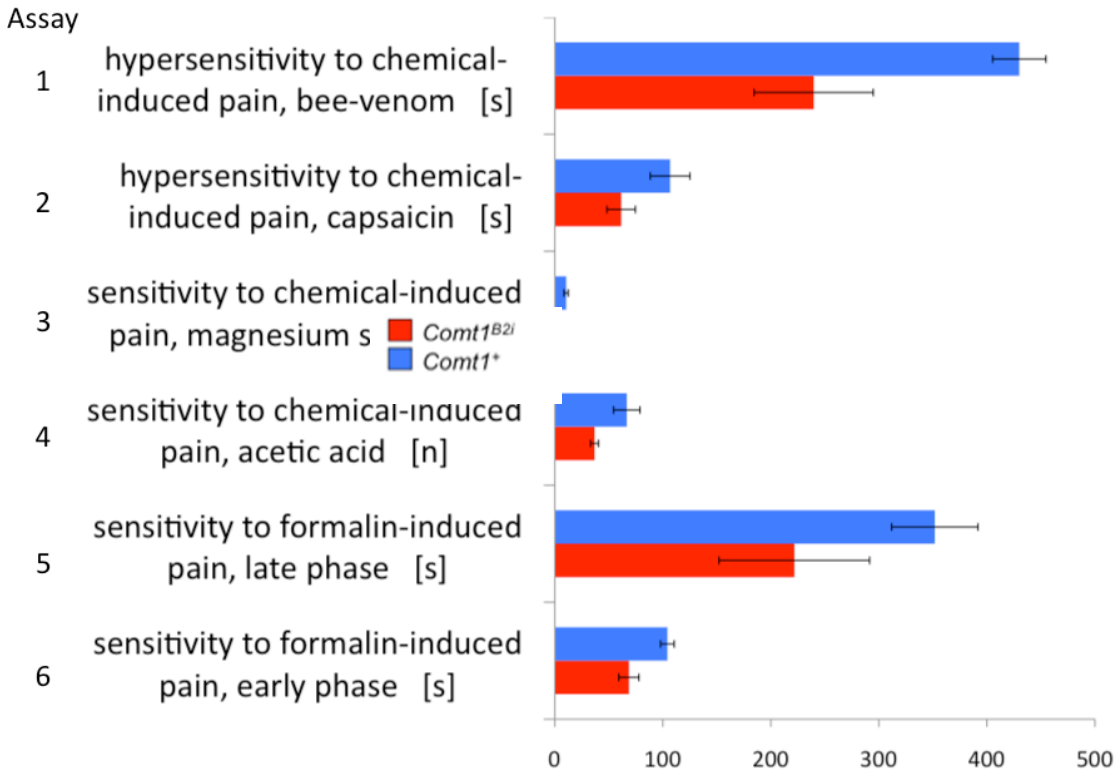

Figure 4.4 continued, (b) Sensitivity to noxious thermal stimulous.

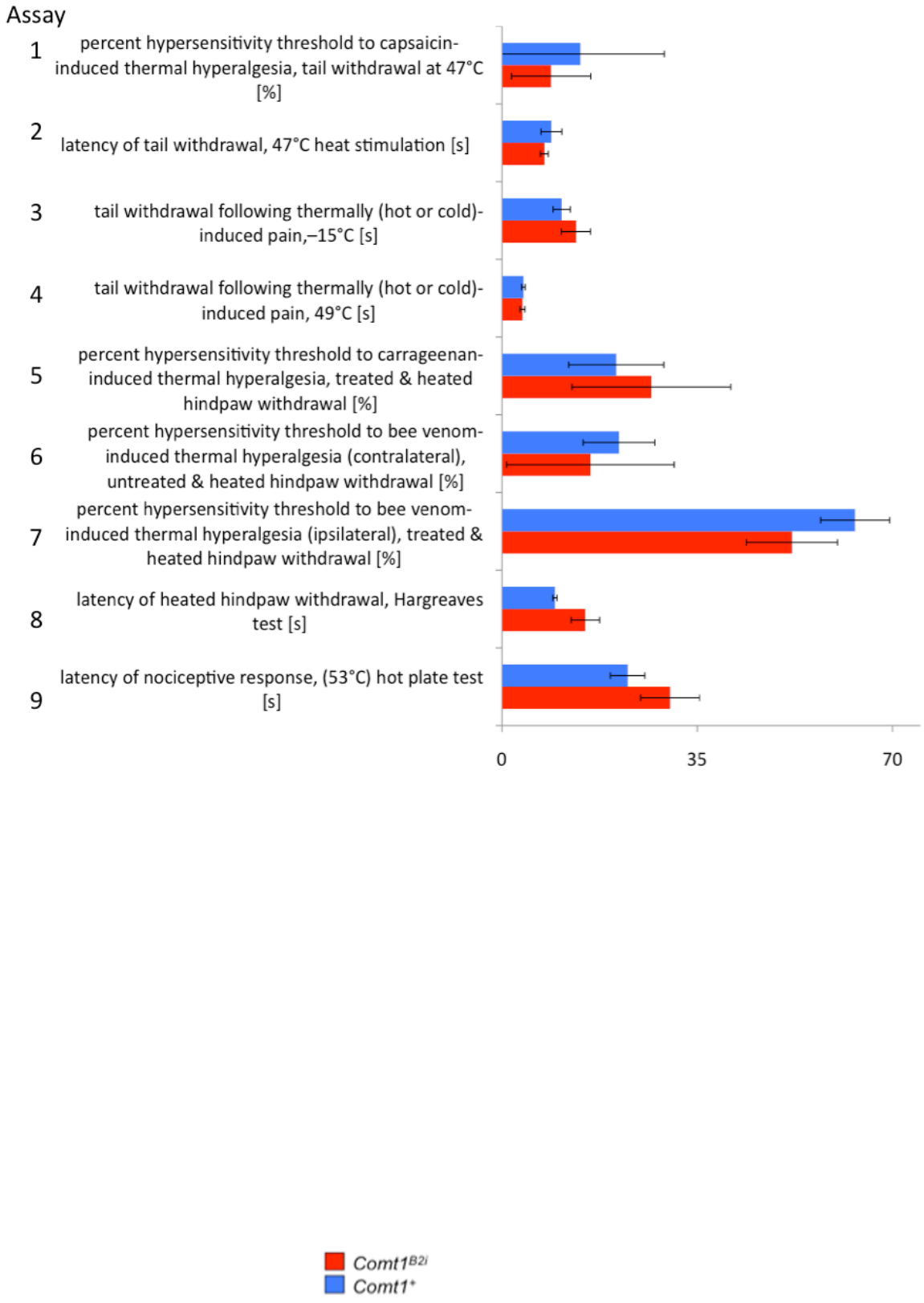

Figure 4.4 continued **(c)** Mechanical pain sensitivity in two assays **(b)** Neuropathic pain, *Comt1*^{B2i} strain means are more sensitive in all assays.

(c)

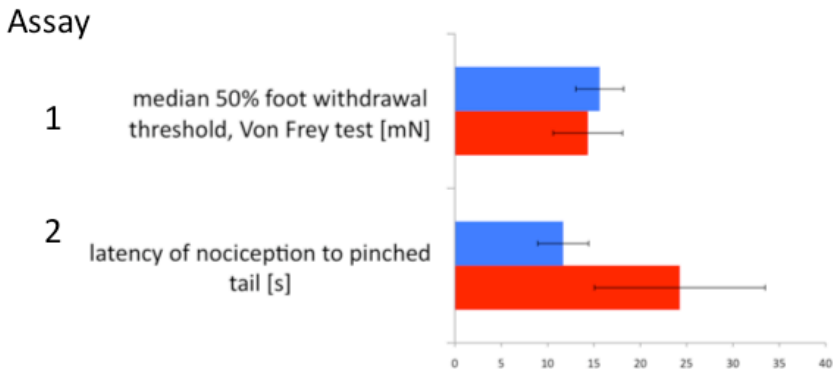

(d)

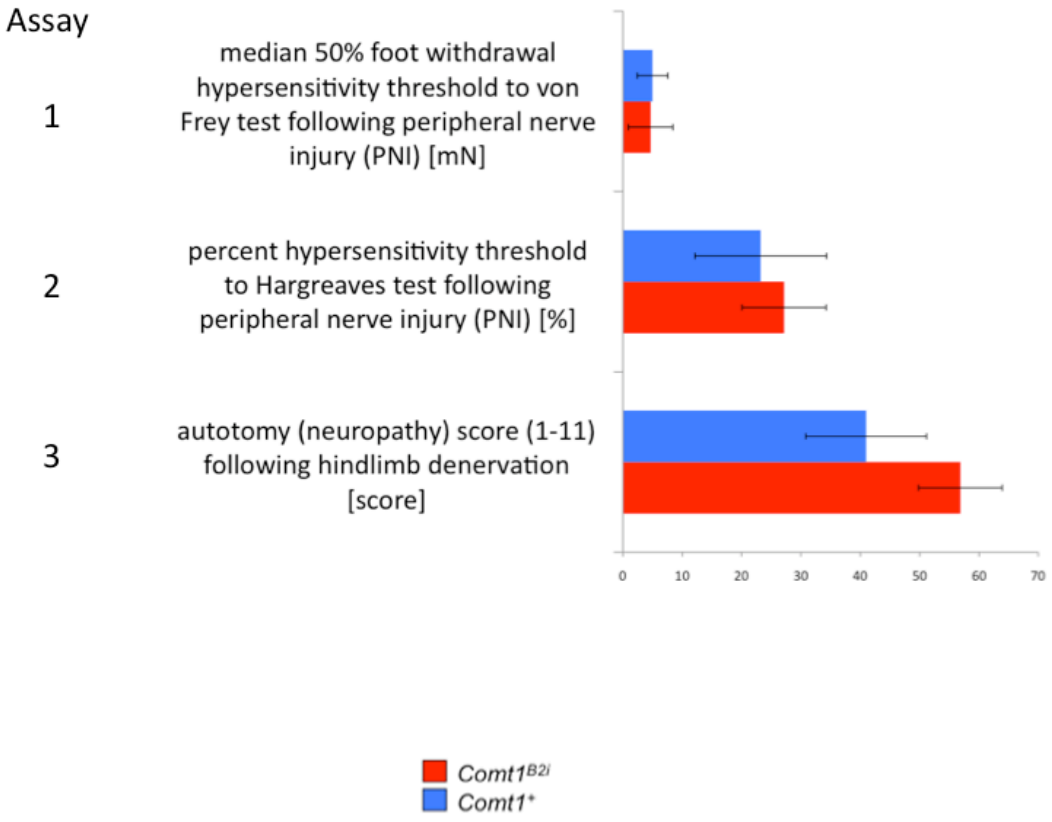

Table 4.1 Correlations between *Comt1* mRNA and behavioral assays. mRNA levels measured by Affymetrix coding probe, 1449183_at.

Behavioral Assay	Brain region	Correlation	Number of strains	P value
Forced Swim Test: Immobility Time	Nucleus Accumbens	0.6293	23	0.0013
Elevated Plus Maze: Total Distance Traveled	Striatum	0.5243	20	0.0176
Elevated Plus Maze: Total Distance Traveled	Amygdala	0.4494	24	0.0276

Table 4.2 Comparison of P values between strain means and individual animals for correlations between eleven behavioral measurements and *Comt1* haplotype.

	Individual Animals				***Strain Means***			
	Female		Male		Female		Male	
	B2i	*WT+*	*B2i*	*WT+*	*B2i*	*WT+*	*B2i*	*WT+*
Light/Dark Box: Total Distance Traveled	**0.0071		**0.0045		0.3623		0.2057	
n	*73*	*56*	*76*	*51*	*13*	*13*	*13*	*13*
Light/Dark box: % Time Spent in Light	***<0.0001		***<0.0001		*0.0259		*0.0340	
n	*73*	*56*	*76*	*51*	*13*	*13*	*13*	*13*
Light/Dark Box: Total Transitions Between Sections	***<0.0001		***0.0065		**0.0028		0.1731	
n	*74*	*56*	*76*	*51*	*13*	*13*	*13*	*13*
Elevated Plus Maze: Total Distance Traveled	*0.0138		**0.0060		0.1412		0.0601	
n	*71*	*47*	*67*	*46*	*13*	*12*	*13*	*12*
Elevated Plus Maze: Percent Time Spent in Open Quadrant	**0.0046		*0.0291		0.1660		0.1732	
n	*70*	*47*	*67*	*46*	*13*	*12*	*13*	*12*
Open Field: Total Distance Traveled	*0.0338		0.1289		0.4532		0.4287	
n	*219*	*212*	*204*	*218*	*15*	*18*	*17*	*15*
Open Field: Percent Center	0.2161		0.3130		0.2975		0.2569	
n	*218*	*204*	*204*	*218*	*15*	*18*	*15*	*17*
Open Field: Total Rearing Events	**0.0015		***0.0001		0.1520		*0.0493	
n	*218*	*212*	*204*	*219*	*15*	*18*	*15*	*17*

Table 4.2 continued

	Individual Animals				***Strain Means***			
	Female		Male		Female		Male	
	B2i	*WT+*	*B2i*	*WT+*	*B2i*	*WT+*	*B2i*	*WT+*
Forced Swim Test: Immobility Time	*0.0370		0.0982		0.4052		0.2996	
n	*74*	*52*	*76*	*51*	*13*	*12*	*13*	*13*
Percent Immobility the Last Four Minutes of the Tail Suspension Test	*0.0277		0.4160		0.3886		0.4455	
n	*176*	*179*	*192*	*199*	*15*	*18*	*15*	*16*
Change in temperature due to Stress Induced Hyperthermia	0.3878		0.3331		0.2622		0.4920	
n	*208*	*216*	*203*	*213*	*14*	*16*	*14*	*16*
total behavior data points per haplotype	*1474*	*1337*	*1445*	*1363*	*138*	*163*	*154*	*157*
total female or male data points	*2811*		*2808*		*301*		*154*	
total behavior data points	*5619*				*455*			

Table 4.3 DiProPerm Analysis on Subsets of Behavioral Measurements.

	Empirical P	Gaussian fit P
Group 1 Female, all tests on strain mean data	0.251680	0.277610
Group 1 Female, 4 samples for each strain, all tests	0.112510	0.104380
Group 1 Female, 4 samples for each strain, t1 and t2	0.018269	0.003571
Group 1 Female, 4 samples for each strain, t2	0.030188	0.013146
Group 1 Female, 10 samples for each strain, all tests	0.000000	0.000000
Group 1 Female, 10 samples for each strain, t1 and t2	0.000000	0.000000
Group 1 Female, 10 samples for each strain, t2	0.000000	0.000000
Group 1 Female, t1 & t2 on strain mean data	0.066228	0.043534
Group 1 Female, t1 & t2 on raw data	0.000000	0.000000
Group 1 Female, t2 on raw data	0.000000	0.000000
Group 1 Female, t2 on strain mean data	0.127230	0.120290
Group 1 Male, all tests on strain mean data	0.418560	0.044402
Group 1 Male, t1 & t2 on strain mean data	0.082816	0.072761
Group 1 Male, t1 & t2 on raw data	0.000000	0.000000
Group 1 Male, t2 on strain mean data	0.082800	0.056038
Group 1 Male, t2 on raw data	0.000000	0.000000
Group 2 Female, strain means, all tests	0.179440	0.182430
Group 2 Female, 4 samples for each strain, all tests	0.000000	0.000001
Group 2 Female, strain mean, test 4	0.037162	0.014386
Group 2 Female, 4 samples from each strain t4	0.000000	0.000000
Group 2 Male, strain means, all tests	0.205160	0.231900
Group 2 Male, 4 samples for each strain, all tests	0.001218	0.000131
Group 2 Male, strain means, t4	0.040607	0.017757
Group 2 Male, 4 samples for each strain, t4	0.000000	0.000000
Group 1 & 2 Female strain mean t1, t2, t4	0.026917	0.011414
Group 1 & 2 Female, 4 samples for each strain, t1, t2, t4	0.000000	0.000000
Group 1 & 2 Male strain mean t1, t2, t4	0.025333	0.010524
Group 1 & 2 Male, 4 samples for each strain, t1, t2, t4	0.000000	0.000000

t1 = Total Distance traveled in Open Field
t2 = Rearing in Open Field
t4 = % Time in Light Section of Dark/Light Box

Table 4.4 Correlations of Pain Measurements to *Comt1* Haplotype. 1-tailed student's t-test used to determine significance for individual assays and *Z*-scores.

		B2i	S.E.	*WT*+	S.E.	**P**	*Z* score **P**
Chemical pain	sensitivity to formalin-induced pain, early phase [s]	68.6	9.3	104.2	6.3	*0.02	*** P<0.001
	sensitivity to formalin-induced pain, late phase [s]	221.7	69.7	351.8	39.9	0.15	
	sensitivity to chemical-induced pain, acetic acid [n]	36.8	3.7	66.6	12.2	0.07	
	sensitivity to chemical-induced pain, magnesium sulfate [n]	3.0	0.7	10.5	1.9	*0.01	
	hypersensitivity to chemical-induced pain, capsaicin [s]	61.4	13.2	106.7	18.4	0.08	
	hypersensitivity to chemical-induced pain, bee-venom [s]	239.7	55.1	430.0	24.7	*0.02	
Mechanical pain	latency of nociception to pinched tail [s]	24.3	9.2	11.7	2.7	0.25	P=0.4154
	median 50% foot withdrawal threshold, Von Frey test [mN]	14.3	3.7	15.6	2.6	0.79	
Neuropathic pain	autotomy (neuropathy) score (1-11) following hindlimb denervation [score]	56.8	7.0	41.0	10.2	0.24	P=0.3397
	percent hypersensitivity threshold to Hargreaves test following peripheral nerve injury (PNI) [%]	27.2	7.1	23.2	11.1	0.77	
	median 50% foot withdrawal hypersensitivity threshold to von Frey test following peripheral nerve injury (PNI) [mN]	4.7	3.7	5.0	2.6	0.90	

Table 4.4 continued

		B2i	S.E.	*WT+*	S.E.	**P**	*Z* score **P**
Thermal Pain	latency of nociceptive response, (53°C) hot plate test [s]	30.2	5.3	22.5	3.1	0.26	P=0.4514
	latency of heated hindpaw withdrawal, Hargreaves test [s]	14.9	2.6	9.5	0.4	0.10	
	percent hypersensitivity threshold to bee venom-induced thermal hyperalgesia (ipsilateral), treated & heated hindpaw withdrawal [%]	52.0	8.2	63.3	6.2	0.30	
	percent hypersensitivity threshold to bee venom-induced thermal hyperalgesia (contralateral), untreated & heated hindpaw withdrawal [%]	15.9	15.0	21.0	6.4	0.77	
	percent hypersensitivity threshold to carrageenan-induced thermal hyperalgesia, treated & heated hindpaw withdrawal [%]	26.8	14.2	20.5	8.5	0.72	
	tail withdrawal following thermally (hot or cold)-induced pain, 49°C [s]	3.7	0.4	3.9	0.3	0.75	
	tail withdrawal following thermally (hot or cold)-induced pain,–15°C [s]	13.3	2.6	10.7	1.5	0.43	
	latency of tail withdrawal, 47°C heat stimulation [s]	7.6	0.7	8.9	1.9	0.56	
	percent hypersensitivity threshold to capsaicin-induced thermal hyperalgesia, tail withdrawal at 47°C [%]	8.8	7.1	14.1	15.0	0.76	

CHAPTER 5: CONCLUSIONS AND FUTURE EXPERIMENTS

Concluding Remarks

Comt1 contributes to pain sensitivity and several behavioral phenotypes in inbred strains of mice. Based on the data observed in humans and $Comt1^{-/-}$ (knock-out) animal studies, we would expect that $Comt1^{B2i}$ mice with increased enzymatic activity would exhibit decreased pain and anxiety. While we correlated a decrease in pain with the $Comt1^{B2}$ haplotype to several previously reported pain assays, we could not state with certainty from all of our anxiety assays that the increase in COMT1 activity decreases anxiety. We have a few behavioral measurements which could tangentially support the hypothesis of decreased anxiety, such as the increased locomotor activity in the elevated plus maze and open field in $Comt1^{B2i}$ mice, and decreased rearing in $Comt1^{B2i}$ mice.

In a second publication which identified the mutation in *Comt1,* measures relating to anxiety, cognition and depression (elevated plus maze, light/dark box, open field) were not shown to be associated with the $Comt1^{B2i}$ allele (Kember *et.al.,* 2010). To be noted, this study used Heterogeneous Stock (HS) mice, which were generated by recombination from eight progenitor stocks of inbred mice.

The Kember study did find a strong association in the novel object

exploration, which *Comt1*$^{B2i/B2i}$ and *Comt1*$^{B2i/+}$ mice making fewer visits to a novel object, and spending less time exploring, than *Comt1*$^{+/+}$ mice. Our inbred strains were not assayed for the novel object assay. In the Papaleo *et.al.,* 2008 study, the authors found that *Comt1*$^{-/-}$ and *Comt1*$^{+/-}$ mice spent less time exploring a novel object, and exhibited more stretching attempts towards the novel object without touching it. This result is consistent with a hypothesis that decreased COMT1 enzymatic activity would cause an animal to be more anxious. The Kember study did not specify stretching attempts, but they did speculate that the open field was an aversive environment and that the mice may not have fully habituated to the novel environment. Although these results appear inconsistent, the mice used to measure the contribution of *Comt1* were on different backgrounds and this makes interpretation of comparative results problematic. Clearly, more sophisticated behavioral tests are in order to clarify the contribution of the *Comt1*^{B2i} allele to this behavior.

What are other possible future directions of the *Comt1*^{B2i} study? Mutants of a gene are often created to study gene function. The *Comt1*^{B2i} allele is a natural occurring polymorphism that increases *Comt1* function. The *Comt1*^{B2i} mice can be compared to the transgenic *Comt-Val Tg* mice and the *Comt1*$^{-/-}$ null mice. One direction would be to use the mutation as a means to study the effects of how and where *Comt1* actually works in the brain, as the studies of the *Comt1*$^{-/-}$ mice have begun to do. The *Comt1*$^{-/-}$ mice are instrumental in determining the contribution of COMT1 enzymatic activity to catecholamine metabolism in a living organism, as demonstrated by the *in vivo* experiments of Huotari *et.al.,*

2002. This study of Huotari used a bolus of the precursor to dopamine, levodopa, to flood the mouse with COMT1 substrate. The important observation was that under basal conditions, the contribution of COMT1 is insignificant. When an acute challenge, such as levodopa loading, is imposed on COMT1 deficient mice, there is a significant accumulation of dopamine. Therefore, the authors conclude COMT1 to have an important role in the catecholaminergic system when catecholamines flood the system.

Why would this be important to keep in mind? Stress is not a basal condition. The effect of an increase or decrease in COMT1 enzymatic activity isn't apparent until the animal is stressed. Our study, as many others, examined gene expression in *unstressed* animals, which may be different from stressed animals.

How COMT metabolism has such a profound effect on behavior is in itself a mystery as COMT activity has not been shown in presynaptic neurons (Karhunen *et.al.,* 1995, Lundstrom *et.al.,* 1995, Mannisto & Kaakkola, 1999). As the catecholamine leaves the presynaptic cell, it is either returned to a storage vessel back in the presynaptic cell or metabolized by monoamine oxidase ($uptake_1$) (Kopin 1985, Cass *et.al.,* 1993). COMT eliminates catecholamines in glial cells and postsynaptic dendritic spines ($uptake_2$) (Huotari *et.al.,* 2002).

The protein made from $Comt1^{B2i}$ transcript could quantified before and after a stressful event. This would tell you if more protein is being generated, or if it is post-translational modification. RNA *in situ* probes of *Comt1* run on pre-

and post-stressed brain sections in *Comt1*^{B2i} and *Comt1*$^{+}$ animals would tell you if the mutant *Comt1*^{B2i} is now being expressed in a different cell type. Fluorescent markers can be added to the cell constructs of both *Comt1*^{B2i} and *Comt1*$^{+}$ alleles to determine where in the cell the protein resides, and if the mutation causes the protein to be sequestered in a cellular compartment. As in the experiments of Overbye & Seglen, lysates of *Comt1*^{B2i} brain can be compared to *Comt1*$^{+}$ to see if the B2 mutation confers a difference in phosphorylation or N-acetylation.

The other future direction of the *Comt1*^{B2i} study is the study of the B2 repeat element: function and origin. Insertions of repeat elements into the human genome commonly result in negative outcomes, as mutations cause a decrease in gene function (Batzer & Deininger 2002). We put forward a few thoughts about the B2 insertion into a domesticated laboratory animal. First, the B2 insertion is the first example we can find of a mutation where the end result is an *increase* in function. Second, for a mouse *not* in a laboratory setting, we believe the recent B2 insertion would indeed result in a negative outcome i.e., *being eaten by a predator.* The B2 insertion would not give the animal any survival advantage in the wild, as not only is basal catecholamine metabolism higher in *Comt1*^{B2i} mice, but COMT1 activity increases after an anxiety inducing event in *Comt1*^{B2i} mice (possibly negating the fight-or-flight response, Eleftheriou, 1975, Figure 1.6), the opposite of what a prey animal would need to survive in a natural environment.

Considering that the classic inbred strains display less “wild” behavior

(such as biting and escaping) than the more recently developed wild-derived strains (Wahlsten *et.al.,* 2003), it is temping to speculate that these behavioral differences may be attributed to the *Comt1*^{B2i} allele. With what is known about repeat element insertions, the mutation happened a single time, and was somehow propagated throughout the classic inbred lines.

In previous years, inbred mice were not housed with lids on the cages, and current thought is that mice in all the classic inbred lines were bred together inadvertently by male mice roaming from cage to cage at night (Pardo-Manuel de Villena, 2010). If the *Comt1*^{B2i} allele caused a mouse to be slightly less anxious when handled, this would confer a selective advantage to the mouse, as a person would naturally select the easiest mouse to catch by hand to go into a breeding cage. The breeding paradigm in the Collaborative Cross is computer generated to avoid this confounding effect of human selection of placid mice (Pardo-Manuel de Villena, 2010).

Classic laboratory mice have extremely low genetic variation in two-thirds of the genome (Yang *et.al.,* 2007). The *Comt1*^{B2i} allele is in a region of essentially no genetic diversity, which provides a tantalizing, if unproven, theory that this region was selected for because of the selective advantage offered by the decrease in anxiety the *Comt1*^{B2i} allele conferred.

The following experiments to characterize the B2 SINE insertion are currently underway and will be completed as a Post-doctoral fellowship in the laboratory of Dr. Luda Diatchenko.

Future Experiments to Characterize the B2 SINE Insertion

Our goal is to determine which region of the transcript drives for increased stability. Is it that the transcript lacks B1 sequence, or does the presence of B2 sequence drive the increased stability of the RNA? We know the B2 insertion possesses a polyadenylation signal, which probably causes early polyadenylation, and very little transcript is made 3' of the insertion.

Does the B1 sequence have a regulatory role? We know mouse B1 sequence is similar to human Alu sequence; they are both derived from the RNA component of the signal recognition particle, or 7SL RNA (Ullu & Tschudi 1984). As *Xenopus* is 87% and *Drosophila* 64% homologous to human 7SL RNA sequence, Alu sequence was likely not only present before the mammalian radiation (Ullu & Tschudi 1984), but may have molecular functions other than directing intercellular proteins.

Alu sequences are preferred methylation targets (Hellmann-Blumberg *et.al.,* 1993, Kochanek *et.al.,* 1993, Jeong & Lee 2005) and are not uniformly distributed across chromosomes (Grover *et.al.,* 2003, 2004). B1 distribution correlates with Alu in orthologous areas of the human genome (Waterson *et.al.,* 2002). Most enticing for a simple explanation of decreased stability in the full *Comt1*$^{+}$ transcript, Alu sequence contains miRNA targets (Smalheiser *et.al.,* 2006).

We know: 1) The *Comt1*$^{+}$ construct containing the B1 sequence is less stable

in actinomyocin D experiments,

2) B1 sequence is not made in the *Comt1*^{B2i} constructs.

In view of these findings, our first goal is to establish what role B1 sequence has in the stability of the transcript. Here are three possible mechanisms, which may not be exclusive, for the increased stability of the mutant RNA (Figure 5.1):

1) *The putative early polyadenylation signal and the absence of B1 element is responsible for lower RNA stability. Remove the polyadenylation site.*

To test this hypothesis, we will use the QuickChange II XL Site-Directed Mutagenesis Kit (Stratagene, LaJolla, CA, USA) to remove the polyadenylation signal AATAAA from the transcript, making a construct we term *Comt1*$^{B2i/nullpolyA}$ (Fig.5.1, construct 1). We can then transfect the mutant constructs into mammalian cell lines (such as PC12, HEK293, COS-1, BV-2, SK-N-Be (2) and THP-1) use RT-PCR to measure if the full transcript, containing both B1 and B2 elements, is made in this case, and if its RNA stability and enzymatic activity are equivalent to those without B1 element. If we see that removing the putative polyadenylation signal has no effect, we can continue to experiment 3.

2. The B1 sequence (or sequence including or near B1) is necessary for transcript degradation. Cite directed mutagenesis of B1 sequence (or sequence including or near B1 sequence).

Dr. Svetlana Shabalina was essential in analyzing human *COMT HPS, LPS,* and *APS* transcripts for stability in previous work (Nackley *et.al.* 2006). Dr. Shabalina will analyze the 3'UTR of $Comt1^{+}$ for RNA degradation motifs and RNA folding.

If the first experiment shows that $Comt1^{B2i/nullpolyA}$ is essentially the same as the $Comt1^{+}$ by activity and stability and the entire transcript is made, we can conclude that there is some region of the 3'UTR necessary for degradation. In this case, we will find RNA degradation motifs in the B1 region of the 3'UTR, and use site directed mutagenesis to remove this motif. This construct will be called $Comt1^{B2i/nullpolyA/nullB1}$ (Fig.6.1, construct 2a).

As the most elegant experiments use a double mutant to restore function, we will then attempt a to restore the secondary structure and stability in the 3'UTR by designing a double mutant, $Comt1^{B2i/nullpolyA/B1DM}$ (Figure 5.1, construct 2b).

3) The B2 sequence makes a very strong secondary structure, which is why the $Comt1^{B2i}$ *transcript is more stable, not because of absence of B1 element. Cite directed mutagenesis of B2 secondary RNA structure.*

First, in collaboration with Dr. Shabalina we will build local secondary structure surrounding B2 region. We then will find nucleotide(s) crucial to this RNA structure in the B2 region and use site directed mutagenesis to remove/modify these critical nucleotides to destroy the secondary structure. This construct will be called 3a) *Comt1*$^{B2i/null2nd}$ (Figure.6.1 construct 3a). We then will transfect into mammalian cell lines as before and use RT-PCR to measure if the shorter transcript is still made, and if the ablated secondary structure of the B2 insertion is still causing an increase in stability, and if the enzymatic activity is still increased. If we see that the secondary structure really is crucial to increased transcript stability, we can prove this by making a double mutant, 3b) *Comt1*$^{B2i/null2nd/dm}$, which then restores the secondary structure and stability (Figure 5.1, construct 3b)

Future Protein Quantification:

We have not established that the B2 insertion causes more protein to be made in the *Comt1*^{B2i} transcript, although other labs have reported this finding (Mulligan *et.al.* 2010). We will quantify protein amounts in our cell transfect ion experiments by Western Blot and run control markers (β-actin) to establish equivalent protein loading amounts. This will establish a logical and linear progression of increased RNA, increased protein, increased enzymatic activity, to a phenotype in animals of the *Comt1*^{B2i} haplotype.

Future Experiments to Establish Dichotomous Role of Catecholamine Signaling in the Spinal Chord

Proposed Mouse Experiments:

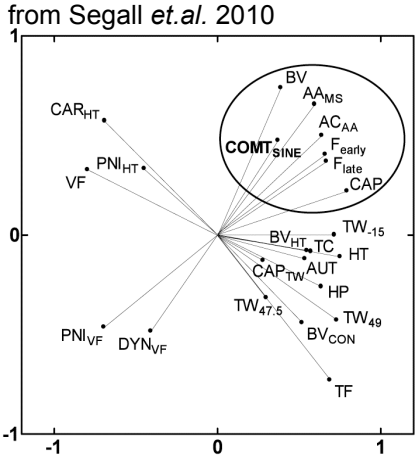

Figure 5.2 Principle Component Analysis Plot of Pain Modalities , from Segall *et.al.* 2010

Peripheral neuropathic injury, as measured by a Von Frey Filament (PNI_{VF}), is a model of neuropathic pain. A principle component analysis plot showed an inverse correlation with this assay to assays of chemically induced nociception (Figure 5.2). Therefore, this assay may be ideal to test for opposing genotypic effects on neuropathic versus nociceptive pain. *Comt1* $^{-/-}$ and *Comt Val-Tg* mice mirror human studies of low COMT activity in regards to thermal pain perception. Neuropathic pain and spontaneous inflammatory pain have not been tested in these mice. Both the *Comt1*$^{-/-}$ and *Tg* mice in comparison to wild-type littermates will be tested in the PNI_{VF} and inflammatory pain assays. Dr. Joseph Gogos (generated *Comt1*$^{-/-}$) and Dr. Daniel Weinberger (generated *Comt Val-Tg*) have sent letters of confirmation that the mice are available for transfer to UNC-Chapel Hill.

Expected Results of Animal Experimentation:

The *Comt1*$^{-/-}$ mice should be less sensitive to the Von Frey filament assay in the neuropathic pain model and more sensitive in inflammatory assays, while the *Tg* mice should exhibit opposite sensitivities.

Proposed Human Association Study:

Our hypothesis will be tested by examining the association of *COMT* haplotypes with clinical pain in four previously collected cohorts: three cohorts of neuropathic pain and one cohort of inflammatory pain. Dr. Jennifer Haythornthwaite, Dr. Claudia Campbell and Dr. Inna Belfer have sent letters of confirmation that data are available for analysis by our group. *COMT* haplotype associations with chemically induced inflammatory and neuropathic pain have not been published previously; this study will be done the first.

Expected Results of Association Study:

We expect the COMT functional haplotypes for high expression and activity (HPS) to be protective in a model of inflammatory pain. We expect to see a negative correlation for HPS haplotypes in neuropathic pain.

In conclusion, establishing the directionality of COMT activity in different pain models is needed to translate basic molecular genetic findings into findings that have meaning in clinical setting. If our hypothesis is correct, *COMT* genotype will be differentially predictive for inflammatory and neuropathic sensitivity, and will bring us closer to diagnostic marker and novel therapeutic targets for these complex human pain conditions.

References

Batzer, M.A. & Deininger, P.L. (2002) Alu repeats and human genomic diversity. *Nat Rev Genet,* **3,** 370-379.

Cass, W.A., Zahniser, N.R., Flach, K.A. & Gerhardt, G.A. (1993) Clearance of exogenous dopamine in rat dorsal striatum and nucleus accumbens: role of metabolism and effects of locally applied uptake inhibitors. *J Neurochem,* **61,** 2269-2278.

Eleftheriou, B.E. (1975) Regional brain catechol-O-methyl transferase: age related differences in the mouse. *Exp Aging Res,* **1,** 99-103.

Grover, D., Majumder, P.P., C, B.R., Brahmachari, S.K. & Mukerji, M. (2003) Nonrandom distribution of alu elements in genes of various functional categories: insight from analysis of human chromosomes 21 and 22. *Mol Biol Evol,* **20,** 1420-1424.

Grover, D., Mukerji, M., Bhatnagar, P., Kannan, K. & Brahmachari, S.K. (2004) Alu repeat analysis in the complete human genome: trends and variations with respect to genomic composition. *Bioinformatics,* **20,** 813-817.

Hellmann-Blumberg, U., Hintz, M.F., Gatewood, J.M. & Schmid, C.W. (1993) Developmental differences in methylation of human Alu repeats. *Mol Cell Biol,* **13,** 4523-4530.

Huotari, M., Gogos, J.A., Karayiorgou, M., Koponen, O., Forsberg, M., Raasmaja, A., Hyttinen, J. & Mannisto, P.T. (2002) Brain catecholamine metabolism in catechol-O-methyltransferase (COMT)-deficient mice. *Eur J Neurosci,* **15,** 246-256.

Jeong, K.S. & Lee, S. (2005) Estimating the total mouse DNA methylation according to the B1 repetitive elements. *Biochem Biophys Res Commun,* **335,** 1211-1216.

Kember, R.L., Fernandes, C., Tunbridge, E.M., Liu, L., Paya-Cano, J.L., Parsons, M.J. & Schalkwyk, L.C. (2010) A B2 SINE insertion in the Comt1 gene (Comt1(B21)) results in an overexpressing, behavior modifying allele present in classical inbred mouse strains. *Genes Brain Behav*.

Kochanek, S., Renz, D. & Doerfler, W. (1993) DNA methylation in the Alu sequences of diploid and haploid primary human cells. *EMBO J,* **12,** 1141-1151.

Kopin, I.J. (1985) Catecholamine metabolism: basic aspects and clinical significance. *Pharmacol Rev,* **37,** 333-364.

Lundstrom, K., Tenhunen, J., Tilgmann, C., Karhunen, T., Panula, P. & Ulmanen, I. (1995) Cloning, expression and structure of catechol-O-methyltransferase. *Biochim Biophys Acta,* **1251,** 1-10.

Mannisto, P.T. & Kaakkola, S. (1999) Catechol-O-methyltransferase (COMT): biochemistry, molecular biology, pharmacology, and clinical efficacy of the new selective COMT inhibitors. *Pharmacol Rev,* **51,** 593-628.

Mulligan, M.K., Z.L., X. Wang, M.F. Miles, L.Lu, R.W. Williams (2010) Functional insertion of a B2 SINE in Comt controls 3'UTR length and generates wide spread expression and behavioral differences amoung inbred strains of mice. . *IBANGS Genes, Brain & Behavior Meeting May 12-16, 2010. .* Dalhousie University, Halifax, Nova Scotia, Canada.

Nackley, A.G., Shabalina, S.A., Tchivileva, I.E., Satterfield, K., Korchynskyi, O., Makarov, S.S., Maixner, W. & Diatchenko, L. (2006) Human catechol-O-methyltransferase haplotypes modulate protein expression by altering mRNA secondary structure. *Science,* **314,** 1930-1933.

Papaleo, F., Crawley, J.N., Song, J., Lipska, B.K., Pickel, J., Weinberger, D.R. & Chen, J. (2008) Genetic dissection of the role of catechol-O-methyltransferase in cognition and stress reactivity in mice. *J Neurosci,* **28,** 8709-8723.

Pardo-Manuel de Villena, F. (2010) The Collaborative Cross: A Mammalian Platform for Systems Genetics. *Friday Pain Seminar.* Health Sciences Library, UNC-Chapel Hill, Chapel Hill, NC, USA.

Segall, S., Nackley, A.G., Diatchenko, L., Lariviere, W.R., Lu, X., Marron, J.S., Grabowski-Boase, L., Walker, J.R., Slade, G., Gauthier, J., Bailey, J.S., Steffy, B.M., Maynard, T.M., Tarantino, L.M. & Wiltshire, T. (2010) Comt1 Genotype and Expression Predicts Anxiety and Nociceptive Sensitivity in Inbred Strains of Mice. *Genes Brain Behav*.

Smalheiser, N.R. & Torvik, V.I. (2006) Alu elements within human mRNAs are probable microRNA targets. *Trends Genet,* **22,** 532-536.

Ullu, E. & Tschudi, C. (1984) Alu sequences are processed 7SL RNA genes. *Nature,* **312,** 171-172.

Wahlsten, D., Metten, P. & Crabbe, J.C. (2003) A rating scale for wildness and ease of handling laboratory mice: results for 21 inbred strains tested in two

laboratories. *Genes Brain Behav,* **2,** 71-79.

Waterston, R.H. & Lindblad-Toh, K. & Birney, E. & Rogers, J. & Abril, J.F. & Agarwal, P. & Agarwala, R. & Ainscough, R. & Alexandersson, M. & An, P. & Antonarakis, S.E. & Attwood, J. & Baertsch, R. & Bailey, J. & Barlow, K. & Beck, S. & Berry, E. & Birren, B. & Bloom, T. & Bork, P. & Botcherby, M. & Bray, N. & Brent, M.R. & Brown, D.G. & Brown, S.D. & Bult, C. & Burton, J. & Butler, J. & Campbell, R.D. & Carninci, P. & Cawley, S. & Chiaromonte, F. & Chinwalla, A.T. & Church, D.M. & Clamp, M. & Clee, C. & Collins, F.S. & Cook, L.L. & Copley, R.R. & Coulson, A. & Couronne, O. & Cuff, J. & Curwen, V. & Cutts, T. & Daly, M. & David, R. & Davies, J. & Delehaunty, K.D. & Deri, J. & Dermitzakis, E.T. & Dewey, C. & Dickens, N.J. & Diekhans, M. & Dodge, S. & Dubchak, I. & Dunn, D.M. & Eddy, S.R. & Elnitski, L. & Emes, R.D. & Eswara, P. & Eyras, E. & Felsenfeld, A. & Fewell, G.A. & Flicek, P. & Foley, K. & Frankel, W.N. & Fulton, L.A. & Fulton, R.S. & Furey, T.S. & Gage, D. & Gibbs, R.A. & Glusman, G. & Gnerre, S. & Goldman, N. & Goodstadt, L. & Grafham, D. & Graves, T.A. & Green, E.D. & Gregory, S. & Guigo, R. & Guyer, M. & Hardison, R.C. & Haussler, D. & Hayashizaki, Y. & Hillier, L.W. & Hinrichs, A. & Hlavina, W. & Holzer, T. & Hsu, F. & Hua, A. & Hubbard, T. & Hunt, A. & Jackson, I. & Jaffe, D.B. & Johnson, L.S. & Jones, M. & Jones, T.A. & Joy, A. & Kamal, M. & Karlsson, E.K., et al. (2002) Initial sequencing and comparative analysis of the mouse genome. *Nature,* **420,** 520-562.

Yang, H., Bell, T.A., Churchill, G.A. & Pardo-Manuel de Villena, F. (2007) On the subspecific origin of the laboratory mouse. *Nat Genet,* **39,** 1100-1107.

Figure 5.1 Proposed cell constructs. **(a)** Mutant *Comt1*^{B2i} transcript compared to ancestral *Comt1*$^{+}$ transcript. **(b)** Destroy the B2 sequence polyA signal. Does construct 1 make the full-length transcript including the B1 sequence? Are these cell constructs now equivalent in RNA degradation, protein, and enzymatic activity?

(a)

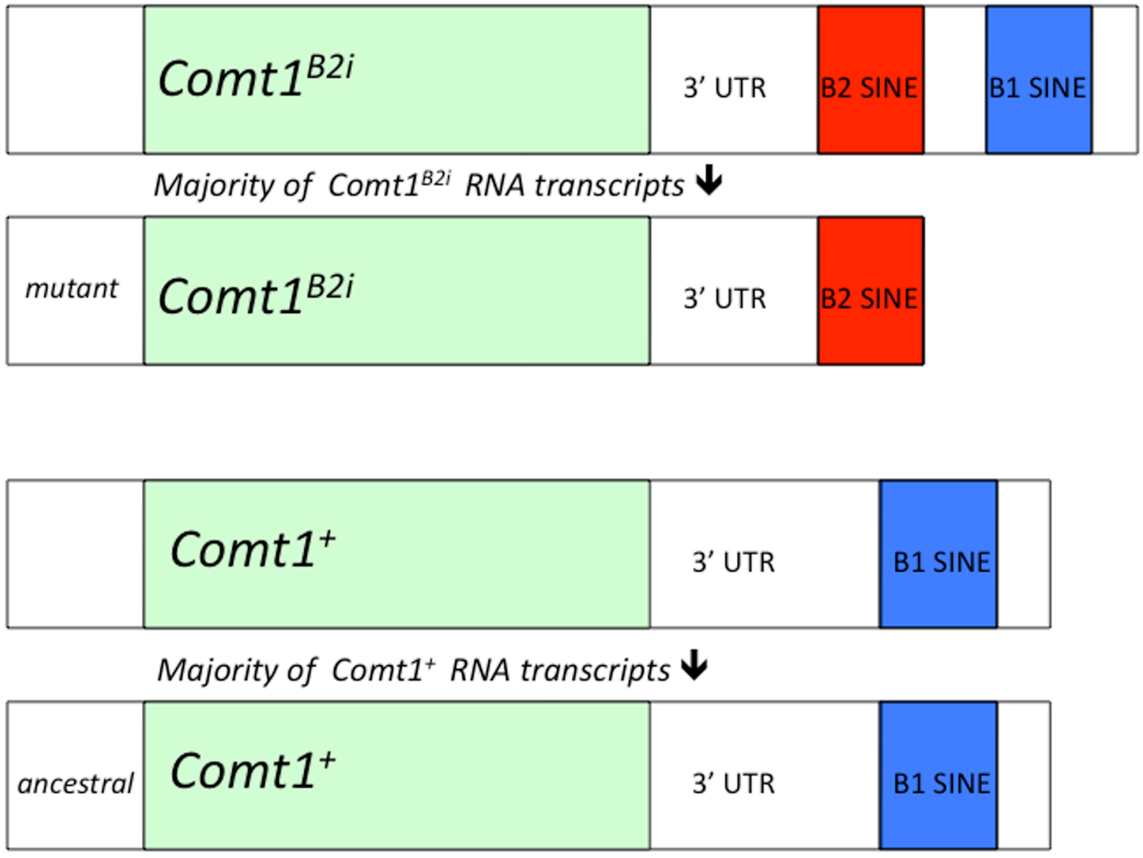

(b)

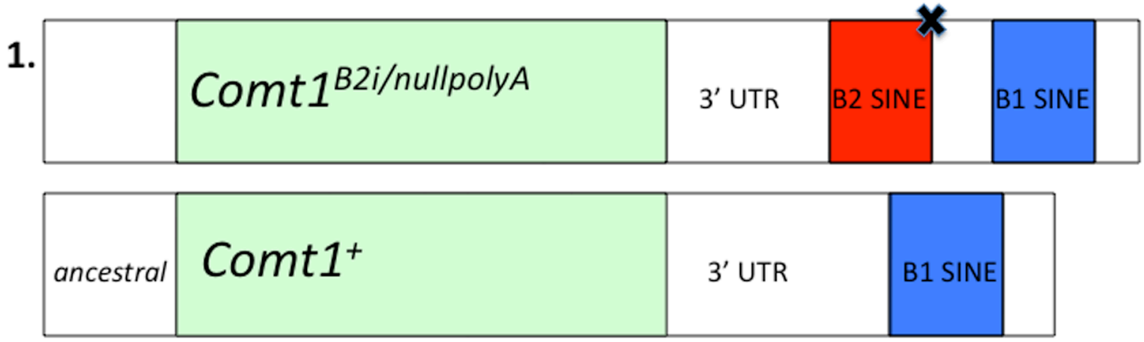

Figure 5.1 (c) Destroy 2^0 structure in B1 sequence. Is construct 2a equivalent to the mutant *Comt1*^{B2i} transcript? This would mean the B1 sequence is crucial to decreased stability, as B1 sequence is not made at high frequency in *Comt1*^{B2}. Is construct 2b equivalent to *Comt1*$^{+}$ transcript? This would confirm the importance of RNA secondary structure in the B1 sequence for RNA degradation.

(c)

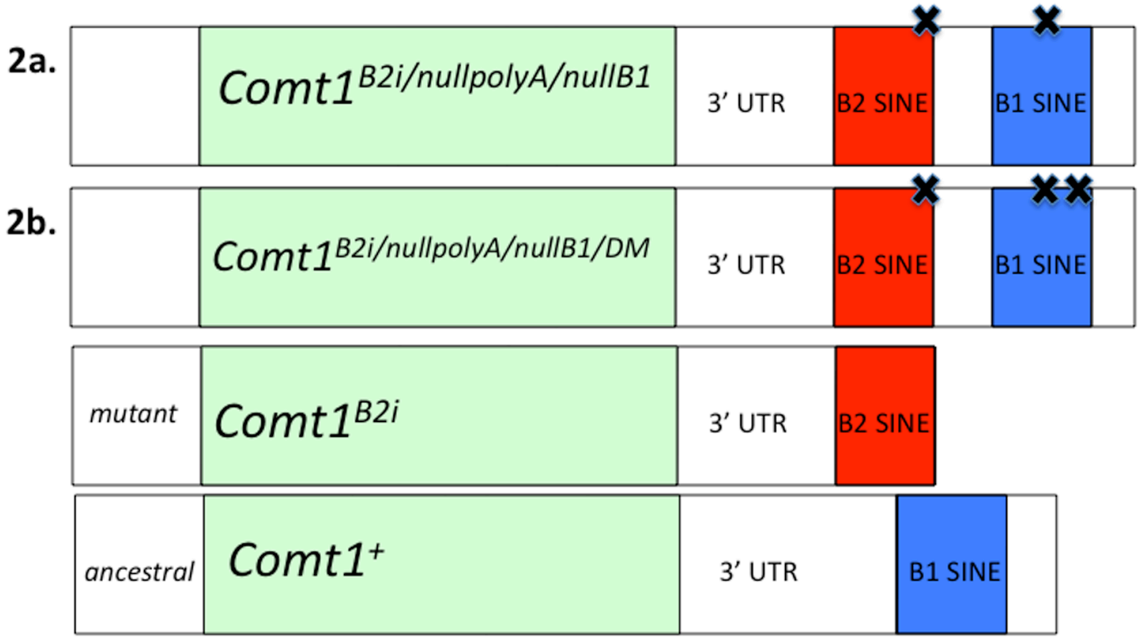

Figure 5.1 (d) Destroy 2^0 structure in B2 sequence. Is construct 3a equivalent to the ancestral *Comt1*$^+$ transcript? This would mean the B2 secondary structure is crucial to increased RNA stability. Is construct 3b equivalent to *Comt1*^{B2i} transcript? This would confirm the importance of RNA secondary structure in the B2 sequence to inhibit RNA degradation.

(d)